About the radiosynthesis and preclinical evaluation of innovative PET-tracers labelled with fluorine-18 and carbon-11 for neuroimaging

“..ubi bene, ibi patria..”

Marcus Tullius Cicero

(Tusculanae disputationes 5, 108)

Table of contents pages

Foreword 4

1. General introduction

1.1. PET basics 6

1.2. Production of radionuclides 10

1.3. PET physics 22

1.4. Radiopharmaceutical chemistry of PET tracers 34

-General development considerations for the design of PET radiotracers 37

-Strategies for labelling techniques with positron emitters 38

2. Experimentals / papers

2.1. Author's contribution 80

Paper 1 *Synthesis and Biodistribution of [^{18}F]FE@CIT, a new potential tracer for the Dopamine Transporter* 81

Paper 2 *Preparation and Biodistribution of [^{18}F]FE@CFN (2-[^{18}F]fluoroethyl 4-[N-(1-oxopropyl)-N-phenylamino]-1-(2-phenylethyl)-4-piperidinecarboxylate), a Potential μ-Opioid Receptor Imaging Agent* 104

Paper 3 *Preparation and first Preclinical Evaluation of [^{18}F]FE@SUPPY as a new PET-Tracer for the Adenosine A3 Receptor.* 127

Paper 4 *The simple and fully automated preparation of [carbonyl-^{11}C]WAY-100635* 146

3. Conclusions, outlook and future perspectives 167

4. Appendix 169

5. Acknowledgments 172

6. Curriculum vitae 174

Foreword

The presented PhD thesis aims at the introduction of three newly developed fluorine-18 labelled radiotracers ([^{18}F]FE@CIT, [^{18}F]FE@CFN and [^{18}F]FE@SUPPY) for the PET neuroimaging and on the improvement of the preparation techniques of one existing PET-tracer, namely the carbon-11 labelled radioligand [carbonyl-^{11}C]WAY 100635. The availability of selective receptor-ligands is a prerequisite for the safe use of these molecules for the purpose of receptor imaging. Since it is known that factors such as reaction time can strongly influence the quality of the radioligand, especially with respects to radiochemical parameters such as specific radioactivity, yield and radiochemical purity, special emphasis is put on these preparative aspects.

The thesis is structured into three main parts :

(I) introduction and methods

(II) papers and discussion

(III) conclusions

The introduction section should provide a brief and general background of the PET technique and the chemistry used for the radiosynthesis of PET-tracers.

The methods/papers section gives experimental details of the newly prepared radiotracers ([^{18}F]FE@CIT, [^{18}F]FE@CFN and [^{18}F]FE@SUPPY) or the improvements performed in case of the existing PET-tracer ([carbonyl-^{11}C]WAY 100635). All papers given in this section are either published (papers 1; 2 and 4) or submitted for publication (paper 3).

Since there are many established abbrevations, which are used on a regular basis in modern PET science, the author of this presented PhD thesis decided not to list the used abbrevations of this work seperately. For a comprehensive and facilitated

reading the abbrevations are always immediately explained at the same page on which they are used for the first time.

Furthermore, for a better overview the references chapter have been divided into several parts. For the general introduction part and also for the four papers the relating used, references are always given at the end of their respective sections.

1.General introduction

1.1. PET basics

PET stands for Positron Emission Tomography

PET is an in vivo imaging technique for the detection of administered radiopharmaceuticals giving the opportunity to visualise physiological processes of the human body. It is a so called **NIRI** (= **N**on-**I**nvasive **R**adiotracer **I**maging) modality [1].

Imaging technique	Mode	Spatial resolution [ranges]	Target sensitivity [ranges]
X- ray/CT	Anatomical	300.0µm	Low [>mM]
MRI	Anatomical	800.0µm	Low [>mM]
Ultrasound	Anatomical	500.0µm	Medium [nM]
SPECT	Functional + molecular	5.0 - 10.0mm	High [nM- pM]
PET	**Functional + molecular**	**2.0 - 8.0mm** [3-6]	**High [nM- pM]**

CT.. Computerized Tomography

MRI.. Magnetic Resonance Imaging

PET.. Positron Emission Tomography

SPECT..Single Photon Emission Computed Tomography

Table 1 shows several complementary non invasive imaging techniques and give an overview of their data key characteristics [2].

The “imaging strength” of PET lies in its non-invasive clinical imaging at the physiological and the molecular level [2]. The obtained spatial resolution and target sensitivities are derived from a combination of intrinsic properties of the techniques themselves and the particular combination of contrast agent and imaging protocol used.

1 CT images (skull,bowels,spine)

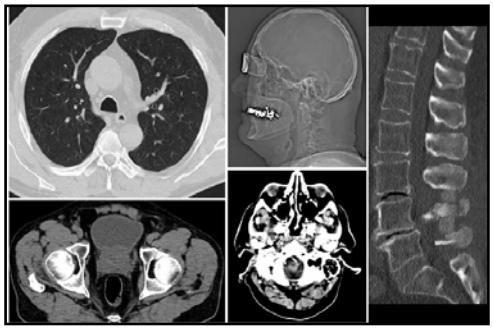

2 X-ray images (skull,upper body,spine)

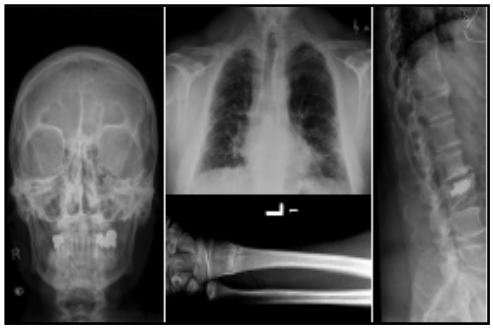

3 MRI images (skull,spine,knee)

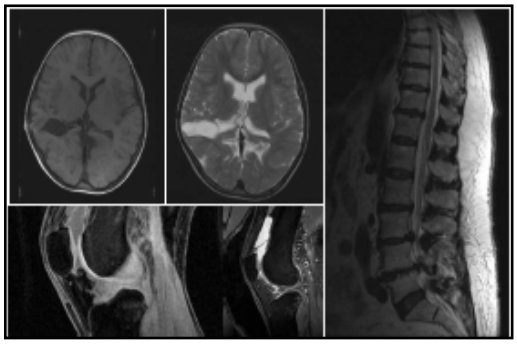

4 Ultrasound images of bowels

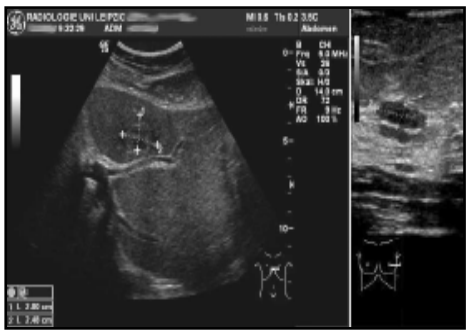

5 [^{18}F]FDG-PET whole body scan

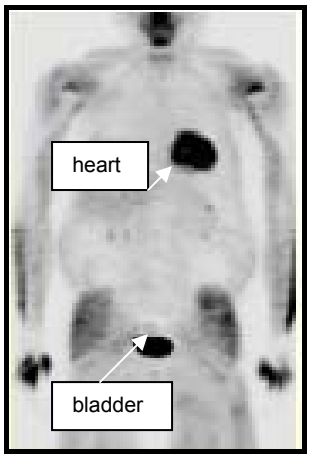

6 [^{99m}Tc]MDP-SPECT whole body scan

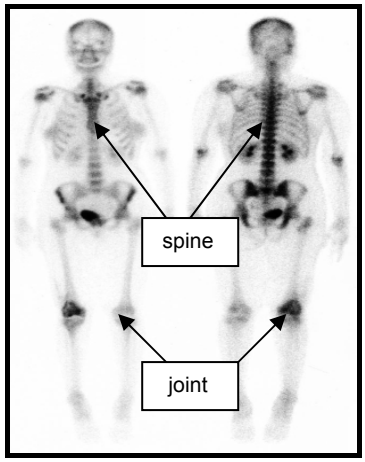

Figures 1- 4 illustrate typical CT, X- ray, MRI and ultrasound images [7],
Figures 5 and 6 show a PET and a SPECT scan [8,9].

The shown images are intended to demonstrate, respectively to compare the obtainable spatial resolution of the introduced imaging modalities of given Table 1.

The interested reader is referred to a recent review article published in 2006 by Cherry SR in which he presented an overview of new advances in PET imaging technology [10]. Furthermore, PET is not only valuable for medical purposes, it is also strongly employed for drug developement research. PET can answering questions of pharmacokinetics and drug dose regimen *(microdosing concept)* and is a helpful tool for the evaluation of the biological selectivity of newly developed drugs for the pharmaceutical industry. However, this PhD- thesis puts its emphasis on interactions between radiochemistry, radiopharmacy, psychiatry working fields and preclinic studies (marked with *blue arrows*).

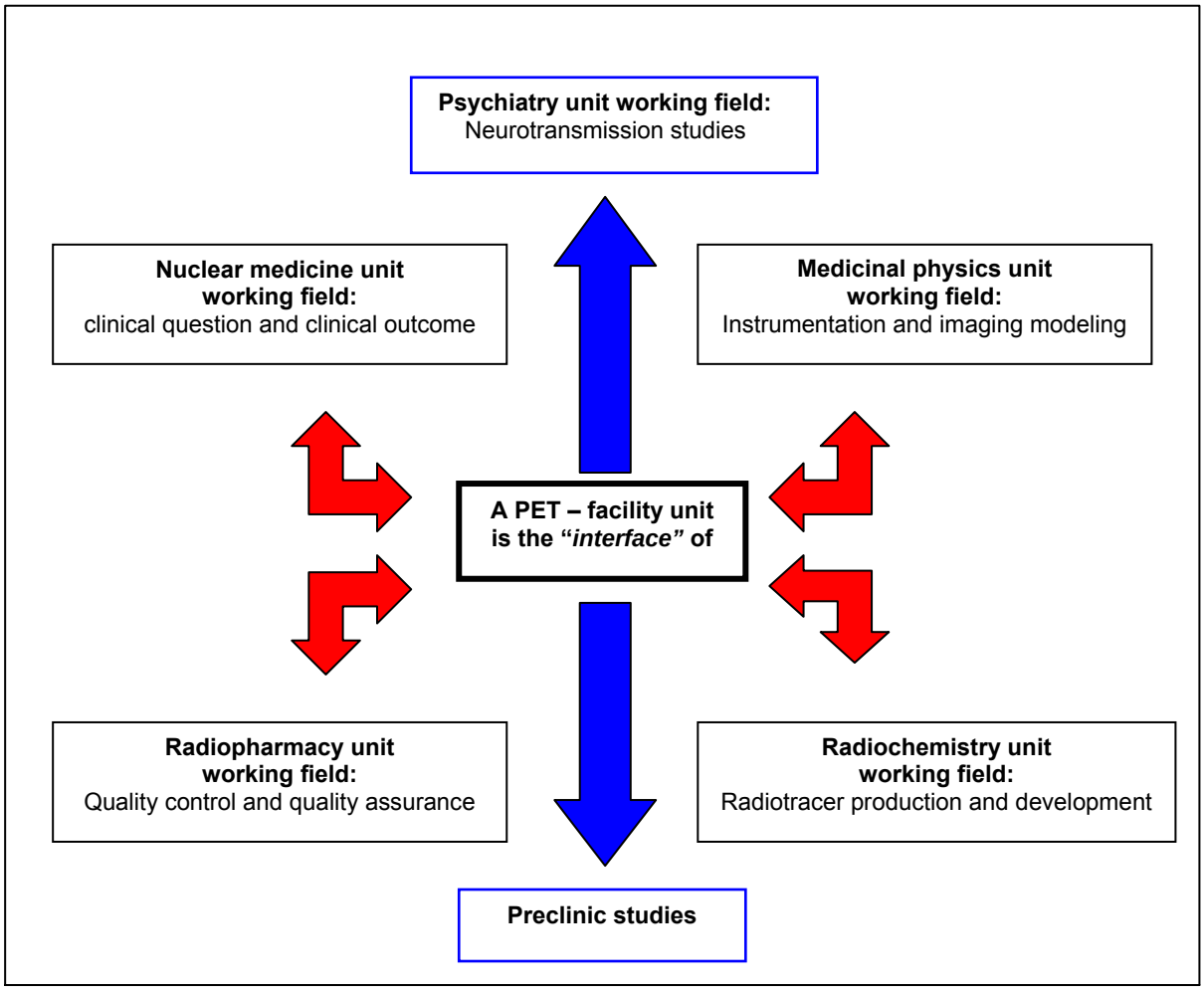

Figure 7 a modern PET facility and its interfaces

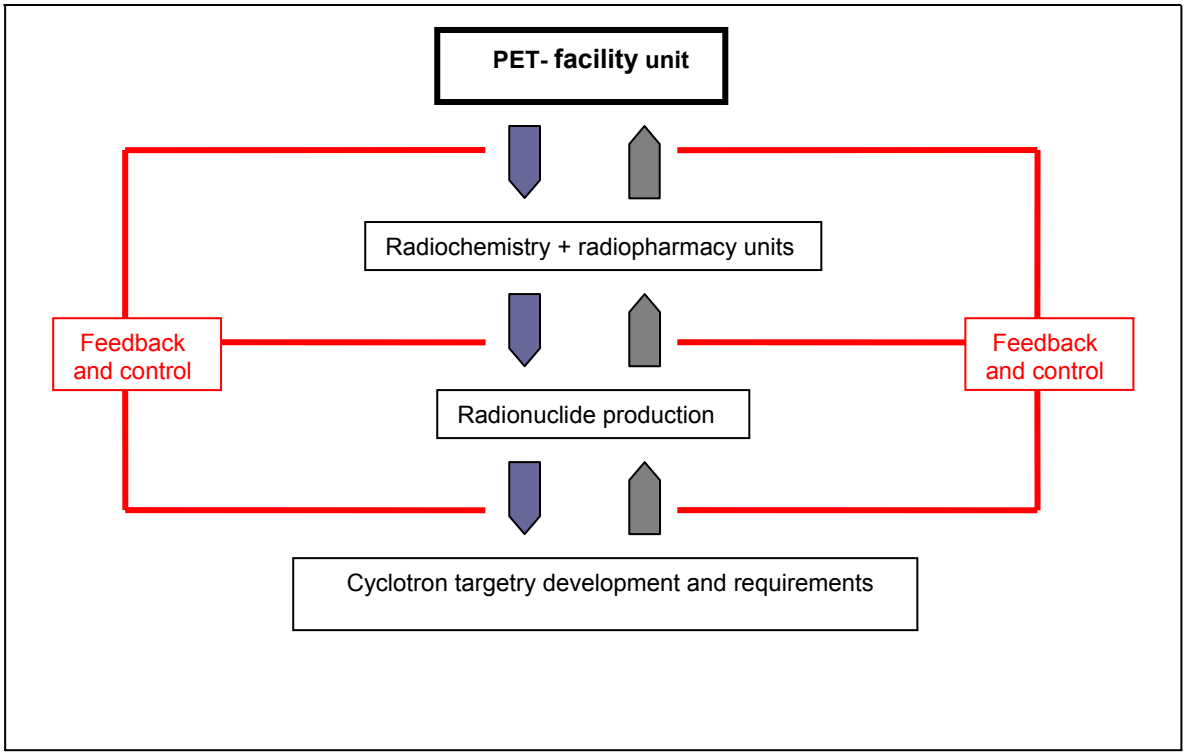

Figure 8 the "feedback and control" working mechanisms of a modern PET-facility and its related units [11].

Overview of PET science and its working fields

1 The particle accelerator (cyclotron) enables the production of desired positron emitters for labelling operations

2 The selected positron emitters carbon-11 and fluorine-18, which are the main focus of this PhD thesis, will be attached to a ligand via different radiochemical syntheses operation steps yielding the PET radiopharmaceutical.

3 The formulated PET radiopharmaceutical will be then administered into patient.

4 The PET scanner is the imaging device which registers the pathway of the administered radiopharmaceutical within the subject It has to be kept in mind that due to short physical half lives of positron emitters (see Table 2) nuclear medicine facilities must be in vicinitiy to the cyclotron site. Only for fluorine-18 labelled PET-tracers a considerable distribution possibility exists. Regional transport of fluorinated PET radiopharmaceuticals such as for the "*working horse*" *2-deoxy-2-[^{18}F]fluoro-D-*

glucose (= [^{18}F]FDG) to other PET sites without cyclotron facility can be performed (so called "*satellite principle*").

Radionuclide	Phys. half life	Decay mode	Max. specific activity*
Carbon-11	20.4 min	$ß^+$	3.4 x 10^{11} GBq/µmol
Fluorine-18	109.7 min	$ß^+$ and EC	6.3 x 10^{10} GBq/µmol

* defined as the number of decay N per second and per mole see also p.36 for detailed explanation

Phys... physical

Max... maximum

$ß^+$.. positron decay

EC.. Electron Capture property

Table 2 compares the physical and radiochemical properties of carbon-11 and fluorine-18 (given values are taken from [12]).

1. Production of radionuclides

In general there are two main approaches for the production of radionuclides which are depicted in the following organigram:

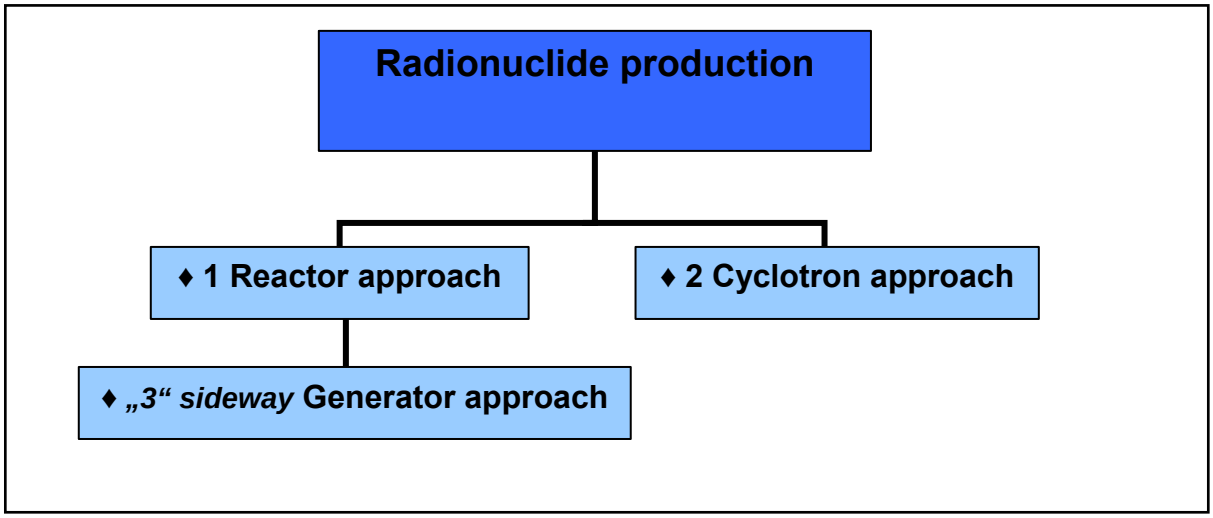

This presented PhD thesis places its emphasis on the second approach and its produced radionuclides. Therefore the first and the "third" production methods have been written with the aim to provide a complete overview of all possible radionuclide production pathways.

As shown, it is possible to produce radionuclides firstly with the nuclear reactor plant approach and secondly using cyclotron production.

Nonetheless, it has to be mentioned (for completeness) that there also exists a "*3 sideway*" option via a generator system. These generator systems are produced in nuclear reactor plants and can be treated as a sideway of the first approach. One can distinguish between neutron deficient/proton rich and neutron rich/proton deficient radionuclides. The latter are generated by nuclear reactors. For PET, only neutron rich/proton deficient compounds are useful for diagnostic imaging.

♦ Approach 1 radionuclide production via a nuclear reactor plant

The main principle for production of this approach I is the bombardment of target material with neutrons. The neutrons are employed as projectiles for the generation of neutron rich nuclides (those products of nuclear reactions are the so called ejectiles).

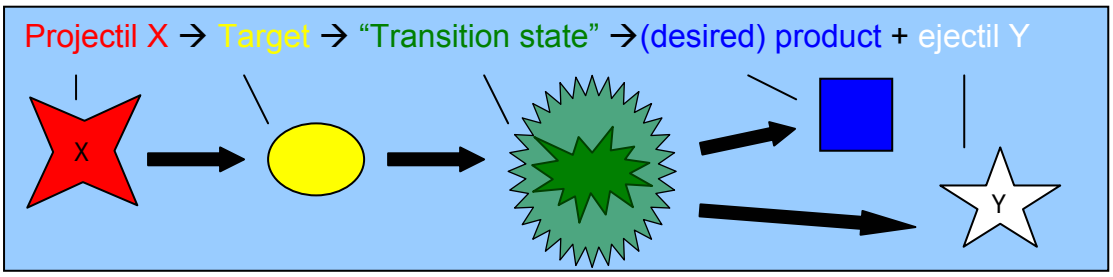

Figure 9a describes general (bombardment) nuclear reaction mechanism

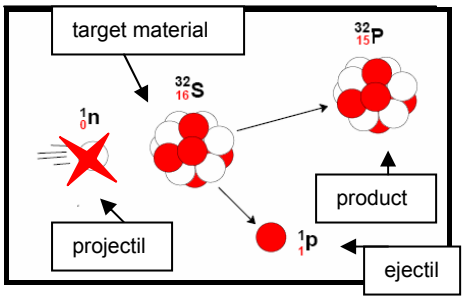

Figure 9b exemplifies the nuclear reaction of $^{32}S(n,p)^{32}P$ using a neutron as projectil [13].

This nuclear reaction can be expressed in following general equation.

$$^{32}S + {}^{1}n \rightarrow {}^{1}p + {}^{32}P$$

(equation 1)

The described (bombardment) nuclear reactions of approach 1 are taking place in a so called nuclear reactor plant.

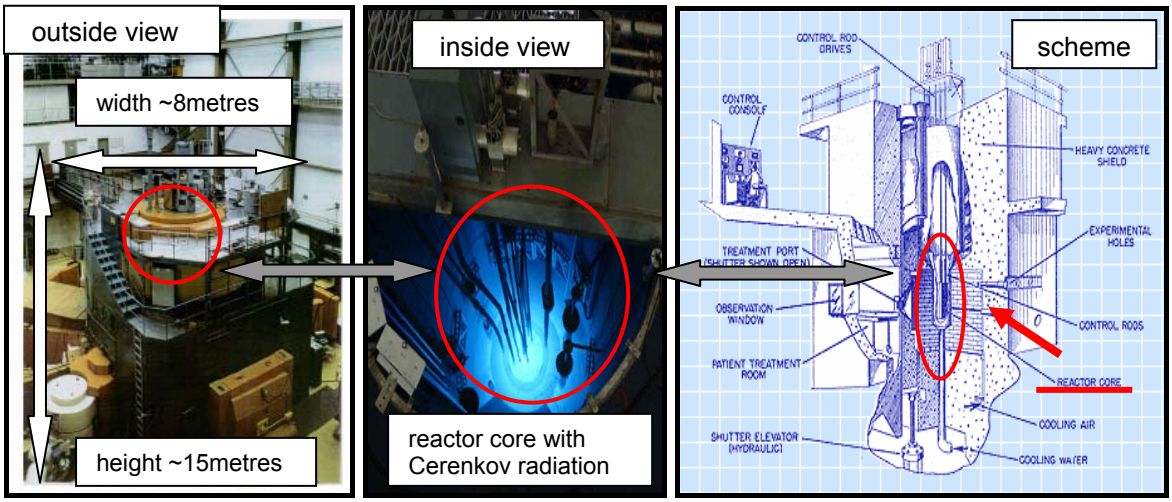

Figure 10 on the left side shows a typical nuclear research reactor (Rossendorf, Germany, decommissioned) [13]. Figure 11 in the middle gives an insight view into nuclear research reactor [14] and Figure 12 on the right hand side illustrates a simplified construction scheme of a nuclear reactor [15].

♦ **“3 sideway” radionuclide production via a generator system**

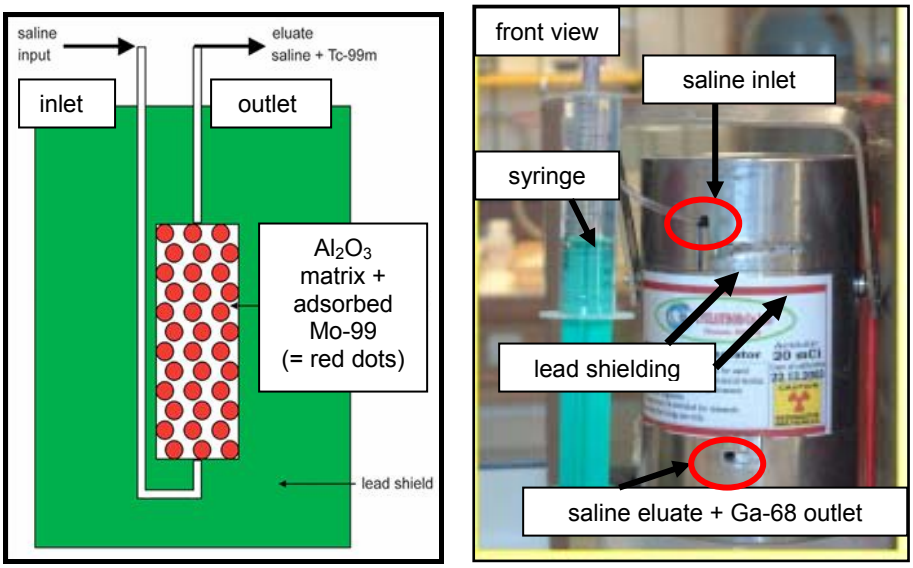

Figure 13 shows on the left hand side a simplified construction scheme of a ^{99}Mo/ ^{99m}Tc generator system [16]. Figure 14 on the right hand side illustrates the ^{68}Ge/ ^{68}Ga generator system which was employed for the first time in fall 2006 at the PET centre of the Vienna General Hospital (AKH Wien) [8]

Technetium- 99m is the most important radionuclide for SPECT imaging tracers in conventional nuclear medicine (Single Photon Computed Tomography) Interestingly, there are also generator systems which produces positron emitters such as the ^{68}Ge/ ^{68}Ga generator. A generator system is employed to seperate and extract the desired radionuclide through the use of a parent nuclide that constantly decays to a daughter nuclide.

Parent nuclide (A) → desired daughter nuclide (B) → granddaughter nuclide (C)

(equation 2).

Furthermore, it is important that the physical half life of *(A)* must be much longer than that of *(B)*, a so called transient equilibrium between mother and daughter nuclide is desired. For example ^{68}Ge is the mother nuclide *(A)* and ^{68}Ga is the desired daughter nuclide *(B)*. The main advantage of a generator is evident for small PET sites, where PET radionuclides become available without cyclotron.

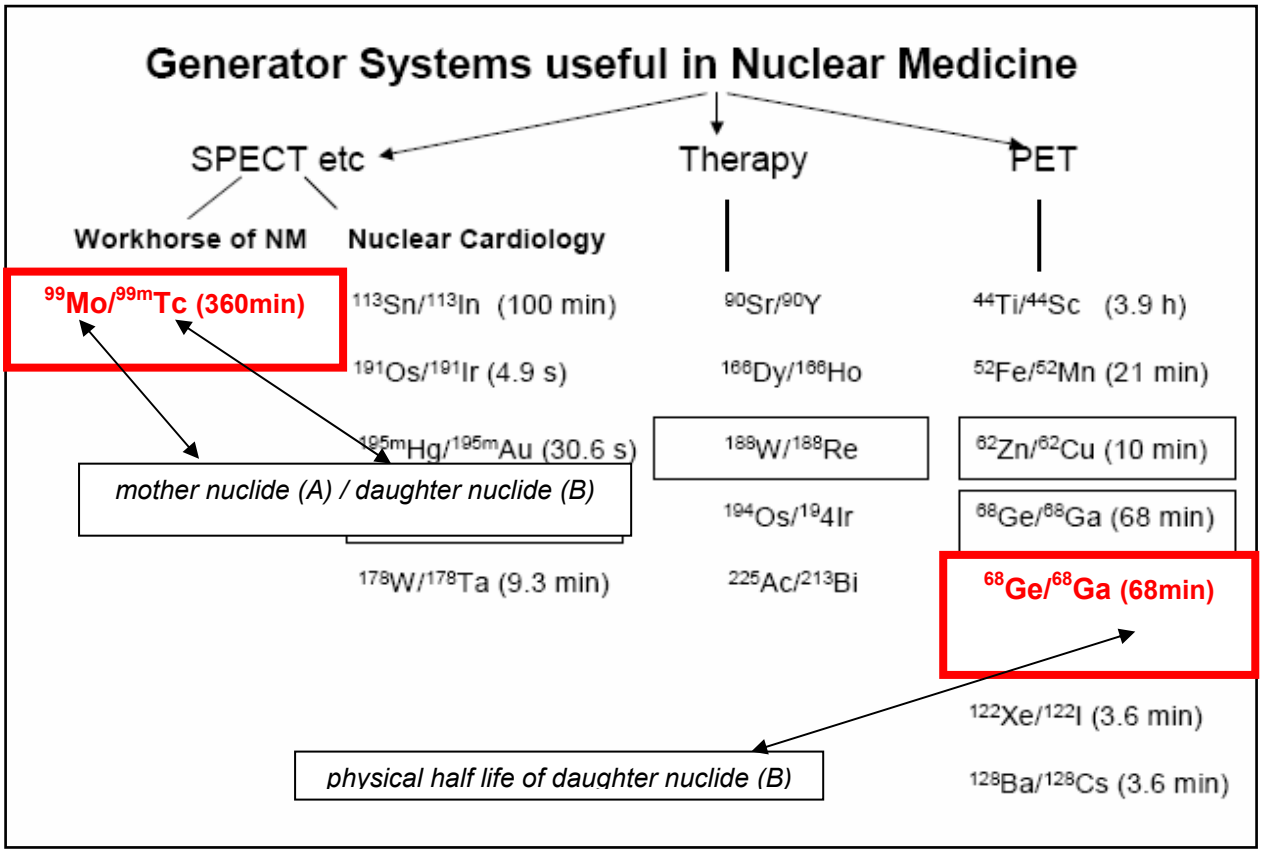

NM..Nuclear medicine

SPECT.. Single Photon Emission Computed Tomography

PET.. Positron Emission Tomography

Figure 15. shows a chart with the two before introduced (red boxes) and other commonly used generator systems employed in conventional nuclear medicine facilities and in PET sites [13].

Out of the so far available PET-generators, the ^{68}Ge/ ^{68}Ga generator system has the best properties concerning the physical half life of the daughter nuclide [68 min] and experiences a real *"boom"* in hospital PET centres. The most prominent ^{68}Ga-

labelled PET-tracer to date is [^{68}Ga]DOTA-TOC which is used for neuroendocrine tumour imaging.

♦ Approach 2 radionuclide production via a cyclotron

The main difference of cyclotron produced radionuclides as compared before to the reactor approach is a wider variety of nuclear reactions. This fact is due to the variation of possible employed projectiles such as protons, deuterons, helium-3 or helium-4 bombarding particles. In practice, however medical cyclotrons mostly use protons as projectiles for the nuclear reactions. Numerous medical accelerators that are used in hospital PET centres are proton accelerators. In some rare cases also alpha particles and deuterons are accelerated. The major advantages of these medical accelerators compared with nuclear reactor plants concerning radionuclide production are:

♦) small construction dimensions

♦) a low activation energy of components

♦) a low neutron background with low lead shielding requirements

♦) to get high specific activity of the desired radionuclide

♦) limited access to reactors

♦) production of fewer radionuclidic impurities by selecting an defined energy window for the employed nuclear reaction

Construction principle of cyclotron

The main parts of a cyclotron comprise:

♦ **1** The ion source located in the cyclotron centre which generates the projectiles

♦ **2** The acceleration chamber for the ions which become projectils for desired nuclear reactions

♦ **3** The magnets to maintain the acceleration of ions and to keep them on a circular path (the so called dee's).

♦ **4** The target chamber where the projectil with high velocity hits the target material and induces the desired nuclear reaction.

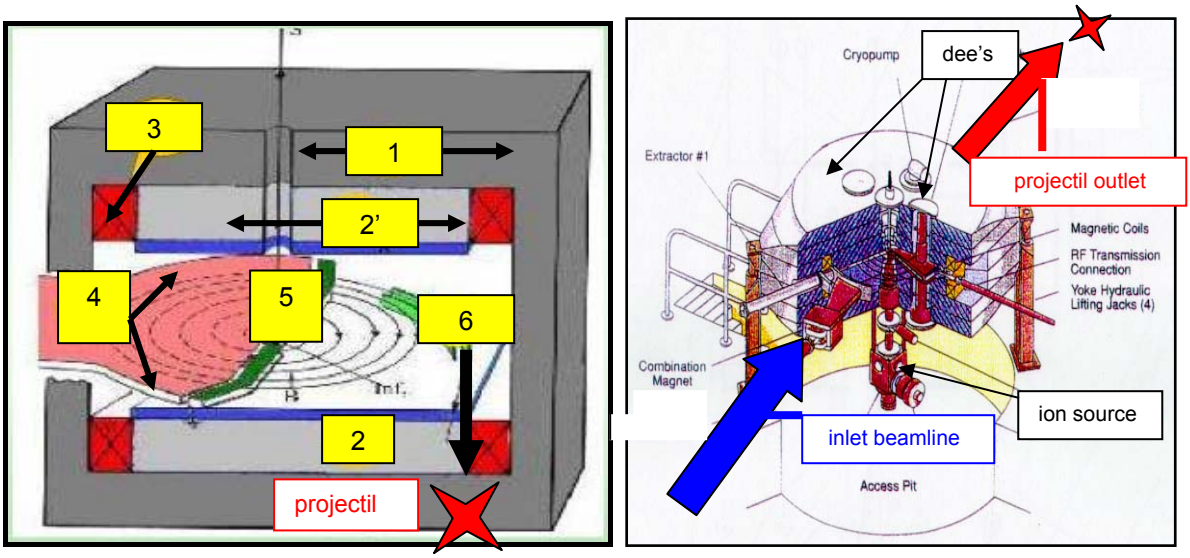

(1) steel yoke (2)+(2') steel poles (3) cooper coils (4) accelerating magnets (dee's) (5) generating ion source (6) accelerated ion (projectil)

Figure 16. on the left side shows a simplified construction scheme of a cyclotron [17].and Figure 17 on the right hand side shows selected details of cyclotron working parts [20].

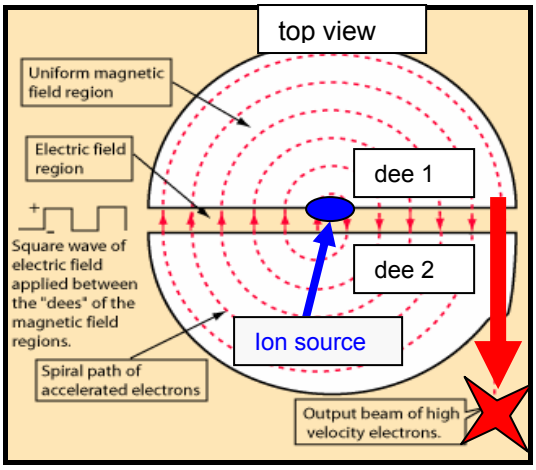

Figure 18. explains the physical mechanisms of the bombarding particle generation within a cyclotron [18].

The dimension size of a cyclotron depends on the function for which they are intended (working pupose).

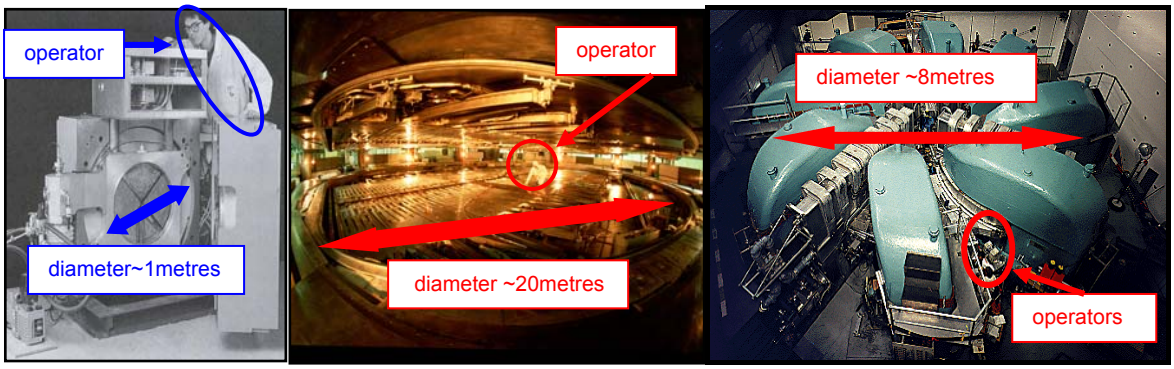

Figure 19 shows on the left hand side a cyclotron which employs deuterons as projectiles especially designed to produce only oxygen-15 for medicinal PET studies for example brain perfusion studies; due to reason of its small size it is also called "baby cyclotron"). Figure 20 illustrates in the middle the particle accelerator at TRIUMF (Tri University Meson Facility) in Vancouver, Canada, where a wide variety of radionuclides are produced and other experiments are carried out (for research purposes). Figure 21 on the right hand side depicts the research cyclotron at the PSI (Paul Scherr Institut) in Villingen, Switzerland, which is also employed for research purposes. (Note the shown diameters (red arrows) of right [19] and middle sided [20] research cyclotrons in comparison to a so called "baby cylotron" on the left hand side (blue arrow) [20] .

To conclude, all such research cylcotrons share another characteristic which sets them apart from medical cyclotrons beside the “bigger” construction dimension, the availability of much higher projectil (mostly proton) energy namely in the range of 50-200MeV compared to baby cyclotron with common proton energy capacity of 2-20MeV. This circumstance leads to a possible high variety of radionuclide production such as Fe-52 (projectil energy (= p.e.) >100MeV); Br-75 (p.e. >60MeV) or I-120 (p.e. >100MeV) with the employment of research cyclotrons. However, there have been also tremendous efforts performed in medical cyclotron construction and target chemistry which resulted in developments of very high intensity small accelerators for the production of common positron emitters especially employed on hospital sites [21-23].

Cyclotron targetry and its design

The main aims of cyclotron targetry are simply summarized:

♦ **1** to construct an optimal containment which accommodates the material being irradiated

♦ **2** to get the target material into the beam of accelerated ions

♦ **3** to keep it there during the irradiation

♦ **4** to remove the generated product radionuclide from the target material quickly and efficiently

General requirements for target design

Following five internal components are mandatory for cyclotron maintenance. There must be :

♦ **1** an area for containment of target material (solid, liquid or gas material) to be irradiated in the beam

♦ **2** a cooling jacket around target containment (cooling liquid like water)

♦ **3** an inert gas cooling flow in the front foil of beam entry (like helium)

♦ **4** a vacuum isolation foil leading to the cyclotron vacuum chamber for beam line.

♦ **5** a target foil leading to the irradiated target material for beam line

These general required five internal components are shown in following Figure on the next page.

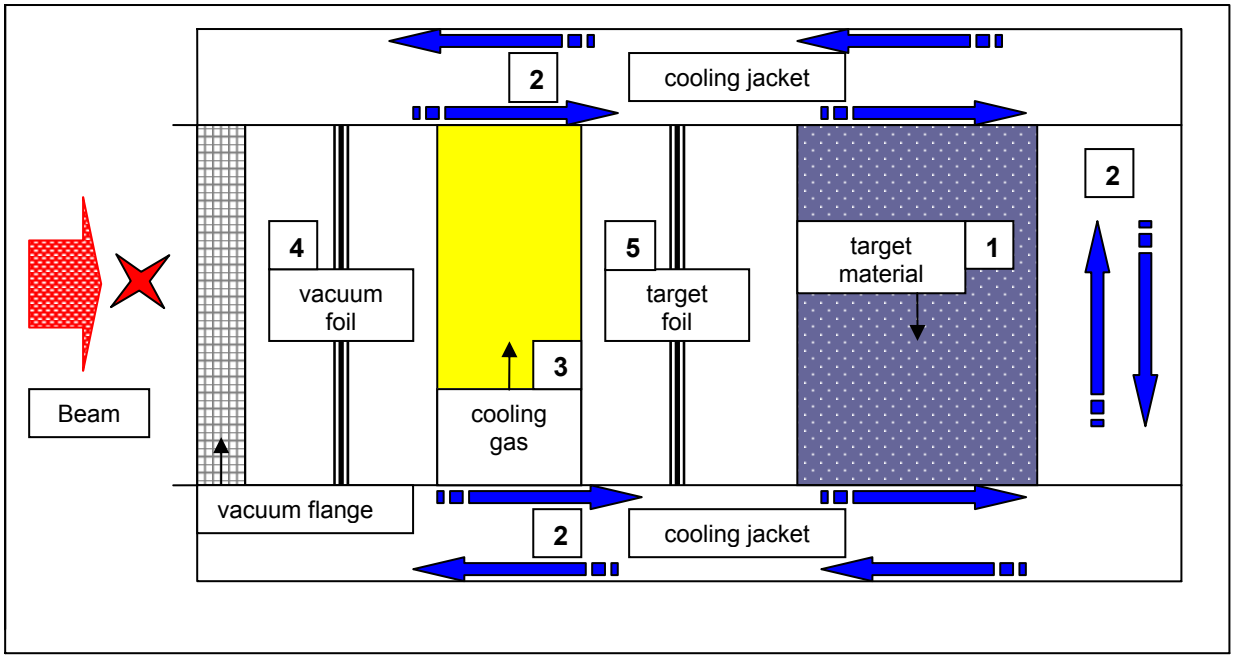

Figure 22 illustrates a simplified target construction scheme showing the five requirements adapted from [20].

1. Solid targets

A solid target can be formed as a foil or as a powder. If the solid target material is a good heat conductor, which is mandatory for optimal achievable cooling efficiency, the beam can hit the solid target in a perpendicular angle and therefore no beam energy loss occurs. Earlier solid powder targets for use with low beam currents or with thermally conductive solids have been designed for the carbon-11 production. These targets are mostly made of solid boron oxide. This *"boron powder"* is pressed into groves of the target plate and irradiated [24]. The main disadvantage of this approach is the removing difficulty of the generated carbon-11 from the boron oxide matrix in comparison to the ease of separation of the desired radionuclide in a gas or liquid target. Complexeous chemical extraction and purification methods have to be employed to remove the desired carbon-11 from the solid boron matrix. Thus this

construction of solid target is not widely used. More detailed information concerning carbon-11 production via the solid target approach is explained on page 42.

2. Liquid targets

In the case of liquids, the target has similar dimensions as compared to the solid target since the target material occupies a specific volume unless the liquid volatilizes. The difference is that the liquid is typically added and removed from the target while it is in place on the cyclotron. The generated radionuclide is conveniently recovered as a reaction product by sparging the volume above the target liquid material with a suitable sweep gas, usually helium (= He). A typical liquid target is the oxygen-18 enriched water (= $H_2{}^{16}O$) target for the production of $[^{18}F]F^-$ for nucleophilic substitution reactions (see on page 48 more detailed information)

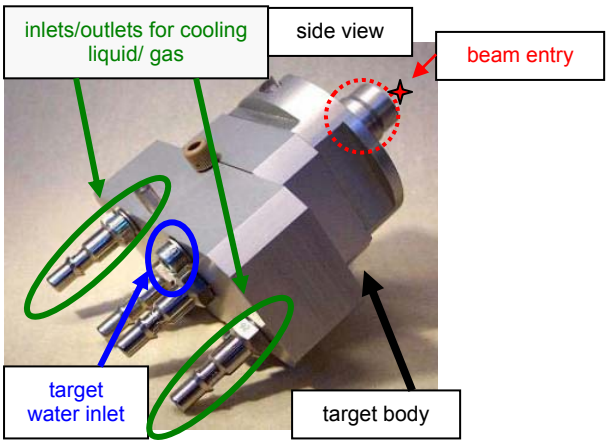

Figure 23 shows an oxygen-18 enriched water (= $H_2{}^{16}O$) generation 2 target from GE®(= General Electric (Schenectady, U.S.A)) [155]

3. Gas targets

Gas targets are widely used, most prominently as the ^{14}N gas target for the production of carbon-11 using the ^{14}N (p,α)^{11}C nuclear reaction. The loading and

unloading of target materials are easily accomplished under remote control and manipulation of the target gas mixture itself also permits some control over the desired radionuclide product quality. To have enough target material in the beam to obtain sufficient radionuclide product, it is mandatory that the target shape has to be designed as a cylinder which holds the target gas under pressure. Thus the foil of beam entry has to withstand this pressure differentials with some reliability, but increased foil thickness also increases beam energy deposition within the foil material (the so called window). Furthermore, since gases have not very good heat conductor properties it is crucial to gurantee the removal of the generated heat during irradation process from the target gas.

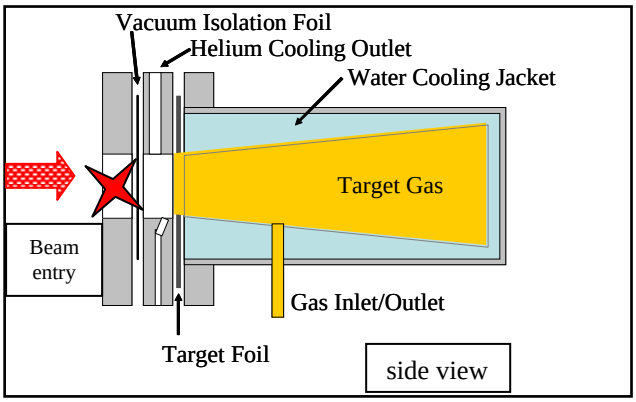

Figure 24. shows a simplified construction scheme for a gas target [20].

A brief guide to PET physics

The PET radiopharmaceutical contains a positron emitter such as carbon-11 or fluorine-18 which enables the detection with PET scanner.

The ß$^+$ decay of positron emitters

Neutron deficient radionuclides (like C-11 and F-18) which are produced by the bfore introduced cyclotron approach (see page 10) have the property to decay via positron particle (ß$^+$ or e$^+$) emission. (particle data: e$^+$ mass has a value of 0.511

MeV, charge +1 and spin value of 1/2 [25]) The consequence for this ß$^+$ decay, for example for carbon-11 is the generation of a new radionuclide in this case boron-10 with one proton fewer and one more neutron in the nucleus under simultaneous emission of a positron and a neutrino (v) particle.

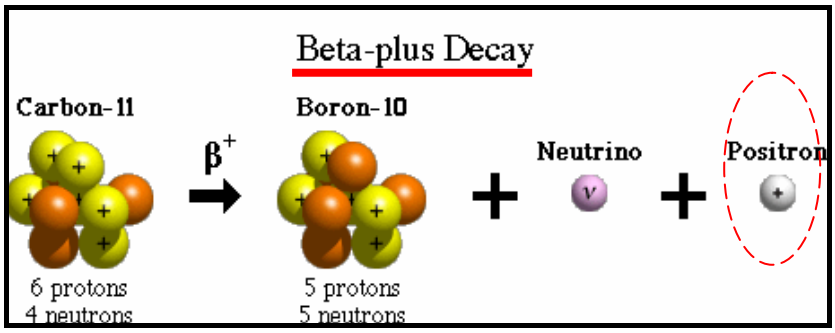

Figure 25. describes graphically the before described carbon-11 nuclear reaction [25]

The annihilation process

The emitted positrons (e^+) shift through matter (e.g. patient's body) and as a consequence undergo the same interactions like electrons (e^-) such as energy loss through ionization and excitation processes of neighbouring atoms and molecules. Is the initial energy loss high enough and the positron traveling distance in the neighbourhood of matter reached (the travel range depends on initial energy of positron see Table 3 on pages 24, 33 and 45), the e^+ will annihilate with a nearby electron since the positron is the antimatter counterpart of the e^-.

The mentioned positron travel ranges in millimeters [mm] and imposes the limit of the physical local resolution aquired with the PET scanner ("*the smaller the initial positron energy values the smaller positron travel range and thus the better the spatial PET resolution*" theoretically can be) [26]. This physical circumstance explains why fluorine-18 labelled PET tracers give better spatial imaging properties compared with carbon-11 labelled PET tracers.

Nuclide	Decay mode	Max. energy	Mean energy	Max. range in water
C-11	100% $ß^+$	0.960 MeV	0.386 MeV	4.1 mm
F-18	97% $ß^+$+ 3% EC	0.690 MeV	**0.250 MeV**	**2.4 mm**

Max...maximum

$ß^+$ ..Positron decay

EC ..Electron Capture property

Table 3. shows positron energy and positron travel range of carbon-11 and fluorine-18 (given values are taken from [12])

This annihilation is always accompanied by an emission of two gamma rays/photons (γ). Both emitted photons leave the nucleus diametrically under an angle of approximatley 180°± 0.3° [122]. The final emitted energy of each photon has the exact value of 511keV. The annihilation process are depicted in following Figures with the intention to give a better overview.for the interested reader.

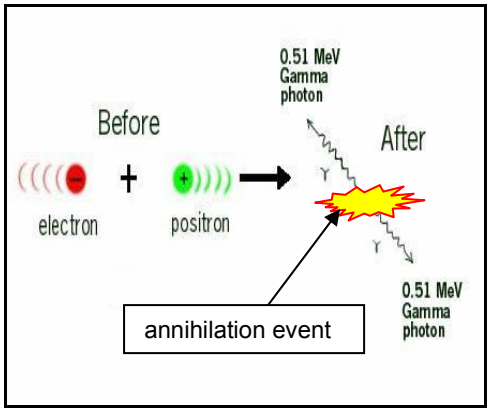

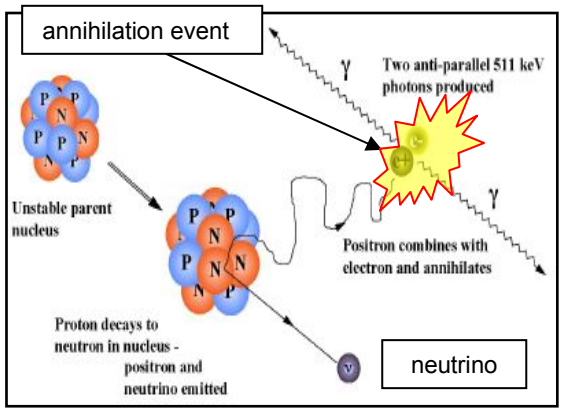

Figure 26 and Figure 27. (right hand side taken from [27] and left hand side is adapted from [28]) are illustrating the annihilation process

The positron ↔ electron pair annihilation can be detected and localized with a modern PET scanner and is essential for "*NIRI*" (= Non- Invasive Radiotracer Imaging) modalities [1] (see pages 6 and 7).

The coincidence detection in a PET scanner

A true coincidence event is defined as the "*simultaneous*" detection of two emitted photons with each 511keV in opposite directions (in an angle of ~180°) within a PET scanner in which the scintillation detectors are circumferencially arranged the so called PET detector ring. As a consequence of thus arrangement a circular and transaxial FOV (= Field Of View) is built. This detector ring is one core part of a PET scanner.

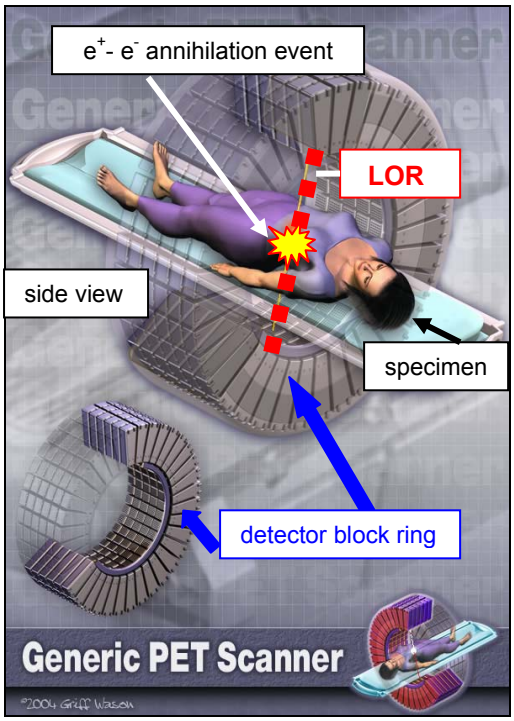

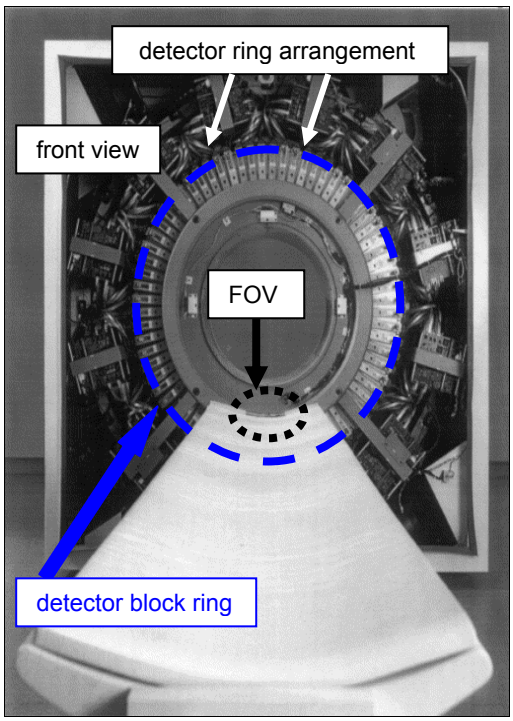

LOR..Line Of Response is referred as the path between two opposite detectors which detect a true coincidence event (further details explained on page 30).

Figure 28 and Figure 29 show PET detector ring arrangements (blue arrows), the LOR (red doted line) and the FOV (black arrow) within a PET scanner) (left hand side a sketch of circular detector block arrangement [121], right hand side a real insight into an opened Siemens CTIECAT EXACT PET scanner [31]).

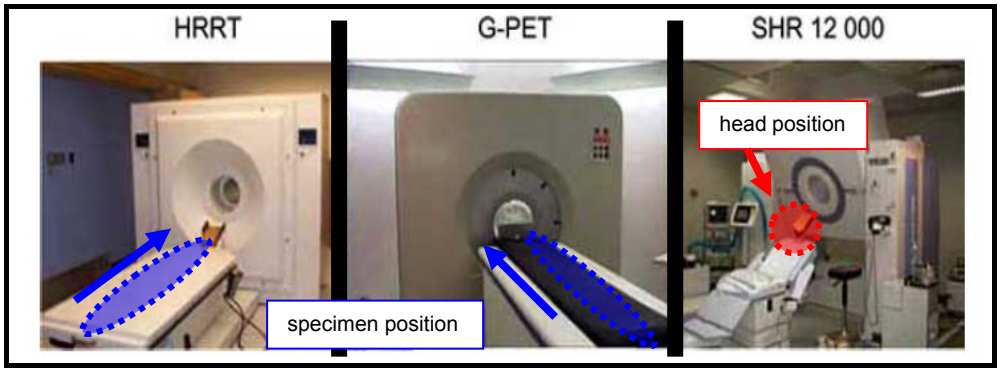

Figures 30-32 are intended to show. state of the art PET scanner models (on left hand side Siemens ECAT-HRRT for whole body imaging (=High Resolution Research Tomograph), in the middle GE G-PET for whole body scans (specimen position blue arrows) and on the right hand side Hamamatsu SHR-12000 PET scanner, which is specialyl designed for neuroimaging modalities (head position red arrow) [30].

PET scanner working parts

Detectors and light distributors

A scintillation detector consists two main parts:

♦ 1 a scintillation crystal

♦ 2 a photomultiplier (= PMT).].

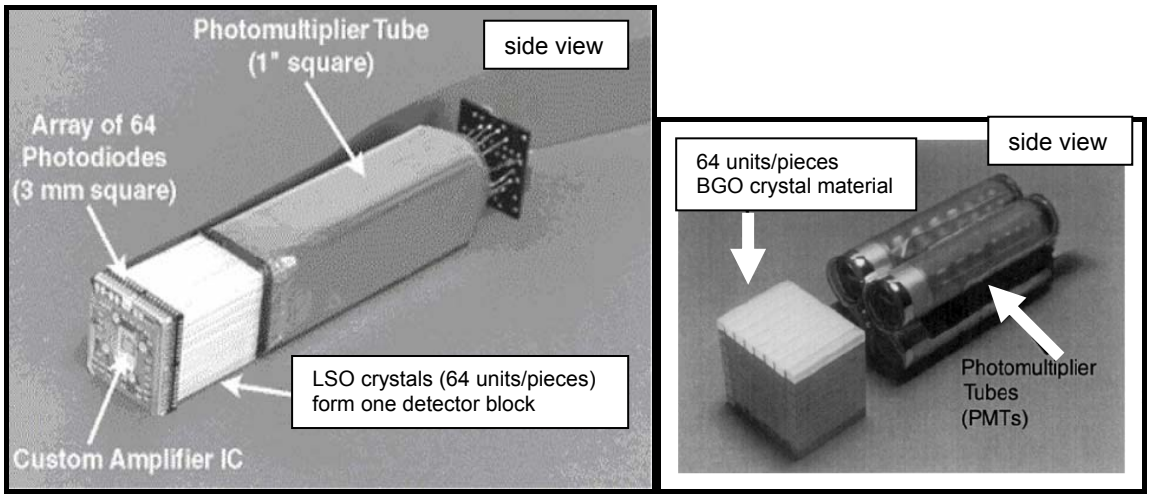

IC.. Integrated circuit unit, this PET read out IC unit (= PETRIC) amplifies the photodiode pulse signals and identifies the highest detector crystal signal

Figure 33 and Figure 34 show scintillation detectors with connected PMT photographs on the left side [29] and on the right hand side adapted from [31]

The current resolution requirements demand a detector crystal size approximately in the range of milimeters [mm].

The adjustment of each single crystal with a single PMT is not possible due to PMT construction limits in miniature. The use of avanlanche photodiodes (= APD) instead of PMT's enables single crystal measurement. So far, this technique is still in development and not available for daily routine use. Detector crystals are positioned in blocks. The scintillation signals which are generated by such arranged crystals are read out by square PTM's classified as *A, B, C,* and *D* that are located behind the crystal matrix as shown right below.

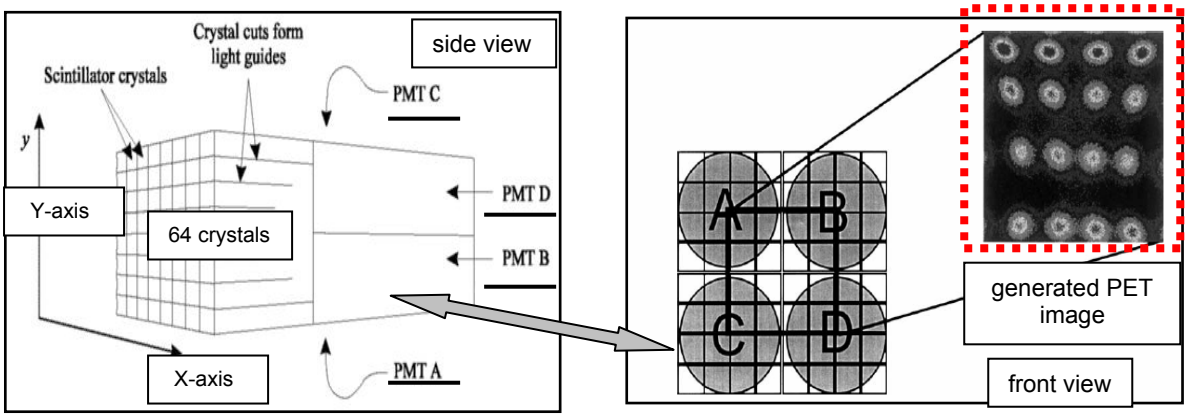

Figure 35 and Figure 36 show schemes of the orientation of PMT's detectors for generating PET images left handed sketch is taken from [27] and right handed side sketch is adapted from [31]).

To avoid crossing signals of the neigbouring single crystals the surfaces of the cuts that seperate them from each other are mirrorplated. If a 511keV photon is entering one of those crystals the interaction will generate a scintillation signal. The arriving photons can only enter from the front of the crystal block.

The block size is a square field of 16 crystals (16 crystals per PMT)

Detectors and lightdistributor are made in one piece. Two scintillation crystal materials are state of the art and used nowadays: Bismuth germanate (= BGO) or

Luthetium orthosilicate (= LSO), LSO is advantageous compared to BGO because LSO can read out more scintillation signals per time interval as BGO and the spatial resolution of LSO is higher. However, LSO is more expensive and so mostly the choice for BGO as a conventional material for detection crystal was made.

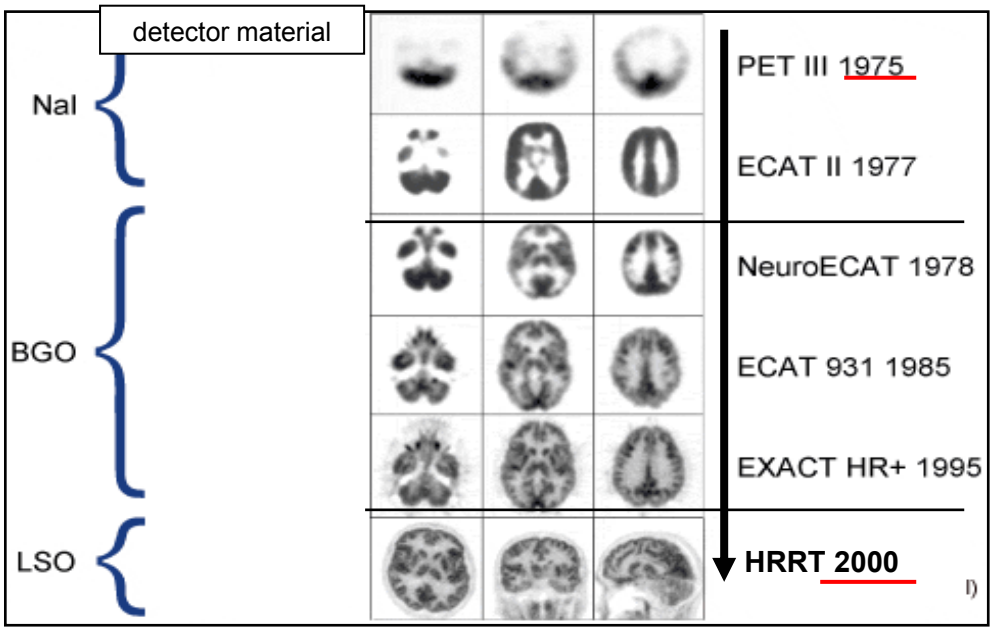

HR.. High Resolution

HRRT..High Resolution Research Tomograph

ECAT.. Emmision Computer Aided Tomography

Figure 37. gives an overview of used PET crystal detectors from the first material Natriumiodid (= NaI) in the 70's to BGO and nowadays employed LSO and their resulting possible related spatial resolution [27].

The coincidence event is the positron ↔ electron- pair annihilation

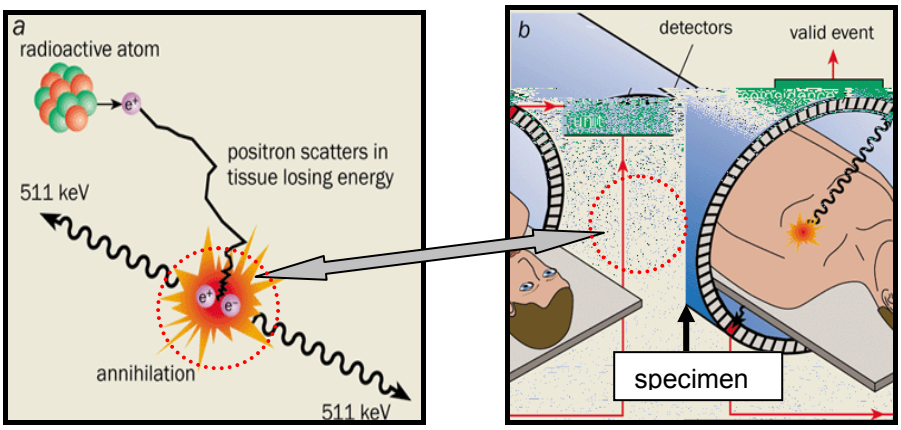

Figure 38 and Figure 39 depicted the desired "coincidence event" which is subsequently registrated within the PET scanner [32].

There has to be made a distinction between three different cases of coincidence events which is illustrated in the following organigram.

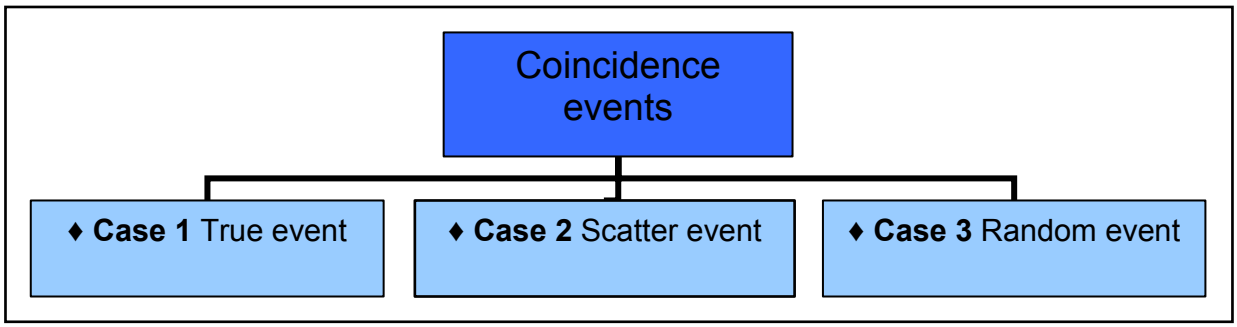

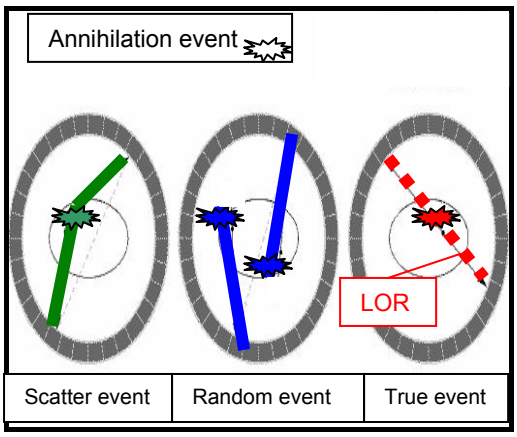

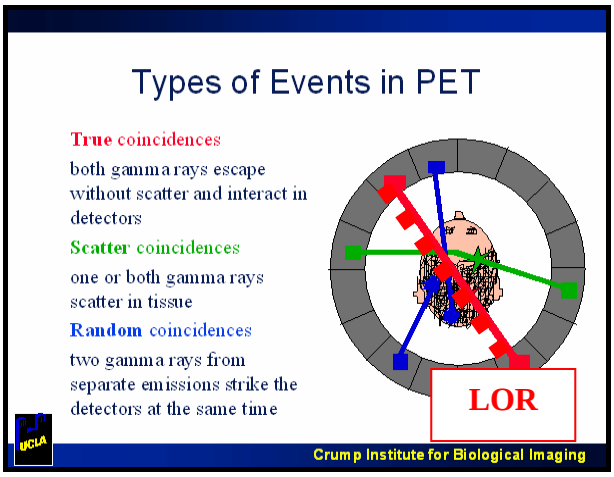

LOR.. Line of response

Figure 40 and Figure 41 are illustrating the three possible cases of coincidence events (left hand side sketch taken from [27] and right hand side from [122]).

♦ **Case 1** The true event

Two opposite located detectors in the PET scanner detector ring were hit by two photons (γ) caused by an annhililation process. The simultaneous pulses from the detectors indicate that our true event occured somewhere along the path between the two detectors. This path is commonly referred to the real line of response (= the LOR). The number of coincidence events occurring between the two detectors indicates how much “radioactivity” there was on the LOR.

♦ **Case 2** The scatter event

Scattered events result from so called Compton scattering where one photon γ is deflected (due to collision with an electron e^-) from its direction prior to detection thus the resulting coincidence event will be assigned to the wrong LOR.

♦ **Case 3** The random event

Randoms events occur when two photons (γ) are not arising from the same annhihilation event, but are incidentally detected within the allowed coincidence interval.

PET imaging quality

As it is shown in below depicted organigram the PET imaging can be degraded by following five factors:

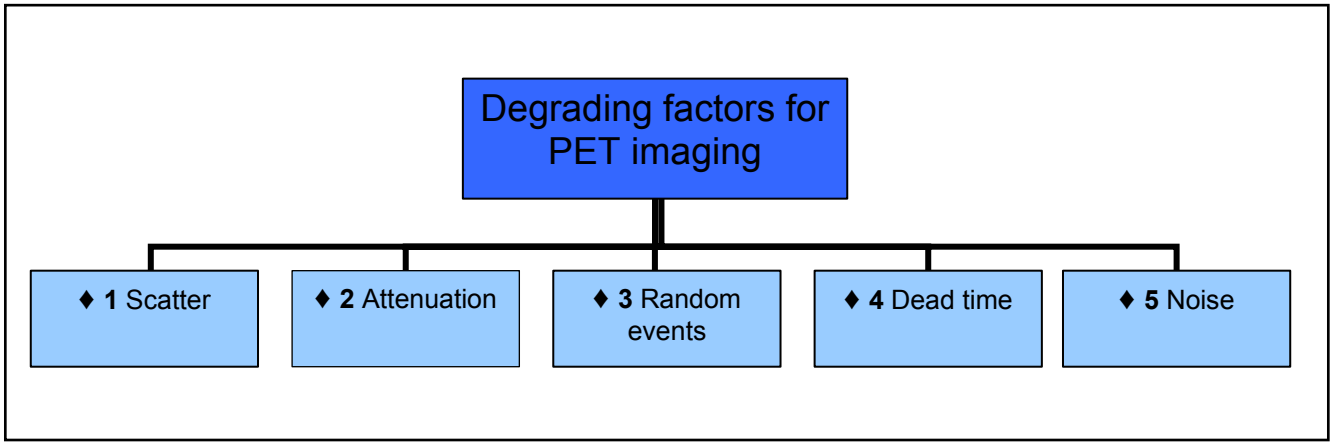

♦ **1** Scatter

Scattered coincidences add a background to the true coincidence distribution causing radioactivity concentration to be overestimated. Statistical noise is also increased by scatter events. The number of detected scattered coincidences depends on the volume and attenuation characteristics of the imaged object and on the camera geometry.

♦ **2** Attenuation

Due to scatter and adsorption effects there is an overall loss of counts (= loss of true events) This can be defined as the attenuation. Both photons (γ) of an annihilation event must leave matter unattenuated to be detected as a true event. Thus, the introduction of body nonuniformities into reconstructed PET images has to be considered. As a consequence, the emitted positrons shifting through different areas of patient's body have different attenuation degrees: radiation emitted from the middle of the body is more likely to be attenuated than from near the patient's body edge area.

♦ **3** Random events

Even if two ring detectors receive the two emitted 511 keV photons of a true event at *"exactly"* the same time, there will be a difference in the detection time at which electronic pulses leave each detector. Thus, the coincidence time window must allow some time difference in detection. The total time window has values of nanoseconds [ns]. This time window should be selected large enough so that all true events are detected. Nonetheless, *"the larger the chosen time window is the more random events will be also recorded"*, resulting in the degradation of PET imaging quality.

Just as with scattered events the random events also add a background to the true coincidence distribution. Like for scatters, the same parameters influence the possible recorded number of random events: the object volume, its attenuation properties and the PET scanner geometry.

♦ **4** Dead time (also the so called refraction time)

With increasing photon rate hitting detectors also the probability of missing photons increases. This fact is due to the detector dead time.

This losses can be reduced by implementing systems of independent detectors, faster scintillators and signal processing for recording events.

♦ **5** Noise

Noise is defined as the random variations in pixel intensity. Noise decreases with increasing counts. Increased countrates can be achieved with longer scanning times, higher administred acitivity doses and improved scanner efficiency performance. In this context the noise quality is also dependend on the background level.

PET spatial resolution

The spatial resolution of a PET image can be impacted by three factors:

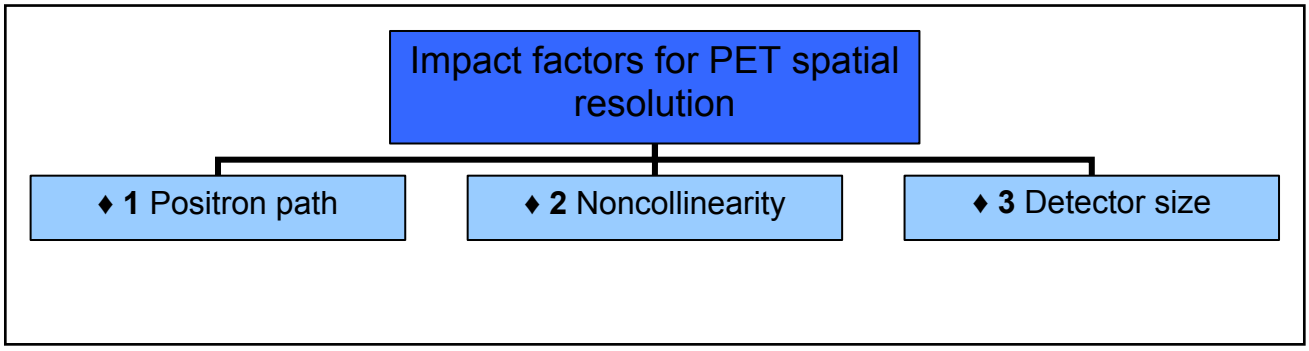

♦ **1** The positron path

The positron has a certain travel range before the e^+ conversion (annihilation event) takes place due to its lower initial energy of fluorine-18 in comparison to carbon-11 the travel distance of fluorine-18 is smaller than of carbon-11.

Nuclide	Decay mode	Max. energy	Mean energy	Max. range in water
C-11	100% $ß^+$	0.960 MeV	0.386 MeV	**4.1 mm**
F-18	97% $ß^+$ + 3% EC	0.690 MeV	**0.250 MeV**	**2.4 mm**

Max..Maximum

$ß^+$ ..Positron decay

EC ..Electron Capture property

Table 3. shows the dependency of positron energy and positron travel range of carbon-11 and fluorine-18 (given values are taken from [20], see also on pages 24 and 45).

♦ **2** The noncollinearity

Due to reason that both 511keV photons are not exactly emitted under an angle of 180°(± 0.3°) noncollinearity is generated [122].

♦ **3** The detector

The size of detector is related directly to spatial resolution *("the smaller the detector size the better the achievable spatial resolution")*.

1.3. PET chemistry

PET is a technique which administers radiopharmaceuticals into the human body. The radiolabel allows to follow the fate of the radiotracer throughout the body. A clinical diagnosis can be based upon the receptor binding, pathological physiology and metabolism, differences in blood flow, or simply by following the distribution of these radiotracers. The most commonly PET-radionuclides are fluorine-18, carbon-11, nitrogen-13, oxygen-15 and gallium-68. Carbon, nitrogen and oxygen can be also called “elements of life” since they are involved in virtually every organic molecule [24]. Therefore, authentic labelling without any change in the chemical properties of the compounds (PET-tracer) can be achieved .Taking into account the half-lives, only carbon-11 (~20min), fluorine-18 (~109min) and gallium-68 (~68min) can be used for the routine synthesis of various PET-tracers.

The differences of PET chemistry to classical organic chemistry

♦ **1** PET chemistry must be always performed in lead shielded enviroments so called hot-boxes/cells with the aim to protect the operator from radiation burden and to fulfill radiation safety guidelines of the authorities. [34].

On the next page two Figures of a typical hot box are presented.

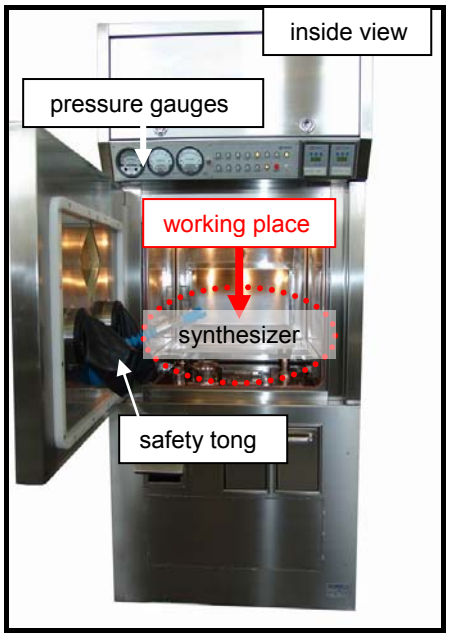

Figure 42 and Figure 43 show state of the art hot-box/cell from outside on the left and on the right side with insight view (hot box model Agatha from Comecer® (Castelbolognese, Italy) for PET chemistry in which the working place is located, respectively the radiosynthesizer module is placed

♦ **2** The most commonly employed primary carbon-11 precursors $[^{11}C]CO_{2(g)}$ and $[^{11}C]CH_{4(g)}$ and also one of the primary fluorine-18 precursors, $[^{18}F]F_{2(g)}$, are gaseous. Thus, for the transformation into secondary precursor molecules for instance $[^{11}C]CH_3I_{(g)}$, or $[^{18}F]XeF_{2(g)}$ online-operations in hot-boxes are mandatory.

♦ **3** The starting amounts for educts in radiosyntheses are "*low*" in comparison to classical organic reactions. The precursor wheight ranges always in [mg] units for applied PET chemistry. No-carrier-added (n.c.a.) products usually are administred in only a few nanogram [ng] amounts.

♦ **4** Time (overall synthesis reaction (time)) is absolutley crucial in PET chemistry due to the short physical half life of the employed positron emitters. Thus, chemical operation processes like radiosynthesis, the high performance liquid chromatography (HPLC) purification and formulation must be done as quickly as possible [36]. Regarding to time duration of each radiosynthesis step **(i-vi)** the

following estimated and approximative time values in minutes for carbon-11 chemistry are enlisted in *"brackets"* :

	(i) The radionuclide production via cyclotron ***(~10-50min)***
	(ii) Preparation set-up of the automated controlled synthesizer modul ***(~60-120min)***
T I M E	**(iii)** Radiosynthesis ***(~10-40min*)***
	(iv) Formulation of radiotracer and documentation ***(~10min)***
	(v) Quality control processes including HPLC and GC methods, furthermore checking of pH and osmolality ***(~10min)***
	(vi) Permission for intravenous administration into patient by physician

*The time duration for the radiosynthesis should not overun more than two physical half lives thus for carbon-11 syntheses approximatley ~40 minutes and in the case for fluorine-18 syntheses approximatley ~200 minutes [36].

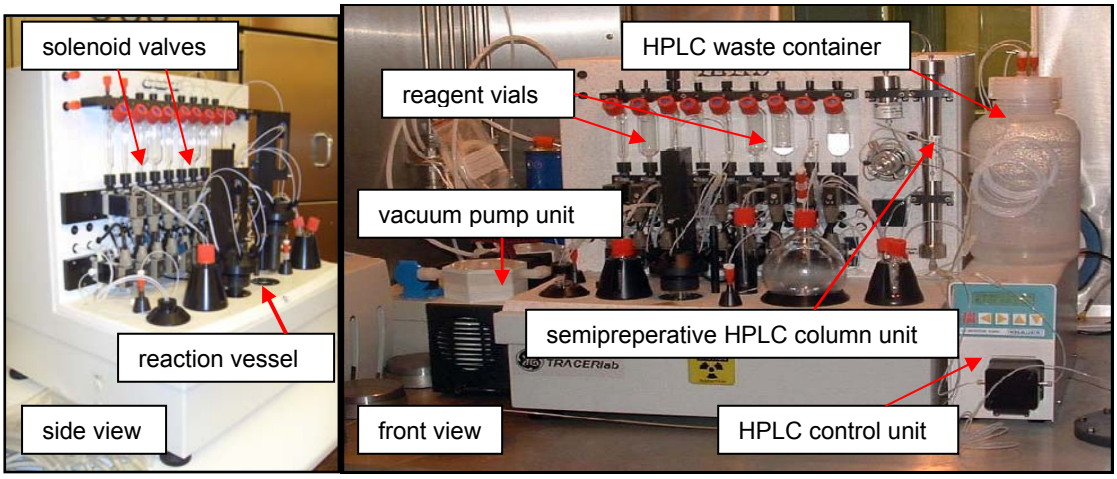

Figure 44. shows a state of the art commercially available synthesizer modul ([^{18}F]-Nucleophilic substitution module Nr.14322 from Nuclear Interface® (Münster, Germany) now GE (= General Electric®,Schenectady, U.S.A) concepted for nucleophlic substitution reaction with [^{18}F]F^{-} for radiosyntheses [35] see more detailed information on page 170).

General development considerations of new PET radiopharmaceuticals:

For the development of a new PET-tracer the following aspects have to be considered:

♦ **1** The choice of labelling position of employed positron emitter (multiple position possible within the compound)

♦ **2** The stereochemistry aspects

♦ **3** The specific radioactivity requirement *

♦ **4** The choice of cyclotron generated primary precursor and related online produced secondary precursors

♦ **5** The choice of inactive precursor which has to be radiolabelled (e.g. free acid/base or the corresponding salt compound) and also the choice of reaction solvents (e.g. lipophilic/hydrophilic media) resulting in the selection of purification conditions (e.g. preperative HPLC column type)

♦ **6** The choice of solvent composition for final formulation (obtaining the desired physiological pH of ~7.4 and physiological osmolality range of ~250-300 osm/kg)

♦ **7** The clinical outcome for nuclear medicine issues of the performed PET study

* The specific activity is an important issue for the preparation of radionuclides. It is important in several applications and particulary of importance in PET where the positron emitter is in incorporated into a molecule that is used to probe some physiological processes in which very small amounts of the molecule are being used. To repeat it once more, PET is basically a tracer method and the goal is to probe the process without perturbing physiology. If the amount of labelled molecules is very small in comparison to the amount of native compound or its competitor then the perturbation will be neglectable. When performing such studies with focus on probing the number of receptors or the concentration of an enzyme these considerations become a main issue [37]. The common way to express the concept of specific activity is in terms of the amount of radioactivity per mole of compound, for example in GBq/µmol or in MBq/nmol.

Specific activity for	Theoretically calculated	Practically measured
Carbon-11	3.4×10^5 GBq/µmol	50 GBq/µmol
Fluorine-1	6.3×10^4 GBq/µmol	500 GBq/µmol

Table 4 illustrates the specific activity values for carbon-11 and fluorine-18 (values taken from [38])

1.3.1. Carbon-11 radiochemical considerations

The targetry for carbon-11 precursor production of $[^{11}C]CO_{2(g)}$ and $[^{11}C]CH_{4(g)}$ is commercially available and can be performed on a daily routine basis.

The short physical half life of 20.3min allows repeated PET studies in the same subject on the same day with different carbon-11radiotracers (so called multitracer studies). Furthermore the effect of multiple labelling positions on the metabolism and uptake of the carbon-11 tracer can be investigated resulting in optimization of target specificity and background minimization.

Nowadays, a wide variety of available carbon-11 labelled radiopharmaceuticals have been developed for the application in biomedical and pharmacological PET studies with the increasing interest in investigations of receptor ligand interactions. Hence, it has become mandatory for radioligands to be prepared with high specific radioactivity.

$[^{11}C]$ PET-tracers	Selected biological targets	Selected references
♦ $[^{11}C]$ Methionine	Brain tumor imaging [39]	[40-43]
♦ $[^{11}C]$ Acetate	Prostate cancer imaging [44]	[45-48]
♦ $[^{11}C]$ DASB	SERT imaging	[49-52]
♦ $[^{11}C]$ WAY 100635	$5\text{-}HT_{1A}R$ imaging	[53-55]
♦ $[^{11}C]$ Flumazenil	$GABA_AR$ + BZR imaging	[56-59]

SERT .. Serotonin transporter

$5\text{-}HT_{1A}R$ .. 5-Hydroxytryptamin (= serotonin) subtype Receptor $_{1A}$

$GABA_AR$.. Gamma butyric acid subtype Receptor $_A$

BZR.. Benzodiazepine Receptor

Table 5 shows selected synthesized carbon-11 PET labelled tracers of the PET centre of the Vienna General Hospital

Generally, the starting primary precursor for radiosyntheses with carbon-11 is $[^{11}C]CO_{2(g)}$. For some radiosyntheses, $[^{11}C]CH_{4(g)}$ is prepared in target as well. However, for a majority of carbon-11 labelling radiosyntheses the secondary precursor $[^{11}C]CH_3I_{(g)}$ is the most important one for the attachment of a $[^{11}C]CH_3$ label into the target compound.

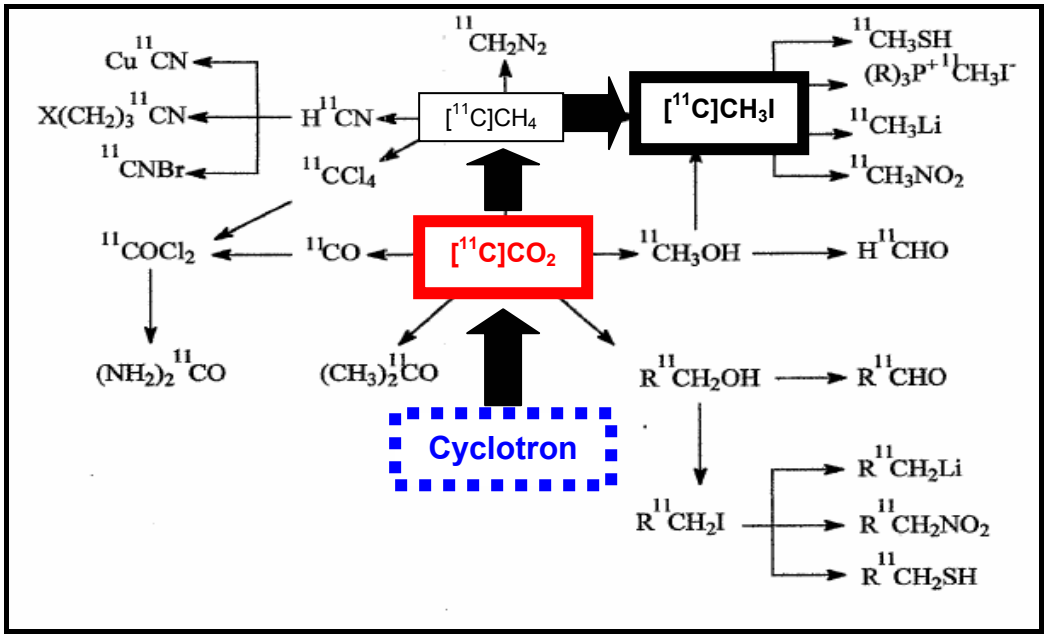

Figure 47 illustrates the complexeous precursor carbon-11 chemistry and the main generation pathway from $[^{11}C]CO_{2(g)}$ to $[^{11}C]CH_3I_{(g)}$ [60].

Carbon-11 is most commonly produced in the target using the before described $^{14}N(p,\alpha)^{11}C$ nuclear reaction [61]. The target is usually a N_2 gas target with a trace of oxygen to convert carbon-11 directly into $[^{11}C]CO_{2(g)}$. Almost all syntheses involving carbon-11 start with $[^{11}C]CO_{2(g)}$ as the primary product [24,61].

$[^{11}C]CO_{2(g)}$, originating from the target, can be easily and quickly processed into $[^{11}C]CH_3I_{(g)}$ by simple reduction and iodination. The reduction is accomplished either by lithium alumimium hydride ($LiAlH_4$) which leads to $[^{11}C]CH_3OH$ or with hydrogen which leads to $[^{11}C]CH_{4(g)}$. $[^{11}C]CH_3I_{(g)}$ can be synthesized "*online*" from both these precursors and there are commercial devices to carry out these syntheses. Starting

from $[^{11}C]CH_3OH$, hydrogen iodide (HI) is added resulting in the production of $[^{11}C]CH_3I_{(g)}$. Starting from $[^{11}C]CH_{4(g)}$ the gas is passed through a heated tube containing gaseous iodine and the "*in situ*" generated $[^{11}C]CH_3I_{(g)}$. is extracted in a recirculating system [62].

The above illustrated pathways demonstrate the wide variety of secondary precursor molecules, which can be synthesized from the labelled primary precursor $[^{11}C]CO_{2(g)}$.

For the desired generation of secondary precursors "*online*" synthetic manipulations cyclotron bombardment are necessary. Nowadays the N, O, S or C- alkylation with $[^{11}C]CH_3I_{(g)}$ is the most widely employed method for incorporating carbon-11 into organic molecules [63].

Moreover, concerning the $[^{11}C]CH_3I_{(g)}$ production via $[^{11}C]CH_{4(g)}$ approach there are several advantages in comparison to the $[^{11}C]CO_{2(g)}$ approach [62].

♦ **1** Higher specific activity value due to reason that the enviromental air does not contain as much inactive $[^{12}C]CH_{4(g)}$ as inactive $[^{12}C]CO_{2(g)}$

♦ **2** Aggressive chemicals like $LiAlH_4$ and HI are not employed for the $[^{11}C]CH_3I_{(g)}$ generation via the $[^{11}C]CH_{4(g)}$ approach

♦ **3** The "*online*" automation of the $[^{11}C]CH_{4(g)}$ approach is more straight forward (one conversion step less)

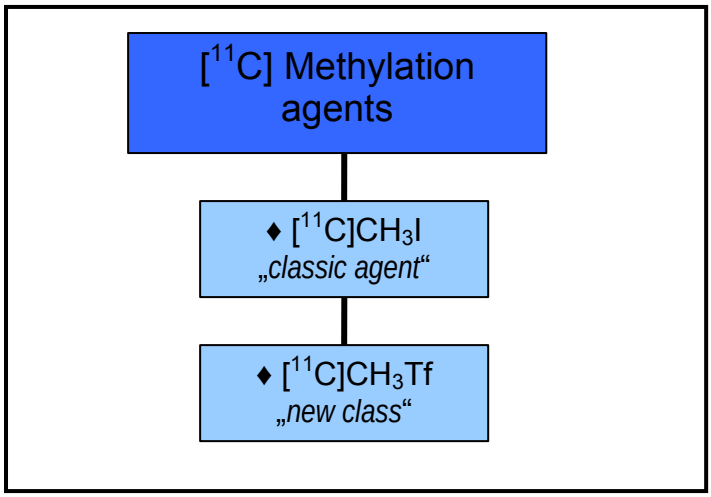

As shown in above organigram, Jewett et al developed a “new class of methylation agent” the highly reactive and convenient [^{11}C]methylation agent [^{11}C]$CH_3Tf_{(g)}$ ([^{11}C]methyltriflate) [64]. [^{11}C]$CH_3Tf_{(g)}$ as a [^{11}C]methylation agent has following striking advantages in comparison to [^{11}C]$CH_3I_{(g)}$ for N, O, S or C-alkylation reactions:

♦ **1** Higher radiochemical yield values

♦ **2** Shorter synthesis time

♦ **3** Higher specific activity values

♦ **4** Lower used precursor amounts

♦ **5** Simplification of an*“online”* automation

♦ **6** Reduction of radioactive waste

1.3.1.1. Carbon-11 labelling methods

On the next page several selected carbon-11 labelling strategies are summarized in following organigram with the intention to give an idea of the complexeous precursor carbon-11 chemistry for the interested reader.

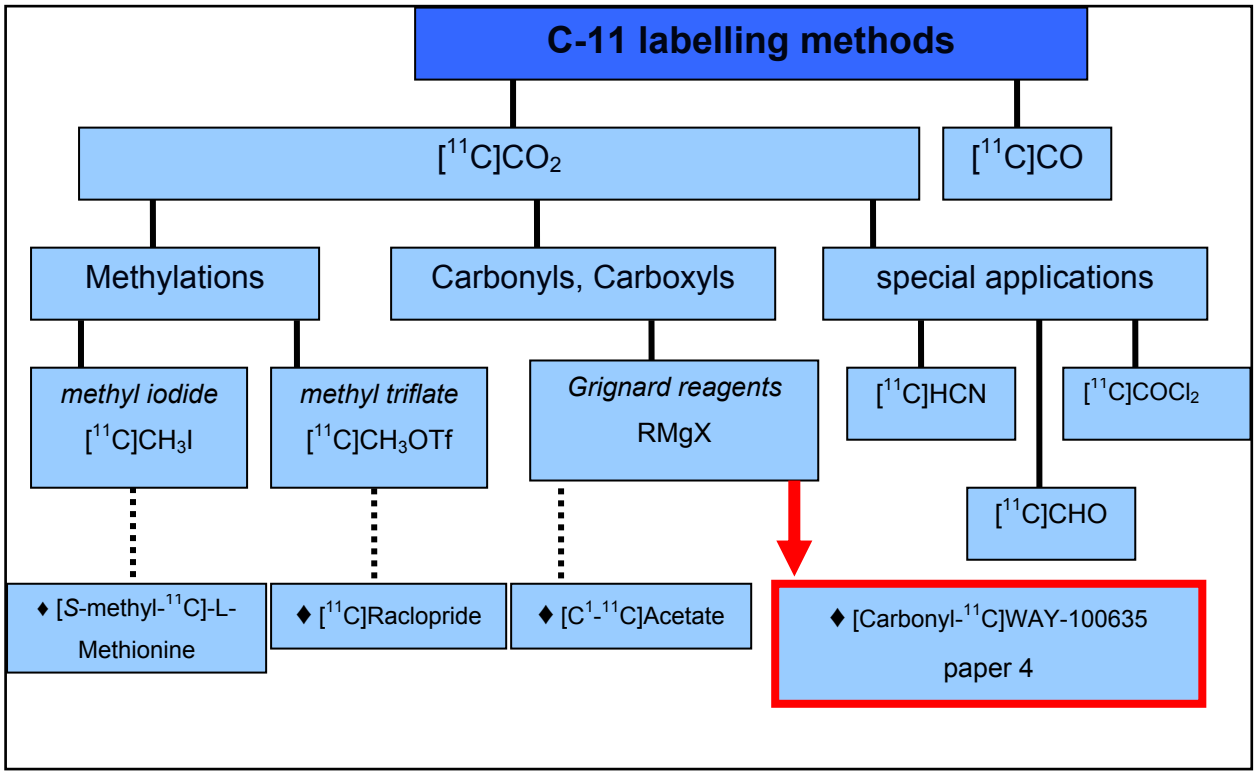

Nuclear reactions for the carbon-11 production

For the carbon-11 production several nuclear reactions are known, two selected approaches are introduced.

	Approach 1	Approach 2
Nuclear reaction	**$^{14}N(p,\alpha)\,^{11}C$ ***	$^{11}B\ (p,n)\ ^{11}C$**
Target	**$N_{2\,(g)}$**	Enrich.^{10}B + Al powder $_{(s)}$
Projectil energy range [MeV]	**13→3MeV**	10→0MeV
Main product form	**$[^{11}C]CO_{2(g)}$**	$[^{11}C]$ in $[^{10}B]$+Al matrix$_{(s)}$ ***
Expected yield [MBq/µAh]	**~3820**	~3400

g..gaseous

s..solid

enrich. ..enriched

*[65] **[66] *** generated carbon-11 must be extracted from the [^{10}B]+Al target matrix through chemical extraction or combustion methods of the matrix

Table 6. shows two selected nuclear reaction for carbon-11 production, whereas the approach 1, the $^{14}N(p,\alpha)\,^{11}C$ nuclear reaction, is most commonly used.

Carbon-11 target containment

Metal materials are the choice for target body construction like Al (aluminium) [65]. Stainless steel foils are suitable for target windows. The target should be made in a conical form with respect to beam profile and penetration, in order to achieve high specific radioactivity and fast emptying properties.

Target hardware

The target gas for carbon-11 production should be of high purity and especially as free from carbon containing impurities as possible. Great care must be taken to prevent any contamination of the target by trap contents. Furthermore, to restrict the entry of inactive $[^{12}C]CO_{2(g)}$ it is preferred to employ polymers as material for tubings between the gas supply and target.

$[^{11}C]CO_2$ recovery methods

The generated $[^{11}C]CO_{2(g)}$ has to be led from the cyclotron target to the hot-box/cell. To maintain high specific activity the $[^{11}C]CO_{2(g)}$ should be recovered from the target as quickly as possible (time range of 1-3min). There are two established methods which are employed for $[^{11}C]CO_{2(g)}$ seperation.

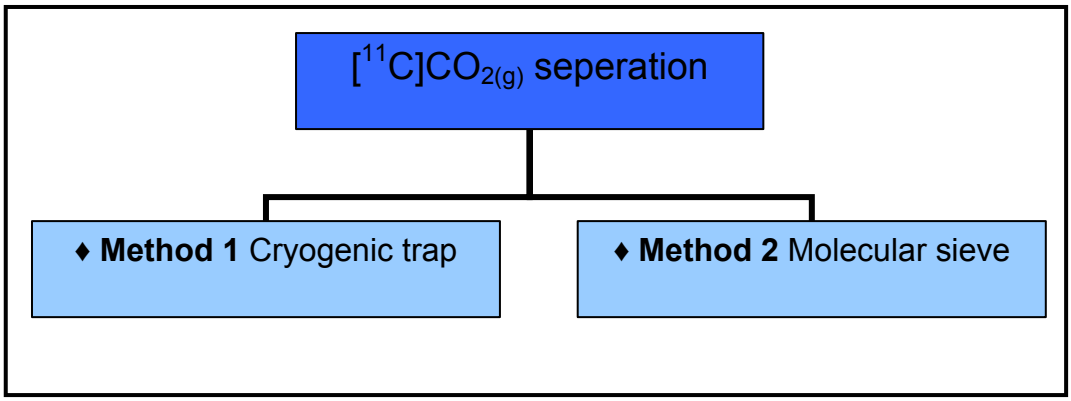

♦ **Method 1 The cryogenic trap**

[^{11}C]$CO_{2(g)}$ is trapped in a stainless steel tube immersed in cooling liquids such as liquid nitrogen (boiling point -196°C) or liquid argon (boiling point -186°C). The desired temperature is maintained by using a temperature controller. The [^{11}C]$CO_{2(g)}$ is recovered simply by passing a slow stream of inert sweep gas for instance helium through the trap while it is warmed up 0°C or room temperature. The trapping efficieny are almost quantitiative and also the recovery performance [>98%] both referring to the end of bombardment (EOB) [60].

♦ **Method 2 The molecular sieve trap**

Using this method, the generated [^{11}C]$CO_{2(g)}$ is collected in a pre-activated molecular sieve column. Column pre-activation is performed by heating up to 400°C under vacuum followed by cooling in a flow of inert gas like nitrogen down to 100°C. Entrapment yield of [^{11}C]$CO_{2(g)}$ is almost quantitative [>98%] and the trapped [^{11}C]CO_2 is recovered in an inert sweep gas like nitrogen by trap heating up to >200°C. The recovery ratio of [^{11}C]CO_2 is about 90% referring to the end of bombardment (EOB) [60].

1.3.2. Fluorine-18 radiochemical considerations

As just discussed before the fluorine-18 labelling strategies, respectively its radiosyntheses are not so *"straight forward"* as compared with the positron emitter carbon-11, which is an element of life [20]. The carbon-fluorine bond forms strong covalent values and can be incorporated into a variety of organic molecules Fluorine-18 can be substituted for a hydroxy group *(as in the case for the most prominent molecule in PET 2-deoxy-2-[^{18}F]fluoro-D-glucose ([^{18}F]FDG))* or can be

substituted for a hydrogen atom. The van der Waals radius of a fluorine atom has a value of 1.47Å (= 1 Ångstrom = 10^{-9}m = 1nm) and is similar to that of a hydrogen atom with 1.20Å and oxygen 1.52 Å and thus substitution of fluorine for hydrogen and oxygen causes "*minimal*" steric alteration of the modified molecule [156]. However, the major concern of substitution with fluorine-18 for hydrogen is the high electronegative (= EN) fluorine with EN 3.980 in comparison with hydrogen with EN 2.200 which can alter the electron distribution in a way that can alter the binding poperties of the new substituted molecule. Furthermore, the fluorine-18 label incorporation can influence parameters such as the pKa value, dipole moments and thus overall the molecule reactivity, the stability of chemical functions neighbouring to the incorporated F-18 label and the lipophilicity (facilitating hydrophobic interactions with specific binding sites). Nonetheless, fluorine-18 is an attractive positron emitter nuclide for the use in PET chemistry, especially due to its convenient physical half-life [12,38,67,68]. Following characteristics underline this attractiveness of fluorine-18 label in comparison to carbon-11 labelled radiopharmaceuticals. Firstly, the *"low"* positron energy in comparison to C-11, which decays from the fluorine-18 emitter, thus F-18 gives the higher spatial resolution [26].

Nuclide	Max. energy	Mean energy	Max. range in water
C-11	0.960 MeV	0.386 MeV	4.1 mm
F-18	0.690 MeV	**0.250 MeV**	**2.4 mm**

Table 3. shows the dependency of positron energy and positron travel range of carbon-11 and fluorine-18 (given values are taken from [20] also on pages 24 and 33)

Secondly, the higher achievable specific activity property of F-18 radiopharmaceuticals (via the enriched oxygen-18 $H_2{}^{16}O$ target approach compared to C-11 labelled radiotracers. Especially, for high affinity receptor PET studies, high specific radioactivity ratios of the synthesized radiopharmaceuticals are prerequisites.

Specific activity	Theoretically calculated	Practically measured
C-11	3.4×10^5 GBq/µmol	50 GBq/µmol
F-18	**6.3×10^4 GBq/µmol**	**500 GBq/µmol**

Table 4. shows the superior theoretical and practical specific activity values of fluorine-18 compared to carbon-11 [38].

Moreover, the physical half life of fluorine-18 of approximatley 109.3 minutes allows complex radiochemical radiosyntheses and “long time consuming” PET scanning procedures in comparison to carbon-11 labelled PET tracers (with a physical half life of 20.4 minutes). Additionally, the incorporation of fluorine-18 into a radiopharmaceutical allows the modulation of electronic, lipophilic and steric parameters all of which can critically influence both the pharmacodynamic and pharmacokinetic drug properties like drug receptor interactions and aiding translocation across lipid bilayers or absorption.

[^{18}F] radiotracer	Selected biological target	Selected References
♦ [^{18}F]FETO	11ß-Hydroxylase	[69-72]
♦ [^{18}F]FDG	glucose metabolism/ utilization	[73-75]
♦ [^{18}F]FE@CIT	DAT	[76-78]
♦ [^{18}F]FE@CFN	μOR	[79-81]
♦ [^{18}F]FE@SUPPY	A3AR	[82-85]
[^{18}F]FFMZ	$GABA_AR$	[86-89]

DAT.. Dopamine Transporter

μOR.. Opioid receptor subtype mu

A3AR.. Adenosine receptor subtype 3

$GABA_AR$.. Gamma butyric acid receptor subtype $_A$

Table 7. illustrates selected available fluorine-18 labelled tracers of the PET centre of the Vienna General Hospital:

Two selected nuclear reactions for the fluorine-18 production

There are existing more than twenty discovered nuclear reaction yielding fluorine-18 for the interested reader the review article of Qaim S is recommended [90]. However, there are two common pathways to introduce which have been worldwidely established and are described in Table 8 on the page 48 comparing their production data characteristics. The approach 1 is the $^{18}O(p,n)^{18}F$ nuclear reaction on an oxygen-18 enriched water (= $H_2{}^{16}O$) target yielding in [^{18}F]$F^-_{(aq)}$. This obtained F-18 labelling agent form has to be specially “activated” prior to its employment This introduced approach 1 of the oxygen-18 enriched water target is the most effective and thus, nowadays the most widely employed in hospital PET centres due to reason of its obtainable high specific activity values, its easy and convenient handling.

The approach 2 is the $^{20}Ne(d,\alpha)^{18}F$ nuclear reaction carried out in a neon gas target wit carrier addition (c.a.) of $[^{19}F]F_{2(g)}$. therefore only *"low"* achievable specific radioactivities can be obtained. Moreover, the hazardous nature of $[^{19}F]F_{2(g)}$ makes it difficult to handle in a hospital enviroment [91].This generated fluorine-18 labelling agent $[^{18}F]F_{2\ (g)}$ can be used in the synthesis directly without any *"pre-activation"* procedures which may be an advantage compared to approach 1 concerning overall radiosyntheses time saving effects [92].

	Approach 1	Approach 2
Nuclear reaction	**$^{18}O(p,n)^{18}F$**	$^{20}Ne(d,\alpha)^{18}F$
Target	**Enr. $H_2{}^{18}O_{(aq)}$**	$Ne_{(g)}$*
Projectil energy range [MeV]	**16→3**	14→0
Main product form	**$[^{18}F]F^-_{(aq)}$**	$[^{18}F]F_{2(g)}$
Expected yield [GBq/µAh]	**~2.22**	~0.40
Specific activity [MBq/µmol]	**~6.10^5**	~100

aq..aqueous

g..gaseous

Enr.. enriched

* Carrier addition (c.a.) of inactive elemental $[^{19}F]F_{2(g)}$ to target neon gas is a prerequisite. In pure neon, nucleogenic fluorine-18 diffuses to the target wall and is chemically adsorbed, when a low proportion of carrier fluorine-19 [~ in µmol range] is present exchange of nucleogenic fluorine-18 can compete with surface adsorption and recovery of most of the generated radioactivity from the target becomes then possible [93] Due to this carrier addition, high specific activities can not be achieved. Due to the necessity of carrier in the $[^{18}F]F_{2\ (g)}$ production and the fact that every $[^{18}F]F_{2\ (g)}$ molecule carries only one active $[^{18}F]$ atom, the theoretical achievable maximum specific activity in subsequent electrophilic fluorine-18 reaction is limited always to 50%.

Production of c.a. [^{18}F]F_2 by the ^{20}Ne(d,α)^{18}F nuclear reaction

Target hardware

Target bodies of approach 2 should be constructed of pure metal material. Usually, the target is made of Nickel (= Ni) [93,95]. The window foil is preferably made of Aluminium (= Al). The cooling of the window foil is normally performed with an inert gas like Helium (= He).

Target gas

The neon gas must be as pure as obtainable in order to recover the radioactivity mainly as elemental [^{18}F]$F_{2(g)}$ [90,91,96]. Thus, the used neon gas should be as free from nitrogen and carbon oxides as these incorporate substantial proportions of the fluorine-18 into inert substances, namely nitrogen[^{18}F]trifluoride and carbon[^{18}F]tetrafluoride. Contamination by fluorocarbons should also be avoided. Corrosion of target and auxillary components is not a significant problem if only dilute mixtures of [^{19}F]F_2 [< 2%] in neon is used. Given the highly hazardous nature of fluorine gas, it is emphasized that additional safety requirements have to be fulfilled.

Target operating conditions for the production of c.a. [^{18}F]F_2

The main factor that determines [^{18}F]$F_{2\ (g)}$ recovery is the chemical state of the target surface [91-92]. Passivation (= perfluorination) of the surface is necessary before bombardment to avoid a significant loss of fluorine-18 along with fluorine-19 carrier. Two passivation methods have been proposed firstly, thermal passivation and secondly the beam induced passivation. Thermal passivation requires the target to be heated after filling with dilute fluorine-19 gas (in neon). The beam-induced passivation is achieved by deuteron bombardment of the gas target.

Target operating conditions for the production of n.c.a. [^{18}F]F^{-}

The proton irradiation of [^{18}O] enriched water is the most effective method for the production of n.c.a. [^{18}F]F$^{-}_{(aq)}$.

The primary consideration in design was to consume as little of the costly [^{18}O] enriched water as possible during production. The requirement for small target volume in turn means that target thickness has to be selected carefully for effective use of the beam. Effective target cooling of the front of the entrance window with helium and the back side with water is mandatory. The decision to operate a low pressure or high pressure target is fundamental since it influences the target construction and the strategy for coping with the adverse effects of radiolysis and heat. In the low pressure mode of operation without taking appropriate precautions radiolysis and boiling can cause a significant loss of [^{18}O] enriched water and render the use of high beam currents impractical for high yields. Requirements for effective venting or the catalytic recombination of radiolytically generated oxygen and hydrogen must therefore be considered [92,93]. On the other hand, for high pressure targets considerations have to be made regarding the ratio between irradiated target water volume and the amount of water available for recirculation on the *"overhead space"* inside of the target water cavity, additionally the density reduction effects as a consequence of elevated temperature operation due to high pressure levels have to be considered.

The most efficient water target is simply composed of a cavity for the target water bounded by two rigid metal foils which the rear foil being efficiently cooled by a suitable fluid e.g. water. Target volume range is usually up to 2.5ml of oxygen-18 enriched water $H_2{}^{16}O$. Other parameters of importance are the type of target seals,

the chemical nature of the metallic insert and foils, the type of transfer tubing and the facility for recovery of the oxygen-18 enriched water $H_2{}^{16}O$ [94].

Target hardware

Pure metal material is the optimal choice for target body construction, e.g. Copper (= Cu) or Silver (= Ag) [97]. Refrigarated Helium (= He) and deionized water are used for cooling down the window foil and the target containment.

Target water

The purity of the oxygen-18 enriched water used in target is of major concern. Organic impurities must be absent as these can prevent recombination of radiolytically generated oxygen and hydrogen atoms causing target burst. In order to eleminate traces of organic solvents purification can be achieved using reflux methods. the yielded purity of the oxygen-18 enriched water can be assesed by gas chromatography (GC). Furthermore, undesired metal cation contaminants coming from the window foil material can be also detected thus decreasing the reactivity of $[^{18}F]F^-_{(aq)}$ [98]. The elimination of such undesired metal cations can be performed by the employment of an ion exchange resin column [99]. which also enables the recovery of enriched oxygen-18 water $H_2{}^{16}O$ [100].

$[^{18}F]F^-$ and $[^{18}F]F_2$ recovery methods

There are two seperation methods for fluorine-18 recovery

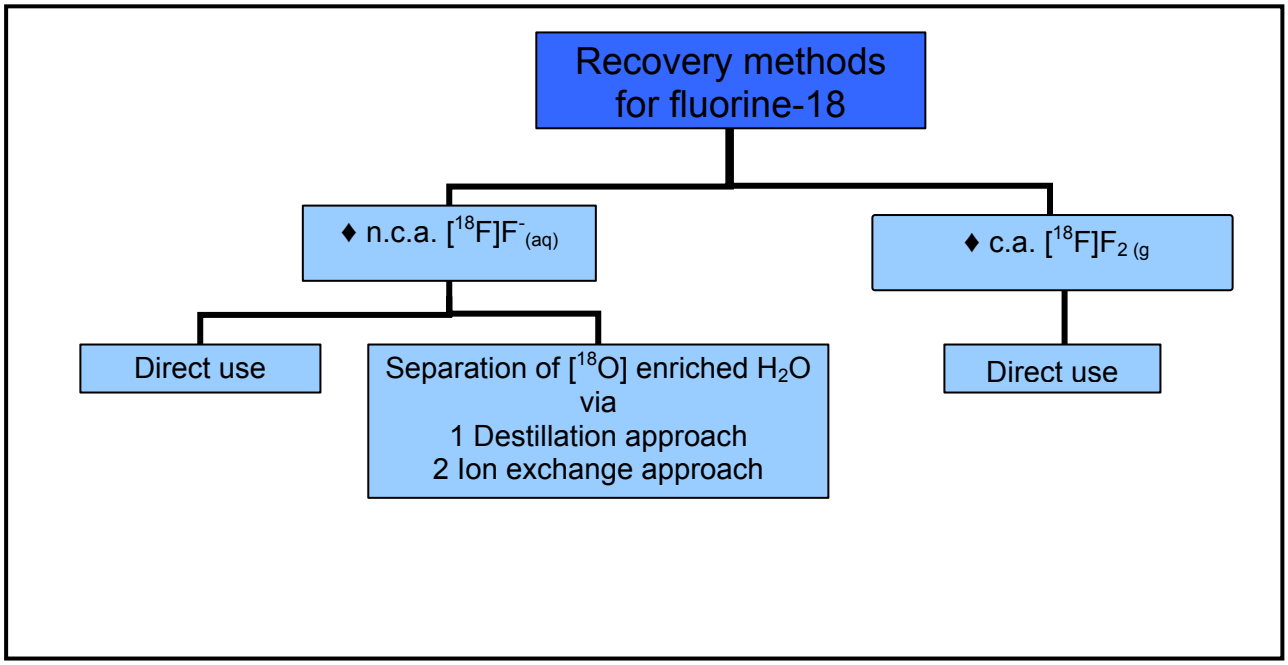

c.a..carrier added (= addition of inactive $[^{19}F]F_{2\,(g)}$)

n.c.a..non carrier added

Figure 49. shows the two methods for fluorine-18 recovery.from an $[^{18}O]$ enriched water target and ^{20}Ne gas target. For the $[^{20}Ne]$ gas target the fluorine-18 is recovered as elemental $[^{18}F]F_{2(g)}$. It is removed by target filling with carrier addition (c.a.) of inactive $[^{19}F]F_2$ in an inert carrier gas such as for example Argon (= Ar) [101]. The resulting mixture of $[^{18}F]F_{2(g)}$ in Argon can be used in following radiosynthesis directly.

In the case of the $[^{18}O]$ enriched water target the fluorine-18 activity is removed in the aqueous phase. The enriched $[^{18}O]$ water containing $[^{18}F]$fluoride ion can be directly used in the radiosynthesis (this method can be employed for small volume water targets and if the cost of losing the $[^{18}O]$ water is minor compared to the cost of the cyclotron run). As shown in above organigram there is also a possibility for seperation of $[^{18}F]F^-_{(aq)}$ from the $[^{18}O]$ enriched water either by distillation or by using a resin column [102-103]

With the knowledge of these generation pathways the next issue is the introduction of fluorine-18 into the desired compounds requiring for carbon-fluorine bonds formation. The labelling agent $[^{18}F]F^-_{(aq)}$ is employed for all nucleophilc substitution

reactions (S^N) and the generated $[^{18}F]F_{2(g)}$ enables the electrophilc substitution mechanism (S^E) or, electrophilic addition mechanism (A^E)

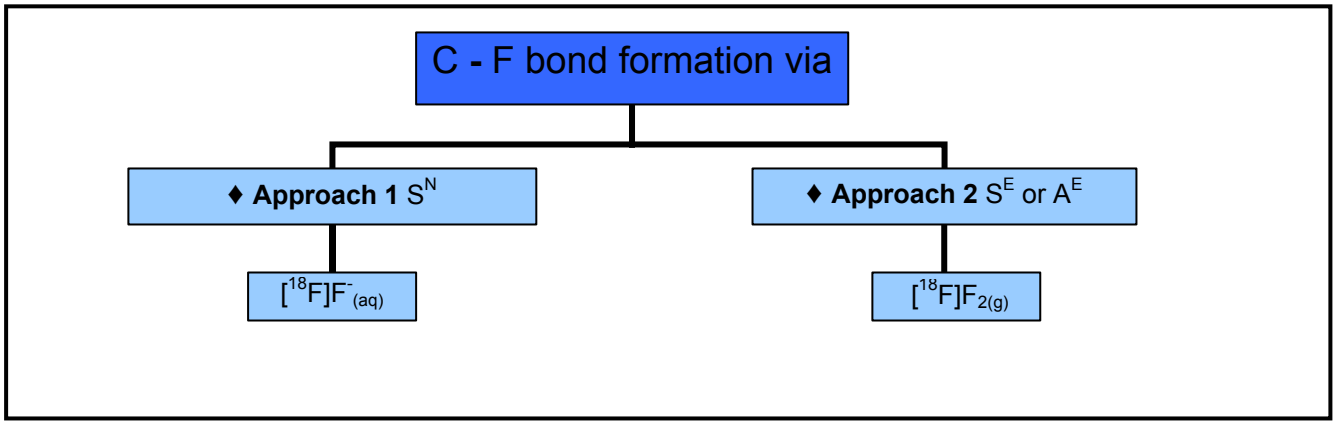

aq..aqueous

g..gaseous

Figure 50 shows the two possible approaches for the C-F bond formation and their relating labelling agent

1.3.2.1. Fluorine-18 labelling methods

There are two main labelling methods for fluorine-18 which are depicted in following organigram.

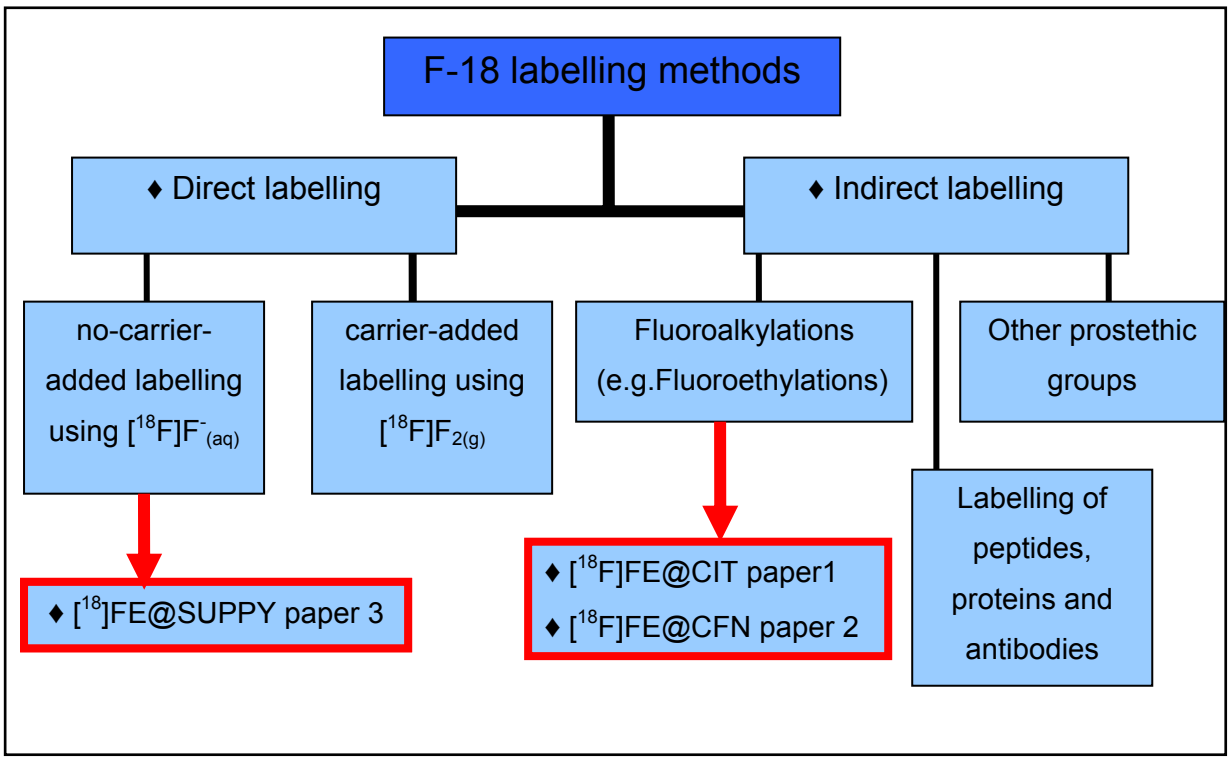

Figure 51. gives an overview of fluorine-18 labelling techniques.

For fluorine-18 labelling - perhaps more than for any other radionuclide- labelling yields depend on factors that are determined by radionuclide production (regarding the electrophilic or the nucleophilic approach).

Nucleophilic reactions (S^N)

For nucleophilic fluorination, the F-18 labelled fluoride ion is almost always obtained as an aqueous solution. $[^{18}F]F^-_{(aq)}$ is unreactive due to the high charge density of the fluoride anion. It is strongly hydrated and thus inactivated for nucleophilic substitution reactions. Therefore, $[^{18}F]F^-_{(aq)}$ requires some simple but very important

manipulations to become a reactive nucleophilic reagent. Thus, methods for the preparation of reactive fluoride ion in organic solvents suitable for radiochemical syntheses have been evaluated. The steps in preparing reactive fluoride are crucial to the success of the labelling reactions and its worthwhile to examine the methods commonly being used. In any aqueous solution, $[^{18}F]F^-$ anion must be accompanied by a positively charged counter ion (such as metal ions). As $[^{18}F]F^-_{(aq)}$ is removed from the water target, there are metal ions present within which were rinsed off the wall surface of the target containment during irradiation [104]. However, such metal counterpart ions of target material like for example Silver (= Ag) generally decrease the reactivity of $[^{18}F]F^-_{(aq)}$ Therefore, employment of an anion exchange resin column for $[^{18}O]$ water seperation is also advantageous for the removal of such metal impurities [99-100].

For labelling by nucleophilic substitutions, $[^{18}F]F^-_{(aq)}$ is required to be essentially free of water. In general, the strategy for generating reactive $[^{18}F]F^-_{(aq)}$ involves the use of phase transfer agents (e.g. cryptand) that incorporate suitable positively charged counter-ion addition $[^{18}F]F^-_{(aq)}$ with a large counter-ion, phase transfer agent (so called cryptand) and addition of a base in a polar aprotic solvent. Where required traces of water (or other solvent) are removed by azeotropic distillation.

First point $[^{18}F]F^-_{(aq)}$ reactivity can be enhanced by the addition of selected cationic counter ion prior to the evaporation of the water. Three types of counter ions have been used: (1) large metal ions such as rubidium or cesium, (2) potassium complexed by a cryptand such as the aminopolyether Kryptofix® 2.2.2 (4,7,13,16,21,24-hexaoxa-1,10-diazabicyclo[8.8.8]hexacosane) [99,100] or another approach is the use of tetrabutylammonium salts [71,105]. The addition of a cation also involves the inclusion of another anion coming from base addition to the reaction mixture. Anions such as $[OH]^-$ or $[CO_3]^{2-}$ are often employed which do not

effectively compete with the $[^{18}F]F^-$ anion in nucleophilic displacement reactions. Carbonate is usually the anion of choice since it is less likely to cause base catalysed side reactions. Moreover, since $[^{18}F]F^-_{(aq)}$ has in dipolar aprotic solvents also a strong basic character, and generally the resulting reaction medium is basic (due to addition of $[CO_3]^{2-}$ or $[OH]^-$ anions), elimination reactions can compete with the nucleophilic substitution S^N. The Vienna General Hospital uses a K_2CO_3-Kryptofix® 2.2.2 system for $[^{18}F]F^-_{(aq)}$ activation by azeotropic distillation with acetonitrile as apolar and aprotic organic solvent. The activated $[^{18}F]F^-_{(aq)}$ is afterwards resolubilised in the solvent containing the substrate (precursor) for nucleophilic attack (labelling). The resolubilisation efficiency is affected by the material and dimension of the reaction vessel, solvents and other factors such as metal ion contamination [106].

The substitution of $[^{18}F]F^-_{(aq)}{}^-$ against various leaving groups is an excellent method for the synthesis of aliphatic carbon-fluorine bonds [107]. The choice of leaving group will depend on the radiochemical yield, stability of the precursors, ease of subsequent separation of the $[^{18}F]$ fluorinated product from precursors, reagents and solvents and the formation of potential side products. Trifluoromethanesulfonate esters commonly so called *"triflates"* (= Tf) are particularly reactive and provide excellent yields in nucleophilic $[^{18}F]$fluorination reactions such as in the radiosynthesis of 2-deoxy-2-$[^{18}F]$fluoro-D-glucose (= $[^{18}F]$FDG). Halogens are good leaving groups for aliphatic nucleophilic displacements. The exact reaction conditions in terms of solvents and temperatures are variable and must be optimized for each particular reaction. Other groups such as cyclic sulfates, halogenides, mesylates and tosylates are also used as leaving groups although they tend to give somewhat lower yields than triflates.

Fluorine-substituted aromatic rings are common in many types of biologically active organic molecules. As mentioned before, fluorine is similar in size to the hydrogen atom and thus does not employ serious steric effects. But its high electronegativity (= EN) is likely to significantly alter the electronic characteristics of the aryl ring system. The generally good metabolic stability of the resulting [^{18}F]-labelled aromatic compounds is a major advantage. Nucleophilic aromatic [^{18}F]-fluorination requires for activated aromatic molecules, electron withdrawing substituents in ortho- or para-position to the leaving group are indispensable. Particulary substituents with strong electron withdrawing properties such as $[NO_2]^-$, $[CN]^-$ and carbonyl groups are suitable for the activation [108-109]. Halogens, nitro and the trimethylammonium salts show increasing reactivity as leaving group.

Direct [^{18}F]-labelling methods

Depending on the procedure that is used for the production of fluorine-18 in the cyclotron, fluorine-18 is obtained in a particular chemical form i.e. as $[^{18}F]F_{2\,(g)}$ or as $[^{18}F]F^-_{(aq)}$ which determines the possible subsequent reaction (→ electrophilic or → nucleophilic substitution).

S^E reaction

C.a. $[^{18}F]F_{2(g)}$ is directly form the Neon gas target available for the electrophilic reactions, but only in low specific activity [110]. $[^{18}F]F_{2(g)}$ is not a selective fluorinating agent due to reason of its *"high reactivity"*, $[^{18}F]F_{2(g)}$ can be modified into somewhat less reactive and thus, more selective such as fluorine-18 acetylhypofluorite or fluorine-18 xenon difluoride [111-112]. These selective agents offer fluorine-18 labelling possibilities of electron rich compounds like alkenes which

can not be labelled via the nucleophilic approach. To repeat again, the main disadvantage of $[^{18}F]F_{2(g)}$ is its low obtainable specific radioactivity value. Concluding, the electrophilic $[^{18}F]$-labelling routes are only useful for radiopharmaceuticals where a high specific activity value is not a requirement like for 6-$[^{18}F]$fluoro-L-DOPA [113]. As mentioned before the electrophilic $[^{18}F]F_{2(g)}$ agent has a low labelling selectivity due to its high reactivity and thus, undesired radical side reactions can occur. Extensive purification procedures have to be performed for fulfilling the requirements of high purity radiopharmaceuticals.

S^N reaction

To obtain $[^{18}F]$-labelled compounds based on n.c.a. $[^{18}F]F^-_{(aq)}$), which is directly available from the target without any carrier addition, the nucleophilic approach (S^N) is nowadays the most important practical route for the production of fluorine-18 labelled radiopharmaceuticals with possible highest specific activity. This is generally preferable but is a prerequisite for investigations of low concentration binding sites, as for example for imaging of neuronal receptors which have to be studied without perturbation of the physiological equilibrium. N.c.a. $[^{18}F]F^-$ is obtained in aqueous solution therefore; the labelling approach has to be performed under aprotic but polar conditions. For $[^{18}F]F^-_{(aq)}$ seperation and recovery anion exchange resins are employed and generally prior the labelling approach via nucleophilic substitution the water excess is subsequently removed by azeotropic distillation process with acetonitrile as the polar and aprotic solvent [103]. The direct nucleophilic ^{18}F-fluorination of aliphatic compounds in dipolar aprotic solvents proceeds according to an SN^2 mechanism. Halogens or sulphonic acid ester functions like mesylate, tosylate and triflate function can be used as leaving groups. Showing that triflate precursors give the best result [99,105]. The replacement of the

leaving group proceeds via a *"Walden inversion"* according to the stereospecific SN^2 mechanism. This is exemplified by the radiosynthesis of the most widely used PET-radiopharmaceutical [^{18}F]FDG [99,100].

[^{18}F]-fluorinated prosthetic groups

Here, a primary F-18 fluorine labelled functionalized compound is coupled with a second molecule. Important procedures via prosthetic groups are the [^{18}F]-fluoroalkylation [107] the [^{18}F]-fluoroacylation [114] and the [^{18}F]-fluoroamidation [115]. Applications of these [^{18}F]-labelling pathways via prosthetic groups are widespread and can be realized with almost every molecule carrying a protic function such as thiol, amino or hydroxyl function. This is exemplified by the fluoroalkylation of several biorelevant molecules like for example for receptor ligands of the dopaminergic system [76,110] the serotoninergic system [111] and benzodiazepine receptors (respectively, $GABA_A$ receptors) [86,87,118]. Many more tracers were synthesized using this route and especially [^{18}F]-fluoroethylation was the subject of recent improvements

Fluoroalkylations

Since many biologically active compounds contain alkylic side chains, e.g. methyl- and ethyl-groups, these structural units may be targets for the affixation of a radiolabel. In fact, many compounds have been labelled with a [^{11}C]methyl-group for PET. Thus, the development of [^{18}F]fluoroalkylated tracers was the logical consequence. A variety of different fluoroalkylating agents have been developed so far: [^{18}F]bromofluoromethane [123,124], [^{18}F]fluoroiodomethane [125] 2-[^{18}F]bromofluoroethane[126,127]], 2-[^{18}F]tosyloxyfluoroethane [107,128] 3-

[^{18}F]bromofluoropropane [129-140], 3-[^{18}F]fluoroiodopropane [140,141] and 3-[^{18}F]tosyloxyfluoropropane [133]. The thus labelled synthons are restricted to small alkyl-chains to avoid too large structural differences. The most important fluoroalkylated tracers, already introduced into clinical application, are [^{18}F]FET (*O*-(2-[^{18}F]Fluorethyl)-L-Tyrosin) [134] and [^{18}F]FP-CIT (2β-carbomethoxy-3β-(4-iodophenyl)-8-(3-[^{18}F]fluorpropyl)nortropan) [130,135,136].

Fluoroethylations

Fluoroethylations represent the most important class amongst the fluoroalkylations since (1) fluoroethylating agents can be easily produced from commercially available substances and (2) the fluoroethyl-group is sterically close to methyl- and ethyl-groups. Targets for fluoroethylations are amine [77,137-141], hydroxylic [134,142,143], mercapto [144,145] and carboxylic [146,70,71,76,86,87] moieties. 2-[^{18}F]Tosyloxyfluoroethane is widely used since it is easy to prepare, very stable and suitable for a variety of compounds [147]. On the other hand, it is (1) not as reactive as 2-[^{18}F]fluoroethyltriflate [148,149] (2) sensitive to some solvents and bases [148]; (3) not a selective agent [150] and (4) intricate to purify – a semi preparative HPLC is unavoidable. Hence, microwave enhanced conditions were proposed that increased the selectivity and the radiochemical yields [151].

2-[^{18}F]Bromofluoroethane can also be produced rapidly. Thus, a lot of effort was put into investigations to optimize yields and quality of this intermediate compound by addition of sodium iodide and application of solid phase extraction for purification [149,152,153].

References

For all quoted hyperlinks „hyperlink http:// references " which are taken from the "*world wide web",* the date of publishing are listed within the brackets.

[1] Gibson RE, Burns HD, Hamill TG, Eng W-S, Francis BE, Ryan C. 2000. Non-Invasive radiotracer imaging as a tool for drug development. Curr Pharm Des **6**: 973-89.

[2] Pither R. 2003. PET and the role of in vivo molecular imaging in personalized medicine. Exper Rev Mol Diagn **3**: 703-13.

[3] Fahey FH. 2001. Positron emission tomography instrumentation. Radiol Clin North Am **39**: 919-29.

[4] Jacobs AH, Li H, Winkeler A. 2003. PET-based molecular imaging in neuroscience. Eur J Nucl Med Mol Imaging **30**:1051-65.

[5] Schäfers KP. 2003. Imaging small animals with positron emissions tomography. Nuklearmedizin **42**: 86-9.

[6] Wang Y, Seide J, Tsui BM, Vaquero JJ, Pomper MG. 2006. Performance evaluation of the GE Healthcare eXplore VISTA dual ring small animal PET scanner J Nucl Med **47**: 1891-1900.

[7] The CT, X-ray,MRI and ultra sound image are adapted from continuing education lecture of postgraduate course radiopharmacy module III Leipzig held by Busse H. (Autumn 2006)

[8] The [^{18}F]FDG PET scan is adapted from continuing education lecture of postgraduate course radiopharmacy module II Zurich Maecke HR. (Fall 2006)

[9] The [^{99m}Tc]SPECT scan was taken from hyperlink http://www-nuk.med.uni-rostock.de/index.htm (14.11.2006)

[10] Cherry SR. 2006. Henry N. Wagner lecture: Of mice and men (and positrons)—Advances in PET imaging technology J Nucl Med **47**: 1735-45.

[11] http:// pet.rh.dk/Lis/Annual .pdf (14.11.2006)

[12] Lasne M-C, Perrio C, Rouden J, Barré L, Roeda D, Dolle F, Crouzel C. 2002. Chemistry of ß$^{+}$-emitting compounds based on fluorine-18 Top Curr Chem **222**: 201-58.

[13] Images are adapted from continuing education lecture of postgraduate course radiopharmacy module II Zurich held by Johanssen B. (Fall 2006)

[14] http:// www.imgc.cnr.it/AR2003/images/miniature/214.ht7.jpg Research nuclear reactor TRIGA MarkII of Pavia University. Cherenkov effect during the operation (10.10.2006)

[15] http://www.bnl.gov/bnlweb/photos/BMRR-cutaway-w.gif Brookhaven scheme (10.10.2006)

[16]http://www.medcyclopaedia.com/library/topics/volume_i/r/radionuclide_generator/radionuclide_generato_fig1.aspx?s=radionuclide+generator&mode=1&syn=&scope (10.10.2006)

[17] http://www.ganil.fr/operation/diaporamas/physicist/sld009.htm (23.09.2006)

[18] http://hyperphysics.phy-astr.gsu.edu/hbase/magnetic/cyclot.html (23.09.2006)

[19] http:// abe.web.psi.ch/accelerators/ringcyc.php (23.09.2006)

[20]http://nuclearmedicine.stanford.edu/education/grand_rounds/050125.pdf (24.04.2007)

[21] Dahl JR, Schlyer D. 1985. Proceedings of first workshop on Targetry and Target chemistry, Heidelberg, pp.: 31-43.

[22] Qaim SM, Blessing G, Stöcklin G. 1987. Routinely used cyclotrons targets for radioisotope production at KFA Jülich. Proceedings of second Workshop on Targetry and Target Chemistry. Heidelberg, pp.: 50-7.

[23] Votowa JR, Nicklesa RJ. 1989. Radionuclide production for positron emission tomography: Choosing an appropriate accelerator. Nuclear Instruments and Methods in Physics research Section B: Beam Interactions with Materials and Atoms **40**: 1093-9.

[24] http:// www.osti.gov/energycitations/product.biblio.jsp?osti_id=784251 Finn R, Schlyer D. Production considerations for the “classic” PET nuclides. (12.08.2006)

[25] http://education.jlab.org/glossary/betadecay.html (11.08.2006)

[26] Levin CS, Hoffman EJ. 1999. Calculation of positron range and its effect on the fundamental limit of positron emission tomography system spatial resolution. Phys Med Biol **44**: 781-99.

[27] http:// www.austin.unimelb.edu.au/ (09.07.2006)

[28]http://sol.sci.uop.edu/~jfalward/elementaryparticles/pairannihilation.JPG (25.02.2007)

[29]http://buffy.eecs.berkeley.edu/PHP/resabs/resabs.php?f_year=2004&f_submit=chapgrp&f_chapter=3 (25.02.2007)

[30] Zaidi H, Montandon ML. 2006. The new challenges of brain PET imaging technology. Curr Med Imaging Rev **2**: 3-13.

[31] Paans MJ, Van Waarde A, Elsinga PH, Willemsen ATM, Vaalburg W. 2002. Positron emission tomography: the conceptual idea using a multidisciplinary approach. Methods **27**: 195-207.

[32] http://www.nucmed.buffalo.edu/b (05.08.2006)

[34]http://www.comecer.com/web2005/content.php?id_lingua=2&id=60# (21.12.2006)

[35] Image is adapted from university lecture *Medizinische Radiochemie Teil* 1 held by Wadsak W. (in summer semester 2005/2006)

[36] Fowler JS, Wolf AP. 1996. Working against time: Rapid radiotracer synthesis and imaging the human brain. Acc. Chem Res. **30**: 181-8.

[37] Musachio JL, Flesher JE, Scheffel UA, Rauseo P, Hilton J, Mathews WB, Ravert HT, Dannals RF, Frost JJ. 2002. Radiosynthesis and mouse brain distribution studies of [11C] CP-126,998: a PET ligand for in vivo study of acetylcholinesterase. Nucl Med Biol **29**: 547-52.

[38] Coenen HH. 2005. Fluorine-18 labelling methods: Features and possibilities of basic reactions. Proceedings of the ESRF Workshop 62, Berlin December 5th

[39] Nakada K. 2004.The role of methionine PET in oncology. Int Congr Ser **1264**: 88-94

[40] Mitterhauser M, Wadsak W, Krcal A, Schmaljohann J, Eidherr H, Schmid A, Viernstein H, Dudczak R, Kletter K. 2005. New aspects on the preparation of [^{11}C]Methionine – a simple and fast online approach without preparative HPLC. J Appl Rad Isot **62**: 441-5.

[41] Becherer A, Karanikas G, Szabo M, Zettinig G, Asenbaum S, Marosi C, Henk C, Wunderbaldinger P, Czech T, Wadsak W, Kletter K. 2003. Brain tumour imaging with PET: a comparison between [^{18}F]fluorodopa and [^{11}C]methionine. Eur J Nucl Med Imaging **30**: 1561-7.

[42] Schmitz F, Plenevaux A, Del-Fiore G, Lemaire C, Comar D, Luxen A. 1995. Fast routine production of L-[11C-methyl]methionine with Al_2O_3KF. Appl Rad Isot **46**: 893-7.

[43] Pascali C, Bogni A,Iwata R, Decise D, Crippa F, Bombardieri E. 1999. High efficiency preparation of L-[S-methyl-11C]methionine by on-column [11C]methylation on C18 Sep-Pak. J Label Compd Radiopharm **42**: 715- 24.

[44] Dimitrakopoulou-Strauss A, Strauss LG. 2003. PET imaging of prostate cancer with [^{11}C]acetate. J Nucl Med **44**: 556-8.

[45] Mitterhauser M, Wadsak W, Krcal A, Schmaljohann J, Bartosch E, Eidherr H, Viernstein H, Kletter K. 2004. New aspects on the preparation of [^{11}C]acetate – a simple and fast approach via distillation. J Appl Rad Isot **61**: 1147-50.

[46] Roeda D, Dolle F, Crouzel C. 2002. An improvement of 11C acetate synthesis-non radioactive contaminants by irradiation- induced species emanating from 11C carbon dioxide product on target. Appl Radiat Isot **57**: 857-600.

[47] Kruijer PS, Linden TT, Mooij R, Visser FC, Herscheid JDM. 1995 A practical method for the preparation of [^{11}C]acetate. Appl Radiat Isot **46**: 317-21.

[48] Moerlein SM, Gaehle GG, Welch MJ. 2002 Robotic preparation of sodium C-11 acetate injection for use in clinical PET. Nucl Med Biol **29**: 613-21.

tomography in patients with acute myocardial infarction. Am J Cardiol **78**: 1230-5.

[49] Wilson AA, Ginovart N, Schmidt M, Meyer JH, Threlkeld PG, Houle S. 2000. Novel radiotracers for imaging the serotonin transporter by positron emission tomography: synthesis, radiosynthesis and in vitro and ex vivo evaluation of ^{11}C-labeled 2-(phenylthio)araalkylamines. J Med Chem **43**: 3103-10.

[50] Solbach C, Reischl G, Machulla H-J. 2004. Determination of reaction parameters for the synthesis of the serotonin transporter ligand [^{11}C]DASB:

Application to a remotely controlled high yield synthesis. Radiochim Acta **92**: 341-344.

[51] Frankle WG, Huang Y, Hwang D-R, Talbot PS, Slifstein M, Van Heertum R, Abi-Dargham A, Laruelle M. 2004. Comparative evaluation of serotonin transporter radioligands [^{11}C]-DASB and [^{11}C]-McN 5652 in healthy humans. J Nucl Med **45**: 682- 94.

[52] Ginovart N, Wilson AA, Meyer JH, Hussey D, Houle S. 2003. [^{11}C]DASB, a tool for in vivo measurement of SSRI-induced occupancy of the serotonin transporter: PET characterization and evaluation in cats. Synapse **47**: 123-33.

[53] McCarron J, Turton DR, Pike VW, Poole KG. 1996. Remotely-controlled production of the 5-HT_{1A} receptor radioligand, [carbonyl-^{11}C]WAY-100635, via ^{11}C-carboxylation of an immobilized Grignard reagent. J Label Compd Radiopharm **38**: 941-53.

[54] Matarrese M, Soloviev D, Todde S, Neutro F, Petta P, Carpinelli A, Brussermann M, Kienle MG, Fazio F. 2003. Preparation of [^{11}C]radioligands with high specific radioactivity on a commercial PET tracer synthesiszer. Nucl Med Biol **30**: 79-83.

[55] Matarrese M, Sudati F, Soloviev D, Todde S, Turolla EA, Kienle MG, Fazio F. 2002. Automation of [^{11}C]acyl chloride syntheses using commercially available ^{11}C-modules. Appl Radiat Isot **57**: 675-9.

[56] Tsukamoto M, Katoh C, Shiga T, Kaji T, Kuge Y, Nakada K, Tamaki N. 2004. Use of a standardized uptake value for parametric in vivo imaging of benzodiazepine receptor distribution on [11C]flumazenil brain PET. Eur J Nucl Med Mol Imaging **31**: 846-51.

[57] Magata Y, Mukai T, Ihara M, Nishizawa S, Kitano H, Ishizu K, Saji H, Konishi J. 2003. Simple analytic method of 11C-flumazenil metabolite in blood. J Nucl Med **44**: 417-21.

[58] Atack JR, Scott-Stevens P, Beech J, Fryer TD, Hughes JL, Cleij MC, Baron JC, Clark JC, Hargreaves RJ, Aigbirhio FI. 2006. Comparison of Lorazepam occupancy of rat brain GABA A receptors measured using in vivo [^{3}H]Flumazenil binding and [^{11}C]Flumazenil microPET. J Pharmacol Exp Ther **12**: in press

[59] Koepp MJ, Labbe C, Richardson MP, Brooks DJ, Van Paesschen W, Cunnigham VJ, Duncan JS. 1997. Regional hippocampal [^{11}C]flumazenil PET in temporal lobe epilepsy with unilateral and bilateral hippocampal sclerosis. Brain **120**: 1865-76.

[60] hyperlink http://www.osti.gov/bridge/product.biblio.jsp?osti_id=781827
Ferrieri RA. Production and application of synthetic precursors labeled with carbon-11 and fluorine-18 (20.08.2006)

[61] Shields AF, Graham MM, Kozawa SM, Kozell LB, Link JM, Swenson ER, Spence AM, Bassingthwaighte JB, Krohn KA. 1992. Contribution of labeled carbon dioxide to PET imaging of carbon-11-labeled compounds. J Nucl Med **33**: 581-4.

[62] Larsen P, Ulin J, Dahlström K, Jensen M. 1997 Synthesis of [^{11}C]methyliodide by iodination of [^{11}C]methane. Appl Radiat Isot **48**: 21 153-7.

[63] Langstrom B Lundqvist H. 1976. The preparation of ^{11}C methyl iodide and its use in the synthesis of ^{11}C methyl-L-methionine. Int Appl Radiat Isot **27**: 357-363.

[64] Jewett DM. 1992. A simple synthesis of [^{11}C]methyl triflate. Appl Radiat Isot **43**: 1383-5.

[65] Bida GT, Ruth TJ, Wolf AP. 1980. Experimentally determined thick target yields for the $^{14}N(p,\alpha)^{11}C$ recation. Radiochim Acta **27**: 181-5.

[66] Firouzbakht ML, Schlyer DJ, Wolf AP. 1998. Yield measurements for the $^{11}B(p,n)^{11}C$ and the $^{10}B(d,n)^{11}C$ nuclear reaction Nucl Med Biol **25**: 161-4.

[67] Ding YS, Fowler JS. 1996. 18F-labeled tracers for positron emission tomography studies in the neurosciences. In: Ojima I, McCarthy J, Welch JT (eds). Biomedical frontiers of fluorine chemistry. ACS Symp Series 639. The American Chemical society, Washington DC, chap 23, p 328

[68] Wüst F. 2003. Organic chemistry with the short-lived ß+ emitters 11C and 18F. Trends Org Chem **10**: 61-70.

[69] Wadsak W, Mitterhauser M, Rendl G, Schuetz LK, Ettlinger DE, Dudczak R, Kletter K, Karanikas G. 2006. [^{18}F]FETO for adrenocortical PET imaging: a pilot study in healthy volunteers. Eur J Nucl Med Mol Imaging **33**: 669-72.

[70] Mitterhauser M, Wadsak W, Wabnegger L, Sieghart W, Viernstein H, Kletter K, Dudczak R. 2003. In vivo and in vitro evaluation of [^{18}F]FETO with respect to the adrenocortical and GABAergic systems in rats. Eur J Nucl Med Mol Imaging **30**: 1398-1401.

[71] Wadsak W, Mitterhauser M. 2003. Synthesis of [^{18}F]FETO, a novel potential 11-ß hydroxylase inhibitor. J Label Compd Radiopharm **46**: 379-88.

[72] Ettlinger D, Wadsak W, Mien LK, Machek M, Wabnegger L, Rendl G, Karanikas G, Viernstein H, Kletter K, Dudczak R, Mitterhauser M. [^{18}F]FETO: metabolic considerations. Eur J Nucl Med Mol Imaging **33**: 928-31.

[73] Tewson TJ. 1983. Synthesis of no-carrier-added fluorine-18 2-fluoro-2-deoxy-D-glucose. J Nucl Med **24**: 235-8.

[74] Hamacher K, Coenen HH, Stoecklin G. 1986. Efficient stereospecific synthesis of no-carrier-added 2-[18F]-fluoro-2-deoxy-D-glucose using aminopolyether supported nucleophilic substitution.J Nucl Med **27**: 235-8.

[75] Fowler JS,Ido T. 2002. Initial and subsequent approach for the synthesis of 18FDG. Semin Nucl Med **32**: 6-12.

[76] Mitterhauser M, Wadsak W, Mien LK, Hoepping A, Viernstein H, Dudczak R, Kletter K, 2005. Synthesis and biodistribution of [18F]FE@CIT, a new potential tracer for the dopamine transporter. Synapse **55**: 73-9.

[77] Goodman MM, Kilts CD, Keil R, Shi B, Martarello L, Xing D, Votaw J, Ely TD, Lambert P, Owens MJ, Camp VM, Malveaux E, Hoffman JM. 2000. 18F-labeled FECNT: a selective radioligand for PET imaging of brain dopamine transporters. Nucl Med Biol **27**: 1-12.

[78] Harada N, Ohba H, Fukumoto D, Kakiuchi T, Tsukada H. 2004. Potential of [(18)F]beta-CFT-FE (2beta-carboxymethoxy-3beta-(4-fluorophenyl)-8-(2-[(18)F]fluoroethyl)nortropane) as a dopamine transporter ligand: A PET study in the conscious monkey brain. Synapse **54**: 37-45.

[79] Jewett, D.M., Kilbourn, M.R. 2004. In vivo evaluation of new carfentanil-based radioligands for the mu opiate receptor. Nucl. Med. Biol. **31**: 321-5.

[80] Henriksen G, Platzer S, Schuetz J, Schmidhammer H, Rafecas ML, Schwaiger M, Wester HJ. 2003. ^{18}F-Fluorinated agonists and antagonists for imaging of μ-opioid receptors: approaches to ^{18}F-Carfentanil, ^{18}F-Sufentanil and ^{18}F-Cyprodime J Lab Compd Radiopharm **46**: 175 (abstract)

[81] Wadsak W, Mien LK, Ettlinger DE, Feitscher S, Toegel S, Lanzenberger R, Marton J , Dudczak R, Kletter K, Mitterhauser M. 2007. Preparation and Biodistribution of [18F]FE@CFN (2-[18F]fluoroethyl 4-[N-(1-oxopropyl)-N-

phenylamino]-1-(2-phenylethyl)-4-piperidinecarboxylate), a Potential μ-Opioid Receptor Imaging Agent. Radiochim Acta **95**: 33-8

[82] Gessi S, Varani K, Merighi S, Morelli A, Ferrari D, Leung E, Baraldi PG, Spalluto G, Borea PA. 2001. Pharmacological and biochemical characterization of A_3 adenosine receptors in Jurkat T cells. Br J Pharmacol **134**: 116-26.

[83] Merighi S, Varani K, Gessi S, Cattabriga E, Iannotta V, Ulouglu C, Leung E, Borea PA. 2001. Pharmacological and biochemical characterization of adenosine receptors in the human malignant melanoma A375 cell line. Br J Pharmacol **134**: 1215-26.

[84] Fishman P, Bar-Yehuda S, Madi L, Cohn I. 2002. A_3 adenosine receptor as a target for cancer therapy. Anticancer Drugs **13**: 437-43.

[85] Li AH, Moro S, Forsyth N, Melman N, Ji XD, Jacobson KA . 1999. Synthesis, CoMFA analysis, and receptor docking of 3,5-diacyl-2, 4-dialkylpyridine derivatives as selective A3 adenosine receptor antagonists. J Med Chem **42**: 706-21.

[86] Wadsak W, Mitterhauser M, Mien LK, Toegel S, Keppler B, Dudczak R, Kletter K. 2003. Radiosynthesis of 3-(2'-[^{18}F]-fluoro)-flumazenil ([^{18}F]-FFMZ) via distillation of 2-bromo-[^{18}F]-fluoroethane. J Label Compd Radiopharm **46**: 1229-40.

[87] Mitterhauser M, Wadsak W, Wabnegger L, Mien LK, Toegel S, Langer O, Sieghart W, Viernstein H, Kletter K, Dudczak R. 2004. Biological evaluation of 2'-[^{18}F]fluoroflumazenil ([^{18}F]FFMZ), a potential GABA receptor ligand for PET. Nucl Med Biol **31**: 291-5.

[88] Chang YS, Jeong JM, Yoon YH, Kang WJ, Lee SJ, Lee DS, Chung JK, Lee MC. 2005. Biological properties of 2'-[^{18}F]fluoroflumazenil for central benzodiazepine receptor imaging. Nucl Med Biol **32**: 263-8.

[89] Yoon YH, Jeong JM, Kim HW, Hong SH, Lee YS, Kil HS, Chi DY, Lee DS, Chung JK, Lee MC. 2003. Novel one-pot one-step synthesis of 2'-[^{18}F]fluoroflumazenil ([^{18}F]FFMZ) for benzodiazepine receptor imaging. Nucl Med Biol **30**: 521-7.

[90] Qaim SM, Clark JC, Crouzel C, Guillaume M, Helmeke HJ, Nebeling B, Pike VW, Stoecklin G. 1993. PET radionuclide production. In: Stoecklin G, Pike VW (eds). Radiopharmaceuticals for Positron Emission Tomography- Methodological Aspects. Kluwer, Dordrecht, pp 1-43

[91] Helus F, Maier-Borst W, Sahm U, Wiebe L. 1979. F-18 cyclotron production methods. Radiochem Radioanal Lett **38**: 395-410.

[92] Lambrecht RM, Neirinckx R, Wolf AP. 1978. Cyclotron isotopes and radiopharmaceuticals. XXIII. Novel anhydrous 18F-fluorinating intermediates. Int J Appl Radiat Isot **29**: 175-83.

[93] Blessing G, Coenen HH, Franken K, Qaim SM. 1986. Production of [^{18}F]F_2,$H^{18}F$ and $^{18}F^-_{aq}$ using the $^{20}Ne(d,\alpha)^{18}F$ process. Appl Radiat Isot **37**: 1135-9.

[94] Bida GT, Ehrenkaufer RL, Wolf AP, Fowler JS, MacGregor RR, Ruth TJ. 1980. The effect of target-gas purity on the chemical form F-18 during 18F-F2 production using the neon/fluorine target. J Nucl Med **21**: 758-62.

[95] Casella V, Ido T, Wolf AP, Fowler JS, MacGregor RR, Ruth TJ. 1980. Anhydrous F-18 labeled elemental fluorine for radiopharmaceutical preparation. J Nucl Med **21**: 750-7.

[96] Iwata R, Ido T, Brady F, Takahashi T, Ujiie A. 1987. [^{18}F]Fluoride production with a circulating [^{18}O] water target. Appl Radiat Isot **38**: 979-84.

[97] Gonzalez-Lepera CE, Dembowski B. 1997. Production of [^{18}F]fluoride with a High-pressure disposable [^{18}O]water target. Appl Radiat Isot **48**: 613-7.

[98] Solin O, Bergman J, Haaparanta M, Reissell A. 1988. Production of 18F from water targets. Specific radioactivity and anoinic contaminants. Int J Appl Radiat Isot **39**: 1065-71.

[99] Hamacher K, Coenen HH, Stoecklin G. 1986. Efficient stereospecific synthesis of no-carrier-added 2-[^{18}F]fluoro-2-deoxy-D-glucose using aminopolyether supported nucleophilic substitution. J Nucl Med **27**: 235-8.

[100] Hamacher K, Blessing G, Nebeling B. 1990. Computer-aided synthesis (CAS) of no-carrier-added 2-[^{18}F]fluoro-2-deoxy-D-glucose: an efficient automated system for the aminopolyether-supported nucleophilic fluorination. Appl Radiat Isot **41**: 49-55.

[101] Nickles RJ, Hichwa RD, Daube ME, Hutchins GD, Congdon DD. 1983. An $^{18}O_2$ target for the high yield production of 18F-fluoride. Int J Appl Radiat Isot **34**: 625-9.

[102] Schlyer DJ, Bastos M, Wolf AP. 1987. A rapid quantitative seperation of fluorine-18 fluoride from oxygen-18 water. J Nucl Med **28**: 764 (Abstract)

[103] Schlyer DJ, Bastos M, Alexoff D, Wolf AP. 1990. Seperation of [^{18}F]fluoride from [^{18}O]water using anion exchange resin. Appl Radiat Isot **41**: 531-3.

[104] Nickles RJ, Gatley SJ, Votaw JR, Kornguth ML. 1986. Production of reactive fluorine-18. Appl Radiat Isot **37**: 649-61.

[105] Kilbourn MR. 1990. Fluorine-18 labelling of radiopharmaceuticals, Nuclear science series NAS-NS-3203, National Academy Press Washington DC, USA

[106] Brodack JW, Kilbourn MR, Welch MJ, Katzenellenbogen JA. 1986. N.c.a. 16α-[^{18}F]fluoroestradiol-17ß: the effect of reaction vessel on fluorine-18 resolubilization, prduct yield and effective specific activity. Appl Radiat Isot **37**: 217-21.

[107] Block D, Coenen HH, Stoecklin G. 1987. The n.c.a. nucleophilic 18F-fluorination of 1,N-disubstituted alkanes as fluoroalkylation agents. J Label Compd Radiopharm **24**: 1029-42.

[108] Angelini G, Speranza M, Wolf AP, Shiue CY, Fowler JS, Watanabe M. 1984. New developments in the synthesis of no carrier added (n.c.a.) 18F-labeled aryl fluorides using the nucleophilic aromatic substitution reaction. J Label Compd Radiopharm **21**: 1223-6.

[109] Angelini G, Speranza M, Wolf AP, Shiue CY. 1985, Nucleophilic aromatic substitution of cationic groups by 18F-labeled fluoride. A useful route to no-carrier – added (nca) 18F-labeled aryl fluorides.J Fluorine Chem **27**: 1223-6.

[110] Hess E, Blessing G, Coenen HH, Qaim SM. 2001. Improved target system for production of high purity [^{18}F]fluorine via the ^{18}O(p,n)^{18}F reaction. Appl Radiat Isot **52**: 1431-40.

[111] Visser GWM, Bakker CNM, Herscheid JDM, Brinkman G, Hoekstra A. 1984. The chemical properties of [^{18}F]-acetylhypofluorite in acetic acid solution. J Label Compd Radiopharm **21**: 1226 (Symposium Abstract)

[112] Chirakal R, Firnau G, Schroblingen GJ, McKay J, Garnett ES. 1984. The synthesis of [^{18}F]xenon difluoride from [^{18}F]fluorine gas. Appl Radiat Isot **35**: 401-4.

[113] De Vries EFJ, Luurtsema G, Brüssermann M, Elsinga PH, Vaalburg W. 1999. Fully automated synthesis module for the high yield one-pot synthesis of 6-[^{18}F]fluoro-L-DOPA. Appl Radiat Isot **51**: 389-94.

[114] Block D, Coenen HH, Stöcklin G. 1988. N.c.a. 18F-fluoroacylation via fluorocarboxylic acid esters. J Label Compd Radiopharm **25**: 185-200.

[115] Shai Y, Kirk KL, Channing MA, Dunn BB, Lesniak MA, eastman RC, Finn RD, Roth J, Jacobson KA. 1989. 18F-labeled insulin: A prosthetic group methodology for incorporation of a positron emitter into peptides and proteins. Biochem **28**: 4801-6.

[116] Coenen HH, Laufer P, Stöcklin G, Wienhard K, Pawlik G, Böcher-Schwarz HG, Heiss WD. 1987. 3-N-(2-[18F]fluoroethyl)-spiperone: a novel ligand for cerebral dopamine receptor studies with PET. Life Sciences **40**: 81-88.

[117] Moerlein SM, Perlmutter JS. 1991. Central serotonergic S2 binding in Papio anubis measured in vivo with N-ω[^{18}F]fluoroethylketanserin and PET. Neurosci Lett **123**: 23-6.

[118] Moerlein SM, Perlmutter JS. 1992. Binding of 5-(2'-[18F]fluoroethyl)flumazenil to central benzodiazepine receptors measured in living baboon by positron emission tomography . Eur J Pharmacol **218**: 109-15.

[119] Baumann A, Piel M, Schirrmacher R, Rösch F. 2003. Efficient alkali iodide promoted 18F-fluoroethylations with 2-[18F]fluoroethyl tosylate and 1-bromo-2[^{18}F]fluoroethane. Tetrahedron Lett **44**: 9165-7.

[120] Musachio JL, Shah J, Pike VW. 2005. Radiosyntheses and reactivities of novel [^{18}F]2-fluoroethylarylsulfonates. J Label Compd Radiopharm **48**: 735-47.

[121]http://www.griffwason.com/gw_images/MRI_scanner/glw-pet_scanner1.jpg (25.02.2007)

[122]http://laxmi.nuc.ucla.edu:8248/M248_98/PET/lec15slides/sld013.htm (25.02.2007)

[123] Coenen HH, Colosimo M, Schüller M, Stöcklin G. 1986. Preparation of N.C.A. [18F]-CH2BrF via aminopolyether supported nucleophilic substitution J Label Compd Radiopharm **23**: 587-95.

[124] Bergman J, Eskola O, Lehikoinen P, Solin O. 2001. Automated synthesis and purification of [^{18}F]bromofluoromethane at high specific radioactivity. Appl Rad Isot **54**: 927-33.

[125] Zheng L, Berridge MS. 2000.Synthesis of [^{18}F]fluoromethyl iodide, a synthetic precursor for fluoromethylation of radiopharmaceuticals. Appl Rad Isot **52**: 55-61.

[126] Elsinga PH, Kawamura K, Kobayashi T, Tsukada H, Senda M, Vaalburg W, Ishiwata K.2001. Synthesis and evaluation of [18 F] fluoroethyl SA4503 and SA5845 as PET ligand for the sigma receptor. J Label Compd Radiopharm **44**: S4.(Poster session)

[127] Wilson AA, DaSilva JN, Houle S.1996 [18F]fluoroalkyl analogues of the potent 5-HT1A antagonist WAY 100635: radiosyntheses and in vivo evaluation. Nucl Med Biol **23**: 487-90.

[128] Skaddan MB, Kilbourn MR, Snyder SE, Sherman PS, Desmond TJ, Frey KA. 2000.Synthesis, (18)F-labeling, and biological evaluation of piperidyl and pyrrolidyl benzilates as in vivo ligands for muscarinic acetylcholine receptors. J Med Chem **43**: 4552-62.

[129] Oh SJ, Choe YS, Chi DY, Kim SE, Choi Y, Lee KH, Ha HJ, Kim BT.1999. Re-evaluation of 3-bromopropyl triflate as the percursor in the preparation of 3-[^{18}F]fluoropropyl bromide. Appl Rad Isot **51**: 293-97.

[130] Lundkvist C, Halldin C, Ginovart N, Swahn CG, Farde L. 1997. [18F] beta-CIT-FP is superior to [11C] beta-CIT-FP for quantitation of the dopamine transporter. Nucl Med Biol **24**: 621-7.

[131] Chesis PL, Welsh MJ.1990. Comparison of bromo- and iodoalkyl triflates for 18F-radiolabeling of amines. Appl Rad Isot **41**: 259-265.

[132] Zijlstra S, de Groot TJ, Kok LP, Visser GM, Vaalburg W.2000. J Org Chem, **43**: 4552.

[133] de Groot TJ, Elsinga PH, Visser GM, Vaalburg W. 1992. 1-[^{18}F]fluoro-2-propanol p-toluenesulfonate: a synthon for the preparation of N-([^{18}F]fluoroisopropyl)amines. Appl Rad Isot **43**: 1335-1339.

[134] Wester HJ, Herz M, Weber W, Heiss P, Senekowitsch-Schmidtke R. 1999. Synthesis and Radiopharmacology of O-(2-[18F]fluoroethyl)-L-Tyrosine for Tumor Imaging. J Nucl Med **40**: 205-212.

[135] Chaly T, Dhawan V, Kazumata K, Antonini A, Margoulef C, Dahl R, Belakhlef A, Margoulef D, Yee A, Wang S, Tamagnan G, Neumeyer JL. 1996. Radiosynthesis of [^{18}F] N-3-fluoropropyl-2-β-carbomethoxy-3-β-(4-iodophenyl) nortropane and the first human study with positron emission tomography. Nucl Med Biol **23**: 999-1004.

[136] Kazumata K, Dhawan V, Chaly T, Antonini A, Margoulef C, Belakhlef A, Neumeyer JL. 1998. Dopamine Transporter Imaging with Fluorine-18-FPCIT and PET. J Nucl Med **39**: 1521-1530.

[137] Gründer G, Siessmeier T, Lange-Asschenfeldt C, Vernaöeken I, Buchholz HG, Stoeter P, Drzezga A, Lüddens H, Rösch F, Bartenstein P. 2001.

18F]Fluoroethylflumazenil: a novel tracer for PET imaging of human benzodiazepine receptors. Eur J Nucl Med **28**: 1463-70.

[138] Satyamurthy N, Barrio JR, Bida GT, Huang SC, Mazziotta JC, Phelps ME. 1990. (2′-[^{18}F]fluoroethyl)spiperone, a potent dopamine antagonist: Synthesis, structural analysis and in-vivo utilization in humans Appl Radiat Isot **41**:113-29.

[139] Satyamurthy N, Bida GT, Barrio JR, Luxen A, Mazziotta JC, Huang SC, Phelps ME. 1986. No-carrier-added 3-(2′-[^{18}F]fluoroethyl)spiperone, a new dopamine receptor-binding tracer for positron emission tomography. Nucl Med Biol **13**: 617-24

[140] Chi DY, Kilbourn MR, Katzenellenbogen JA, Brodack JW, Welsh MJ.1986. Synthesis of no-carrier-added N-([^{18}F]fluoroalkyl)spiperone derivatives. Int J Rad Appl Instr Part A **37**: 1173-80.

[141] Zijlstra S, Visser GM, Korf J, Vaalburg W.1993. Synthesis and in vivo distribution in the rat of several fluorine-18 labeled N-fluoroalkylaporphines. Appl Radiat Isot **44**: 651-58.

[142] Wester HJ, Willoch F, Tölle TR, Munz F, Herz M, Oye I, Schadrack J, Schwaiger M, Bartenstein P. 2000. 6-*O*-(2-[^{18}F]Fluoroethyl)-6-*O*-Desmethyldiprenorphine ([^{18}F]DPN): Synthesis, Biologic Evaluation, and Comparison with [^{11}C]DPN in Humans. J Nucl Med **41**: 1279-86.

[143] Hamacher K, Coenen HH. 2002. Efficient routine production of the ^{18}F-labelled amino acid O-(2-[^{18}F]fluoroethyl)-L-tyrosine. Appl Radiat Isot **57**: 853-6.

[144] Suehiro M, Greenberg JH, Shiue CY, Gonzales C, Dembowski B, Reivich M.1996. Radiosynthesis and biodistribution of the S-[^{18}F]fluoroethyl analog of McN5652. Nucl Med Biol **23**: 407-12.

[145] Tang G, Wang M, Tang X, Luo L, Gan M. 2003. Pharmacokinetics and radiation dosimetry estimation of O-(2-[^{18}F]fluoroethyl)-L-tyrosine as oncologic PET tracer. Appl Radiat Isot **58**: 219-25.

[146] Wilson AA, Dasilva JN, Houle S. 1995 Synthesis of two radiofluorinated cocaine analogues using distilled 2-[^{18}F]fluoroethyl bromide. Appl Radiat Isot **46**: 765-70.

[147] Chin FT, Musachio JL, Cai L, Pike VW. 2003. J Label Compd Radiopharm **46**: S172. (poster session PO2 - Neuroscience p S138-S188)

[148] Skaddan MB, Kilbourn MR, Snyder SE, Sherman PS, Desmond TJ, Frey KA. 2000. Synthesis, (18)F-labeling, and biological evaluation of piperidyl and pyrrolidyl benzilates as in vivo ligands for muscarinic acetylcholine receptors. J Med Chem **43**: 4552-62.

[149] Zhang MR, Furutsuka K, Yoshida A, Suzuki K. 2003. How to increase the reactivity of [18F]fluoroethyl bromide: [18F]fluoroethylation of amine, phenol and amide functional groups with [18F]FEtBr, [18F]FEtBr/NaI and [18F]FetOTf. J Label Comp Radiopharm **46**: 587-98.

[150] Schirrmacher R, Mathiasch B, Schirrmacher E, Radnic D, Rösch F. 2003. Syntheses of novel N-([18F]fluoroalkyl)-N-nitroso-4-methyl-benzenesulfonamides and decomposition studies of corresponding 19F- and bromo-analogues: potential new compounds for the 18F-labelling of radiopharmaceuticals. J Label Compd Radiopharm **46**: 959-77.

[151] Lu SY, Chin FT, McCarron JA, Pike VW. 2004. Efficient O- and N-(-fluoroethylation)s with NCA [18F]-fluoroethyl tosylate under microwave-enhanced conditions J Label Compd Radiopharm **47**: 289-97.

[152] Comagic S, Piel M, Schirrmacher R, Höhnemannt S, Rösch F. 2002. Efficient synthesis of 2-bromo-1-[^{18}F]fluoroethane and its application in the automated preparation of ^{18}F-fluoroethylated compounds. Appl Radiat Isot **56**: 847-51.

[153] Zhang MR, Tsuchiyama A, Haradahira T, Yoshida A, Furutsuka K, Suzuki K. 2002. Development of an automated system for synthesizing ^{18}F-labeled compounds using [^{18}F]fluoroethyl bromide as a synthetic precursor. Appl Radiat Isot **57**: 335-42.

[154] http:// Anexo F- Especificaciones técnicas ciclotron GE .htm (Barcelona) (29.05.2007)

[156] Smart BE,Banks RE, Tatlow JE.1994. Characteristics of C-F systems in Organofluorine Chemistry. Principles and Commercial Applications.Plenum Press, New York pp.57-88.

2.1. Author's contribution

I hereby declare to have significantly contributed to the realisation of each of the following four studies that are included in the present thesis.

Concerning the first study Synthesis and Biodistribution of [^{18}F]FE@CIT, a new potential tracer for the Dopamine Transporter, I participated in the study design and performed all the radiosyntheses. Furthermore, I fully participated in the bioevaluation studies at Seibersdorf and the conception and writing of the manuscript.

For the second study Preparation and Biodistribution of [^{18}F]FE@CFN (2-[^{18}F]fluoroethyl 4-[N-(1-oxopropyl)-N-phenylamino]-1-(2-phenylethyl)-4-piperidinecarboxylate), a Potential μ-Opioid Receptor Imaging Agent, I participated in the study design, and I performed all the radiosyntheses. Furthermore, I fully participated in the bioevaluation study at ARC Seibersdorf and the conception and writing of the manuscript. Additionally, I oversaw the practical aspects of the diploma thesis of Mrs. Feitscher S.

For the third study Preparation and first Preclinical Evaluation of [18F]FE@SUPPY as a new PET-Tracer for the Adenosine A3 Receptor, I participated in the study design, I performed all the radiosyntheses and I partizipated in the implementation of the automated radiosynthesis via synthesizer module and the conception and writing of the manuscript. Additionally, I oversaw the practical aspects of the diploma theses of Ms. Schmidt B. and Ms. Weber K.

In the fourth study The simple and fully automated preparation of [carbonyl-^{11}C]WAY-100635, I participated in the study design and in the implementation of the automated radiosynthesis via synthesizer module. Additionally, I participated in the design and in the writing of the manuscript.

I carefully corrected each publication especially with emphasis on the practical aspects.

2.2. Paper 1

Synthesis and Biodistribution of [^{18}F]FE@CIT, a new potential tracer for the Dopamine Transporter

Synapse 2005; 55: 73-79

Markus Mitterhauser [1,2,3 *], Wolfgang Wadsak [1,4,5], Leonhard-Key Mien [1,2], Alexander Hoepping [6], Helmut Viernstein [2], Robert Dudczak [1,5], Kurt Kletter [1]

1 Department of Nuclear Medicine, Medical University of Vienna, Austria

2 Department of Pharmaceutic Technology and Biopharmaceutics, University of Vienna, Austria

3 Hospital Pharmacy of the General Hospital of Vienna, Austria

4 Department of Inorganic Chemistry, University of Vienna, Austria

5 Ludwig-Boltzmann-Institute for Nuclear Medicine, Vienna, Austria

6 ABX - Advanced Biochemical Compounds, Radeberg, Germany

Abstract: In the last decade radiolabelled tropane analogues based on ß-CIT have proven undisputable for the imaging of the dopamine transporter. However, further improvements in their pharmacodynamic and pharmacokinetic features are desirable. An important improvement, yielding in higher affinity to the dopamine transporter (DAT) versus serotonin transporter (SERT) can be achieved by a simple replacement of the carboxylic methyl ester group in ß-CIT by a fluoroethyl ester. The preparation and ex vivo evaluation of this new ß-CIT-analogue – [^{18}F]FE@CIT – will be presented herewith. Precursor and standard were prepared from ß-CIT and analyzed by spectroscopic methods. Yields of precursor and standard preparation were 61% and 42%, respectively. [^{18}F]FE@CIT was prepared by distillation of [^{18}F]bromofluoroethane ([^{18}F]BFE) and reaction with (1R-2-exo-3-exo)8-methyl-3-(4-iodo-phenyl)-8-azabicyclo[3.2.1] octane-2-carboxylic acid. After 10 minutes at 150°C the product was purified using a C-18 SepPak. The radiosynthesis evinced radiochemical yields of >90% (based on [^{18}F]BFE), the specific radioactivity was >416 GBq/µmol. An average 30µAh cyclotron irradiation yielded in more than 2.5GBq [^{18}F]FE@CIT. For the ex vivo bioevaluation 20 male Sprague-Dawley rats were sacrifized at 5, 15, 30, 60 and 120 minutes after infection. Organs were removed, weighed and counted. For autoradiographic experiments transversal brain slices of about 100µm were prepared. The ex-vivo evaluation showed highest brain uptake in striatal regions followed by thalamus and cerebellum. Highest striatum to cerebellum ratio was 3.73 and highest thalamus to cerebellum ratio was 1.65. Autoradiographic images showed good and differentiated uptake in striatal regions with good target to background ratio.

Key words: ß-CIT, PET, [^{18}F]FE@CIT, dopamine transporter, autoradiography

1. Introduction

In the last decade radiolabelled cocaine analogues based on ß-CIT have proven undisputable for the imaging of the dopamine transporter (DAT). Alterations of the DAT can be associated with neurodegenerative and neuropsychiatric disorders, including Parkinson´s disease, depression, attention deficit-hyperactivity disorder, Huntington´s chorea and schizophrenia [1]. A multitude of cocaine analogs has been synthesized to date. Among these the so called WIN-compounds exhibit a 2-200-fold higher affinity for the DAT than cocaine. Some of these compounds have been labeled with [^{11}C] or [^{18}F] and were used for positron emission tomography (PET). The major disadvantage of the WIN-compounds is their high affinity for the serotonin transporter (SERT) and the norepinephrine transporter (NET) [2-8]. Basically two functional groups within the molecule can be targeted with the radiolabelled substituent: the amine and the carboxylic function. Replacing the original N-methyl substituent of ß-CIT by a more lipophilic N-fluoroethyl (ß-CIT-FE) or N-fluoropropyl substituent (ß-CIT-FP) resulted in decreased affinity both for DAT and SERT [9] Modifications of the original methyl ester function towards longer more lipophilic fluoroethyl or fluoropropyl substituents resulted in higher affinity for the DAT and from all investigated tropanes, the fluoroethylester of ß-CIT displayed the highest DAT affinity and the highest selectivity DAT over SERT and DAT over NET [8]. We have recently presented a feasible method for the synthesis of [^{18}F]fluoroethyl esters proofing biologically more stable than methyl- or ethyl esters [10-13]. Thus our rationale was the precursor preparation, radiosynthesis and first ex vivo evaluation of this [^{18}F]fluoroethylester of ß-CIT (2ß- carbo-2´-[^{18}F]fluoroethyloxy-3ß-4-iodophenyltropane; 2`-[^{18}F]fluoroethyl (1R-2-exo- 3-exo)-8-methyl-3-(4-iodophenyl)-8-azabicyclo[3.2.1]octane-2-carboxylate; [^{18}F]FE@CIT) using rats.

2. Materials and Methods

Synthesis

Materials Solid phase extraction cartridges (SepPak® C18plus) were purchased from Waters Associates (Milford, MA). ß-CIT was obtained from ABX (Radeberg, Germany). All other reagents and chemicals were purchased from Merck (Darmstadt, Germany), Sigma-Aldrich Chemical Company (Steinheim, Germany) or Riedel-de Haën (Seelze, Germany) and used without further purification. Analytical thin layer chromatography (TLC) was performed using silicagel 60 F_{254} plates from Merck or Macherey-Nagel (Düringen, Germany). Analytical high performance liquid chromatography (HPLC) was performed using a LiChrospher 100 RP-18 column (5µm, 250 x 4mm) from Merck. Preparative HPLC was performed using a Luna RP-18 column from Phenomenex (2.5 x 30 cm; Torrance, CA, USA). Gas chromatography (GC) was performed using an HP-Innowax column (30m x 0.32mm x 0.25µm).

[^{18}F]Fluoride was produced via the ^{18}O(p,n)^{18}F reaction in a GE PETtrace cyclotron (16.5 MeV protons). $H_2{}^{18}O$ was purchased from Rotem GmbH (Leipzig, Germany).

Instruments Analysis of radio-TLC plates was performed using a digital autoradiograph (Berthold Technologies, Bad Wildbad, Germany). Analytical HPLC was performed with a Merck-Hitachi LaChrom L-7100 system equipped with a Merck-Hitachi LaChrom L-7400 UV detector at 235nm and a lead-shielded NaI-radiodetector (Berthold Technologies, Bad Wildbad, Germany). Preparative HPLC was performed with a Knauer 1800 pump and a Knauer K 2501 UV-Detector (Berlin, Germany). Gas chromatography was performed using an HP 6890 series system equipped with a flame ionisation detector (FID, Hewlett Packard, Palo Alto, CA, USA). NMR spectra were recorded on a Varian Inova 400 (Palo Alto, CA, USA) with $CDCl_3$ and methanol-D4 as solvents.

Precursor Synthesis (3-ß-(4-Iodophenyl)tropane-2-ß-carboxylic acid) ß-CIT (500mg, 1.3mmol) was dissolved in 6N hydrochloric acid and refluxed for 24h under an argon atmosphere. Then the hydrochloric acid was evaporated and the residue was purified by preparative HPLC (Phenomenex Luna column, water/acetonitrile/trifluoroacetic acid: 70/30/0.1, flow rate 50mL/min). The solvents were removed and the residue was dried under vacuum to give 300mg (61%) of a colorless solid.

FE@CIT (3-ß-(4-Iodophenyl)tropane-2-ß-carboxylic acid 2-fluoroethyl ester) 3-ß-(4-Iodophenyl)tropane-2-ß-carboxylic acid (122mg, 0.33mmol) was dissolved in 13ml dichloromethane. 2-Fluoroethanol (164mg, 2.56mmol) and N,N-dimethylpyridin-4-amine (DMAP 20.2mg, 0.165mmol) were added and the mixture was cooled to 0-5°C. Then 1-Ethyl-3-(3-(N,N-dimethylamino)propyl)carbodiimide hydrochloride (EDCI, 70mg, 0.36mmol) was added and the mixture was stirred under argon for 18h. The solvent was removed and the residue was subjected to flash chromatography (hexane/ether/triethylamine: 15/10/1) to obtain 58mg (42%) as a white solid.

2-Bromoethyl triflate 2-Bromoethyl triflate was prepared according to a literature method [14] starting from trifluoromethanesulfonic anhydride and 2-bromoethanol.

2-Bromo-1-[^{18}F]fluoroethane ([^{18}F]BFE) No-carrier-added (n.c.a.) aqueous [^{18}F]fluoride was added to a 2.5ml v-vial containing Kryptofix 2.2.2. (13.3µmol), potassium carbonate (10.0µmol) and acetonitrile (1.0ml, 19.1mmol) and heated to 100°C. Azeotropic drying was performed by subsequent addition of at least four 250µl portions of acetonitrile. To the dried complex 2-bromoethyl triflate (20µl, 77.8µmol) and acetonitrile (80µl, 1.5mmol) were added, the vial was sealed and heated at 100°C (10min).

Distillation Volatiles were distilled using a smooth stream of nitrogen (5ml/min) and 1/16" tubing with needles connecting the reaction vessel, a washing flask and the

product trap. The washing flask contained 190µl of DMSO and 10µl of anhydrous DMF at ambient temperature, whereas the product trap contained 600µl of anhydrous DMF at 0°C. A total of 500µl of acetonitrile was added in small portions to the reaction vessel to achieve quantitative distillation of [^{18}F]BFE.

"Wilson Method" [2]. Volatiles were distilled using the same set up as described in *distillation* except: THF was used as distillation solvent (500µl), no washing flask was used and [^{18}F]BFE was trapped into 200µl DMF (-40°C), 3x100µl THF were used for quantitative transfer.

[^{18}F]FE@CIT 5mg (13.4µmol) (1R-2-exo-3-exo)-8-methyl-3-(4-iodo-phenyl)-8-azabicyclo[3.2.1]octane-2-carboxylic acid was dissolved in 300µl dichloromethane, 17.4µl TBAH solution was added and dichloromethane was evaporated. The dried complex was reconstituted in 500µl anhydrous DMF. A calculated aliquot of this solution was added to the distilled [^{18}F]BFE. The reaction was carried out for 10 to 30 minutes at temperatures from 20°C to 180°C. For the "*Wilson Method*" 20min at 80°C were used.

Product purification The product solution was diluted with a total of 20ml water and loaded onto a pre-conditioned (ethanol/water) C18plus SepPak® cartridge. After washing with a further 10ml of water, the purified [^{18}F]FE@CIT was quantitatively eluted with 1.2ml of ethanol (100%).

Quality control Chemical and radiochemical impurities were detected using radio-HPLC (mobile phase: 65% (water/ethanol/acetic acid 87.5/10/2.5 (v/v/v), 2.5 g/l ammonium acetate, pH 3.5), 35% acetonitrile) and radio-TLC (mobile phase: 40% (water/ethanol/acetic acid 87.5/10/2.5 (v/v/v), 2.5 g/l ammonium acetate, pH 3.5) 60% acetonitrile). Residual solvents were analyzed by GC (carrier gas: He; flow: 2.7 ml/min; 45°C (2.5min) – 20°C/min to 110°C – 30°C/min to 200°C – 200°C (10min); FID: 270°C). Residuals of Kryptofix 2.2.2 were analyzed by TLC according

to the [^{18}F]FDG monograph in the European Pharmacopoeia (1999:1325) (mobile phase: 90% methanol/10% ammonia (v/v); iodine chamber).

Animal Experiment.

Materials Organ fractions were counted with a Canberra Packard Cobra II auto-gamma counter (Canberra Packard, Canada). % Doses were calculated using two calibration curves (high and low activity) with known activities and decay corrected for the injection time. Preparation of the doses was done on a Capintec CRC15R dose calibrator and the rest body was counted on a planar NaI crystal assembled with an Ortec Maestro 32MCA emulator data acquisition software. Remaining activity in the rest body was calculated by correlation of the counts with a calibration curve acquired with known activities in the same geometry and decay corrected for the injection time. Autoradiographic images were developed on a Canberra Packard instant imager.

Biodistribution All biodistribution studies followed a protocol for the NIH Animal Care and Use Committee also approved by the Austrian law on animal experiments. Male Sprague-awley rats/Him:OFA (n=20, 206-242 g) were injected with 1.25-2.23 MBq [^{18}F]FE@CIT in 180-225 µl physiological phosphate buffer through the tail vein. Subsequently the rats were sacrificed by exsanguination from the abdominal aorta in ether anaesthesia after 5 (n=4), 15 n=4), 30 (n=4), 60 (n=4) and 120 minutes (n=4). Organs were removed, weighed and counted (Cobra II auto-gamma counter, Canberra Packard, Canada). Radioactivity is expressed as percentage of injected dose per gram tissue (% ID/g). For autoradiography 12.25-17.84 MBq were administered via the tail vein and transversal brain slices of about 100µm were prepared after 5, 15, 30, 60 and 120 minutes and subjected to imaging.

3. Results

Synthesis

A reaction scheme of the synthesis is presented in figure 1.

Synthesis of FE@CIT ß-CIT was hydrolyzed with hydrochloric acid to give the free ß-CIT acid and purified by preparative HPLC (yield 61%). ^{1}H-NMR(methanol-D4): δ 1.95 (dt *J* = 14.37, *J* = 4.0, 1H); 2.14-2.31 (m, 2H); 2.35-2.53 (m, 2H); 2.72 td (*J* = 14.1, J = 2.62, 2 H); 2.84 (s. 3H, CH_3); 3.05 (dd, *J* = 6.3, *J* = 1.87, 1H); 3.53 (m, 1H); 4.00 (m, 1H), 4.12 (dd, *J* = 6.9, *J* = 2.1, 1H); 7.09 (m, 2H); 7.66 (m, 2H)

Fluoroethyl-ß-CIT was obtained by reacting the acid with 2-fluoroethanol in dichlormethane employing EDCI as coupling agent and DMAP as catalyst (yield 42%). ^{1}H-NMR($CDCl_3$): δ 1.54-1.76 (m, 3H); 2.02-2.27 (m, 2H); 2.20 (s, 3H, CH_3); 2.51 (td, *J* = 12.3, *J* = 2.8, 1H); 2.92 (m, 2H); 3.34 (m, 1H); 3.60 (m, 1H); 3.98-4.55 (m, 4H, CH_2-CH_2-F); 6.99 (d, *J* = 8.45, 2H); 7.56 (d, *J* = 8.45, 2H). ^{19}F-NMR: δ 125

Synthesis of [^{18}F]FE@CIT Radiochemical yields depended on reaction temperature and amount of precursor, as presented in figures 2 and 3 whereas reaction time appeared to play a subordinate role: the reaction was complete within 10 minutes (cf. figure 3). The radiosynthesis evinced radiochemical yields of >90% (based on [^{18}F]BFE), the specific radioactivity was >416 GBq/µmol. An average 30µAh cyclotron irradiation yielded in more than 2.5GBq [^{18}F]FE@CIT.

[^{18}F]FE@CIT was identified by co-elution of the radioactive product with the inactive reference standard both on HPLC and radio-TLC (TLC: rf values: precursor: 0.68, FE@CIT: 0.74, BFE: 0.0; HPLC: retention times: precursor: 3.85min; FE@CIT: 8.13min; BFE: 6.05min). Radiochemical yield of the purified product exceeded 96% (specific radioactivity >416 GBq/µmol (11243Ci/mmol)).

Animal Experiment

Results of the biodistribution experiments are presented in table 1 and showed good uptake of [^{18}F]FE@CIT in brain regions. Autoradiographic results are presented in figure 4. Striatal regions are clearly visible at 60 minutes.

4. Discussion

General

ß-CIT has been playing an important role in neuroimaging for more than a decade. A series of analogues have already been synthesized and evaluated for PET mostly showing modifications on the ester function, the amine function and on the para-position in the aromatic ring. [1,2] presented the evaluation of two [^{18}F]fluoroethylesters with a para-methylphenyl and a para-chlorophenyl substituent showing high affinity for DAT-rich regions. These investigations [8] showed that the substitution of the paraphenyl-methyl group by a paraphenyl-halogen group yielded in a higher DAT-affinity and better DAT over SERT selectivity. On the other hand replacing the original methyl-ester of ß-CIT by a fluoroethyl ester yielded in a 1.5 times higher affinity for the DAT, a 10 fold increased selectivity DAT over SERT and a 59 times increased selectivity DAT over NET [8]. Looking at the metabolic pattern of ß-CIT and methylester-analogues, enzymatic ester cleavage appeared to be the major degradation route [6], [15-16]. In previous reports we presented evidence for a higher metabolic stability of esters when the alkyl-rest chain was replaced by a fluoroalkyl-chain [12,13]. This fact supports the strategy of fluoroethylation as a tool for stabilizing ester functions. As another strategy fluoroalkyl groups could be attached to the secondary amine group of the molecule, but concordantly, Kula et al [17], Gu et al [8] and Okada et al [9] presented lower affinity and lower DAT over SERT selectivity when replacing the N-methyl group by N-fluoroalkyl groups. All these data from recent publications and own experiences abounded as the

theoretically optimal structure (1) the fluoroethylester for metabolic stability together with (2) high affinity and (3) best DAT over SERT selectivity with a N-methyl substituent and the para-iodophenyl or a 3,4-dichlorophenyl structure.

Synthesis

The synthesis of the *precursor* for [^{18}F]FE@CIT is based on literature methods. Thus ß-CIT was hydrolyzed with 6N hydrochloric acid to yield the ß-CIT acid [18]. In the author's opinion, this method is superior with respect to the saponification employing dioxane/water requiring several days of reaction [19]. However, neither way gave 100% conversion thus making a purification of the acid by preparative HPLC necessary.

The synthesis of *FE@CIT* was straightforward. ß-CIT acid was reacted with 2-fluoroethanol and 1-ethyl-3-(3-dimethyllaminopropyl)carbodiimide hydrochloride (EDCI) in the presence of 4-dimethylaminopyridine (DMAP). FE@CIT was obtained in 42% yield.

[^{18}F]BFE We evaluated two different set-ups for the purification of [^{18}F]BFE via distillation. Both methods yielded highly purified (>99%) [^{18}F]BFE, but the reactivity for the conversion to [^{18}F]FE@CIT did not abide for the "Wilson Method". Although Wilson et al. [2] presented very high yields (>27%) for the radiosynthesis of [^{18}F]FETT and [^{18}F]FECT using THF as distillation solvent, we could not reproduce these findings in the synthesis of *[^{18}F]FE@CIT*. As already discussed before, the washing flask is essential for successful syntheses [10-11]. The described method uses solid phase extraction (SPE) for product purification and is easy to adopt for a remotely controlled synthesis module.

Animal Experiment

The ex-vivo evaluation showed highest brain uptake in striatal regions followed by thalamus/hypothalamus and cerebellum. The striatal region was selected as an area of binding to the DAT due to its high concentration of dopamine reuptake sites and thalamus/hypothalamus was chosen as an area representative of binding to SERT because it contains many serotonergic nerve terminals and few dopaminergic nerve terminals [20]. Highest uptake in the striatum was found at 15 minutes, with a steady decrease thereafter (figure 5). Lavalaye et al presented another parameter for the evaluation of tracer binding: Striatum to cerebellum ratio and thalamus to cerebellum ratio, both expressed as % ID/g multiplied by the body weight [20]. For [^{18}F]FE@CIT the highest striatum to cerebellum ratio was 3.73 and thalamus to cerebellum ratio was 1.65 both at the maximum (60 and 120 minutes, respectively). Maximum values for [^{123}I]FP-CIT were calculated for 120 minutes [20]: 3.95 for striatum/cerebellum and 2.01 for hypothalamus/cerebellum (cf. figure 6). Goodman et al [7] investigated [^{18}F]FECNT in rats and found in two different studies at 60 minutes striatum to cerebellum ratios of 8 and 4.3, respectively. In the same two studies hypothalamus to cerebellum ratios were 2.24 and 1.76, respectively. Wilson et al [1] evaluated four tropanes using rats: [^{11}C]RTI-31, [^{11}C]RTI-32, [^{18}F]FETT and [^{18}F]FECT and found maximum striatum to cerebellum ratios of 8.7, 26.7, 21 and 14; whereas maximum hypothalamus to cerebellum ratios were 2.3, 3, 8 and 1.69. Striatum to hypothalamus ratios in this study as a sign of DAT/SERT selectivity showed values of 2.3 ([^{11}C]RTI-31), 3.0 ([^{11}C]RTI-32), 8.0 ([^{18}F]FETT) and 1.69 ([^{18}F]FECT). Günther et al [21] calculated striatum to thalamus ratios from autoradiographic slices and found 1.5±0.02 ([^{125}I]ß-CIT), 2.0±0.15 ([^{125}I]ß-CIT-FE) and 2.7±0.44 ([^{125}I]ß-CIT-FP) (Günther et al., 1997). Our study with [^{18}F]FE@CIT showed a striatum to thalamus ratio of 2.99±0.32 (60 min). Amongst the discussed tropanes [^{18}F]FE@CIT does not

show the highest affinity to the DAT, but the DAT/SERT ratio is comparatively high. These findings are also in concordance with the transporter binding affinities presented by Gu et al [8].

Organs with high uptake were liver, lung and kidney (up to 5.1% ID/g at 120 minutes/liver), whereas bowels, bone and muscle showed little uptake (max. 0.56 % ID/g, 120 minutes/bowels). Intermediate uptake was found in heart, thyroid, spleen, pancreas and the pituitary gland (max. 1.1% ID/g, 15 minutes/spleen). The increase in uptake of the kidneys over time without a concomitant increase in uptake in the bowels could be in line with the mainly renal excretion of [^{18}F]FE@CIT. Low levels of fluoride accumulation was shown in bone (max. 0.32±0.03% ID/g; femur). Autoradiographic images showed good and differentiated uptake in striatal regions with good target to background ratio (figure 4).

5. Conclusion

[^{18}F]FE@CIT was prepared via the well established distillation method and followed the expected biodistribution routes. Precursor and standard synthesis were fast and simple with good yields. Optimum reaction conditions are 10 minutes at a temperature of 150°C with a precursor concentration of ≥ 5mM. Uptake in DAT rich regions was high with striatum to thalamus/hypothalamus ratios in the upper range of comparable DAT-tracers. Ex-vivo bioevaluation together with ex-vivo autoradiographic findings support the further evaluation of [^{18}F]FE@CIT for DAT-PET.

6. Acknowledgements

The authors thank Peter Angelberger, Herbert Kvaternik, Robert Hruby and Thomas Wanek at ARCS for support during the animal experiment, Mrs Sylvia Hießberger from BSM Diagnostica for her organisation talents and support. Especially Barbara Wirl, Rupert Lanzenberger and Ulli Müller are acknowledged for lots of helping hands during the animal experiments.

7. References

[1] Wilson AA, DaSilva JN, Houle S. 1996. In Vivo Evaluation of [^{11}C]- and [^{18}F]-Labelled Cocaine Analogues as Potential Dopamine Transporter Ligands for Positron Emission Tomography. Nucl Med Biol 23:141-146.

[2] Wilson AA, DaSilva JN, Houle S. 1995**.** Synthesis of two radiofluorinated cocaine analogues using distilled 2-[^{18}F]fluoroethyl bromide. Appl Rad Isot 46:765-770.

[3] Qi-Huang Z, Mulholland GK. 1996. Improved Synthesis of ß-CIT and [^{11}C]ß-CIT Labeled at Nitrogen or Oxygen Positions. Nucl Med Biol 23:981-986.

[4] Lundkvist C, Halldin C, Ginovart N, Swahn C-G, Farde L. 1997. [^{18}F]ß-CIT-FP Is Superior to [^{11}C]ß-CIT-FP for Quantitation of the Dopamine Transporter, Nucl Med Biol 24:621-627.

[5] Lundkvist C, Halldin C, Ginovart N, Swahn C-G, Farde L. 1999. Different brain radioactivity curves in a PET study with [^{11}C]ß-CIT labelled in two different positions. Nucl Med Biol 26:343-350.

[6] Chaly T, Dhawan V, Kazumata K, Antonini A, Margouleff C, Dahl JR, Belakhlef A, Margouleff D, Yee A, Wang S, Tamagnan D, Neumeyer JL, Eidelberg D. 1996. Radiosynthesis of [^{18}F] N-3-Fluoropropyl-2-ß-Carbomethoxy-3-ß-(4-Iodophenyl) Nortropane and the First Human Study With Positron Emission Tomography. Nucl Med Biol 23:999-1004

[7]Goodman MM, Kilts CD, Keil R, Shi B, Martarello L, Xing D, Votaw J, Ely TD, Lambert P, Owens MJ, CAMP V, Malveaux E, Hoffmann JM. 2000. ^{18}F-labeled FECNT: a selective radioligand for PET imaging of brain dopamine transporters. Nucl Med Biol 27:1-12.

[8]Gu X-H, Zong R, Kula NS, Baldessarini RJ, Neumeyer JL. 2001. Synthesis and biological evaluation of a series of novel N- or O-fluoroalkyl derivatives of tropane:

potential positron emission tomography (PET) imaging agents for the dopamine transporter. Bioorganic & Medicinal Chemistry Letters 11:3049-3053.

[9] Okada T, Fujita M, Shimada S, Sato K, Schloss P, Watanabe Y, Itoh Y, Tohyama M, Nishimura T. 1998. Assessment of Affinities of beta-CIT, beta-CIT-FE, and beta-CIT-FP for Monoamine Transporters Permanently Expressed in Cell Lines. Nucl Med Biol 25:53-58.

[10] Wadsak W, Mitterhauser M. 2003. Synthesis of [^{18}F]FETO, a novel potential 11-ß hydroxylase inhibitor**.** J Label Compd Radpharm 46:379-388.

[11] Wadsak W, Mitterhauser M, Mien L-K, Tögel S, Keppler B, Dudczak R, Kletter K. 2003. Radiosynthesis of 3-(2´-[^{18}F]fluoro)-flumazenil ([^{18}F]FFMZ). J Label Compd Radpharm 46:1229-1240.

[12] Mitterhauser M, Wadsak W, Wabnegger L, Sieghart W, Viernstein H, Kletter K, Dudczak R. 2003. In vivo and in vitro evaluation of [^{18}F]FETO with respect to the adrenocortical and GABAergic system in rats. Eur J Nucl Med Mol Imaging 30:1398-1401.

[13] Mitterhauser M, Wadsak W, Wabnegger L, Mien L-K, Tögel S, Langer O, Sieghart W, Viernstein H, Kletter K, Dudczak R. 2004. Biological evaluation of 2´-[^{18}F]fluoroflumazenil ([^{18}F]FFMZ), a potential GABA receptor ligand for PET. Nucl Med Biol 31:291-295.

[14] Chi D, Kilbourn M, Katzenellenbogen J, Welsh M. 1987. A rapid and efficient method for the fluoroalkylation of amines and amides. Development of a method suitable for incorporation of the short-lived positron emitting radionuclide fluorine-18. J Org Chem 52: 658-664.

[15] Bergström KA, Halldin C, Kuikka JT, Swahn C-G, Tiihonen J, Hiltunen J, Länsimies E, Farde L. 1995. The Metabolite Pattern of [^{123}I]ß-CIT Determined with a Gradient HPLC Method. Nucl Med Biol 22:971-976

[16] Coenen HH, Dutschka K, Müller SP, Geworski L, Farahati J, Reiners C. 1995. N.c.a. radiosynthesis of [^{123}I][^{124}I]ß-CIT, plasma analysis and pharmacokinetic studies with SPECT and PET. Nucl Med Biol 22:977-984.

[17] Kula NS, Baldessarini RJ, Tarazi FI, Fisser R, Wang S, Trometer J, Neumeyer JL. 1999. [^{3}H]beta-CIT: a radioligand for dopamine transporters in rat brain tissue. Eur J Pharmacol. 385:291-4.

[18] Swahn C-G, Halldin C, Günther I, Patt J, Ametamey S. 1996. Synthesis of unlabelled, 3H- and 125I-labelled ß-CIT and its o-fluoroalkylanalogues ß-CIT-FE and ß-CIT-FP, including synthesis of precursors. J. Labelled Comp. Radiopharm. 38:675-685.

[19] Carrol FI, Kotian P, Gray JL, Kuzemko MA, Parham KA, Abraham P, Lewin AH, Boja JW, Kuhar MJ. 1995. Cocaine and 3ß-(4'-substituted phenyl)tropane carboxylic ester and amide analogues. New high-affinity and selective compounds for the dopamine transporter. J Med Chem 38:379-388.

[20] Lavalaye J, Knol RJ, de Bruin K, Reneman L, Janssen AG, Booij J. 2000. [^{123}I]FP-CIT binding in rat brain after acute and sub-chronic administration of dopaminergic medication. Eur J Nucl Med. 27:346-349.

[21] Günther I, Hall H, Halldin C, Swahn C-G, Farde L, Sedvall G. 1997. [^{125}I]ß-CIT-FE and [^{125}I]ß-CIT-FP Are Superior to [^{125}I]ß-CIT for Dopamine Transporter Visualization: Autoradiographic Evaluation in the Human Brain. Nucl Med Biol 24:629-634.

Figures and tables

Figure 1 shows a scheme of the synthesis of FE@CIT and [^{18}F]FE@CIT. Reagents and conditions: a) 6N HCl, reflux; b) standard synthesis: 2-fluoroethanol, DMAP, EDCI, dichloromethane; c) radiosynthesis: TBAH, DMF, [^{18}F]BFE, 150C°.

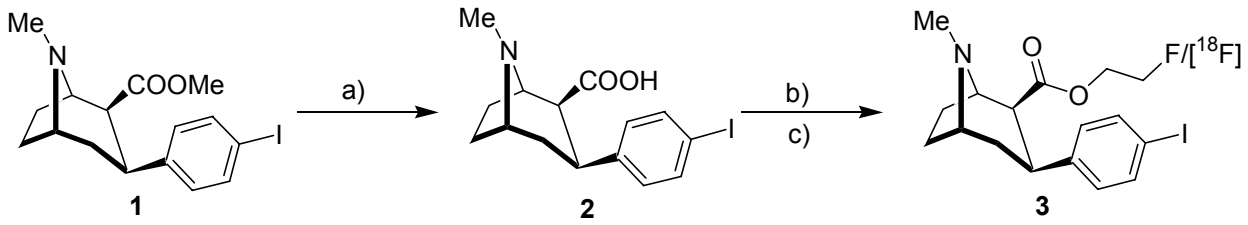

Figure 2 shows the dependence of the radiochemical yield of [^{18}F]FE@CIT and [^{18}F]BFE on reaction temperature (5mM, 20min, means ± SD; n≥4; P=0.95).

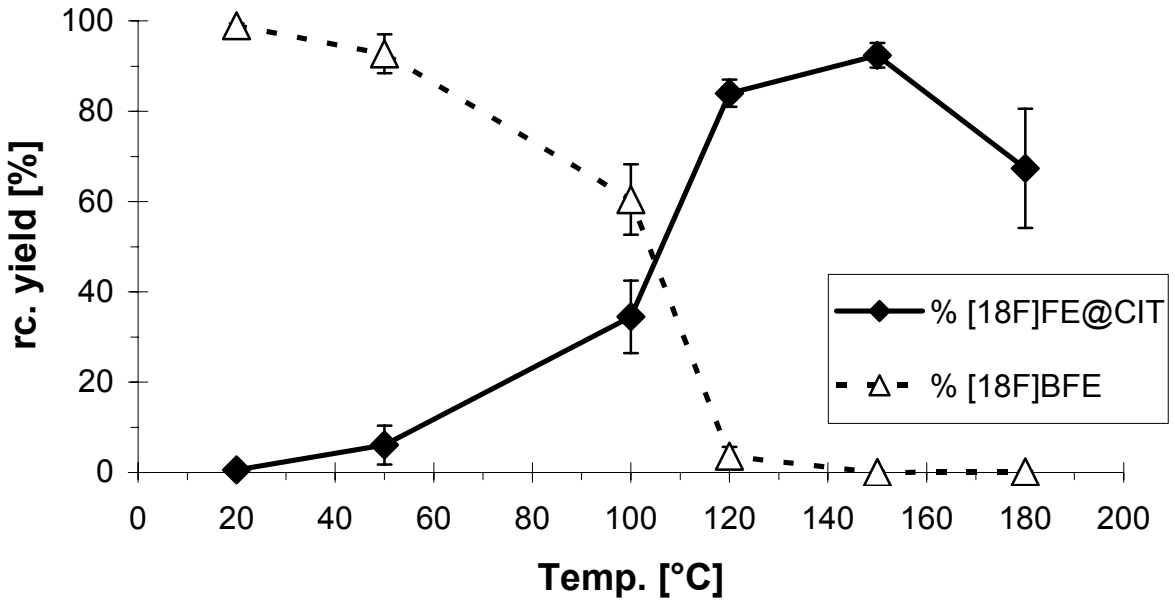

Figure 3 shows the dependence of the radiochemical yield of [^{18}F]FE@CIT on the amount of precursor (150°C; means ± SD; n≥4; P=0.95).

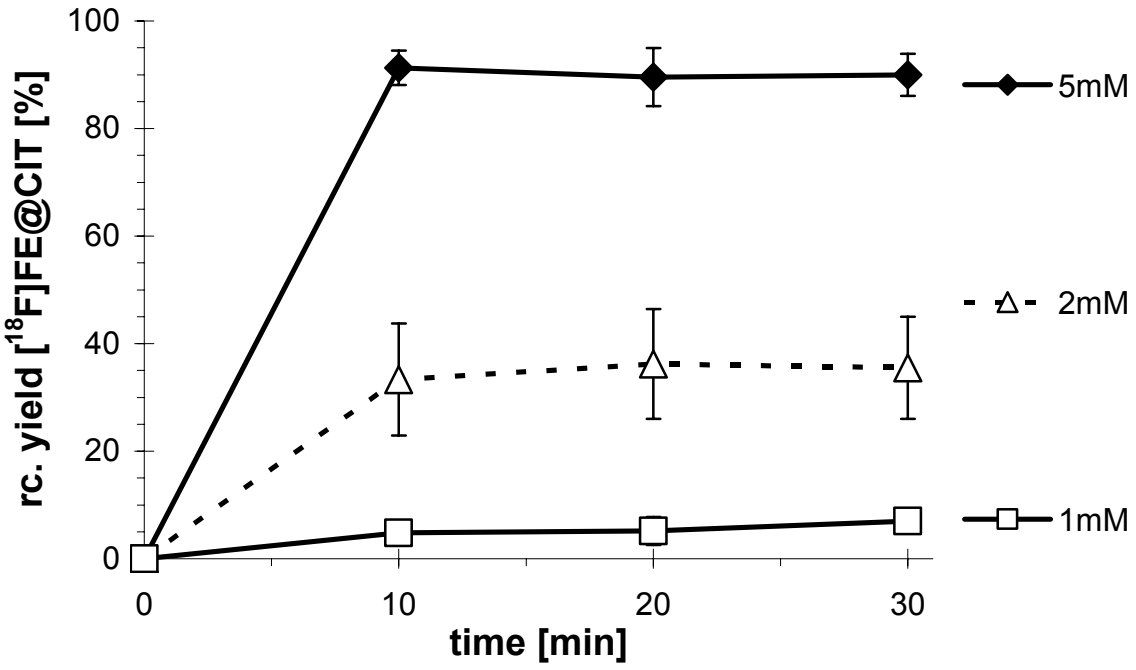

Table 1 on the next page shows the values counted in various organs at different time points after application of 1.25-2.23 MBq [^{18}F]FE@CIT as percent injected dose per gram organ (% ID/g; mean values +/- SD).

Tissue	5min	15min	30min	60min	120min
blood	0,27 ± 0,05	0,23 ± 0,04	0,17 ± 0,01	0,15 ± 0,03	0,10 ± 0,03
bone (femur)	0,32 ± 0,03	0,30 ± 0,02	0,19 ± 0,06	0,14 ± 0,02	0,10 ± 0,03
colon	0,30 ± 0,04	0,27 ± 0,06	0,19 ± 0,08	0,14 ± 0,01	0,14 ± 0,04
fat	0,13 ± 0,03	0,23 ± 0,12	0,21 ± 0,10	0,21 ± 0,04	0,17 ± 0,03
heart	0,63 ± 0,07	0,34 ± 0,04	0,18 ± 0,05	0,14 ± 0,01	0,10 ± 0,02
ileum/ jejunum	0,33 ± 0,12	0,53 ± 0,21	0,37 ± 0,13	0,54 ± 0,33	0,56 ± 0,30
kidney	2,12 ± 0,60	2,54 ± 1,01	2,30 ± 1,44	3,86 ± 2,05	3,14 ± 2,11
liver	0,54 ± 0,11	1,47 ± 0,31	1,68 ± 0,79	3,06 ± 0,46	5,09 ± 0,64
lung	3,57 ± 0,89	2,30 ± 0,48	1,33 ± 0,45	0,86 ± 0,13	0,52 ± 0,08
muscle	0,34 ± 0,05	0,26 ± 0,02	0,16 ± 0,07	0,16 ± 0,09	0,07 ± 0,02
pancreas	0,73 ± 0,09	0,83 ± 0,12	0,44 ± 0,15	0,30 ± 0,02	0,17 ± 0,02
pituitary gland	0,73 ± 0,22	0,61 ± 0,32	0,46 ± 0,24	0,44 ± 0,18	0,24 ± 0,07
spleen	0,54 ± 0,24	1,08 ± 0,13	0,70 ± 0,25	0,49 ± 0,03	0,27 ± 0,04
tail	0,90 ± 0,71	0,84 ± 0,81	0,61 ± 0,63	0,72 ± 0,57	0,28 ± 0,11
testes	0,18 ± 0,02	0,27 ± 0,05	0,24 ± 0,10	0,28 ± 0,06	0,34 ± 0,07
thyroid	0,76 ± 0,46	0,70 ± 0,34	0,41 ± 0,20	0,35 ± 0,23	0,42 ± 0,41
striatum	1,35 ± 0,26	1,96 ± 0,20	1,43 ± 0,06	1,23 ± 0,08	0,48 ± 0,07
thalamus/ hypothalamus	0,89 ± 0,11	0,80 ± 0,04	0,66 ± 0,06	0,42 ± 0,06	0,27 ± 0,04
cerebellum	0,89 ± 0,04	0,82 ± 0,09	0,56 ± 0,02	0,33 ± 0,04	0,16 ± 0,01
carcass	0,42 ± 0,10	0,39 ± 0,12	0,30 ± 0,11	0,22 ± 0,01	0,17 ± 0,08

Figure 4 shows an autoradiography of an ex vivo mid-brain slice from a single rat 60 minutes after i.v. administration of [^{18}F]FE@CIT.

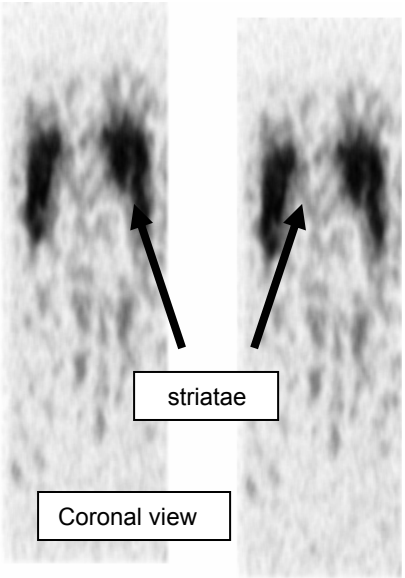

Figure 5 shows the kinetics of three brain regions expressed as % ID/g x g bodyweight (means ± SD; n=4; P=0.95).

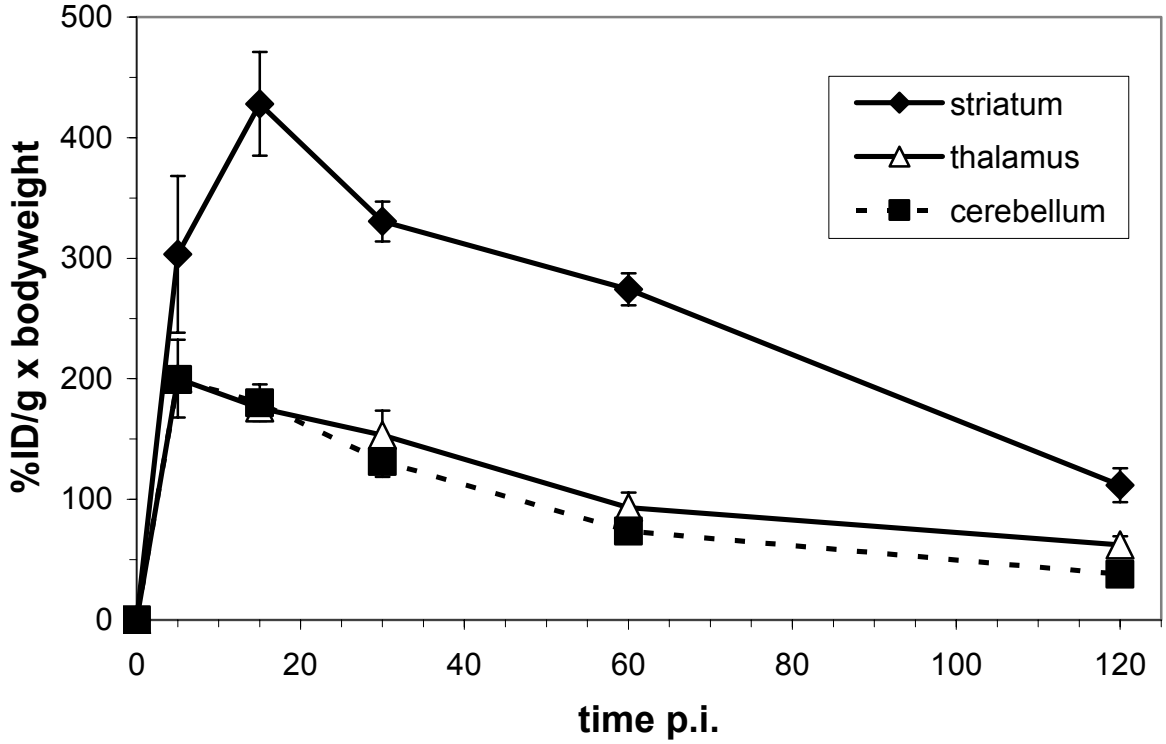

Figure 6 shows distribution volume ratios (DVR) representing tissue to cerebellum ratios at various time points (% ID/g; means ± SD; n=4; P=0.95). The asterisk (*) signs values for [^{123}I]FP-CIT taken from reference [Lavalaye J. et al] for reasons of comparison. Statistical P-values are given for DVR(striatum) vs. DVR (thalamus/hypothalamus) and were determined via t-test for comparison of two means from independent (unpaired) samples with α=0.05.

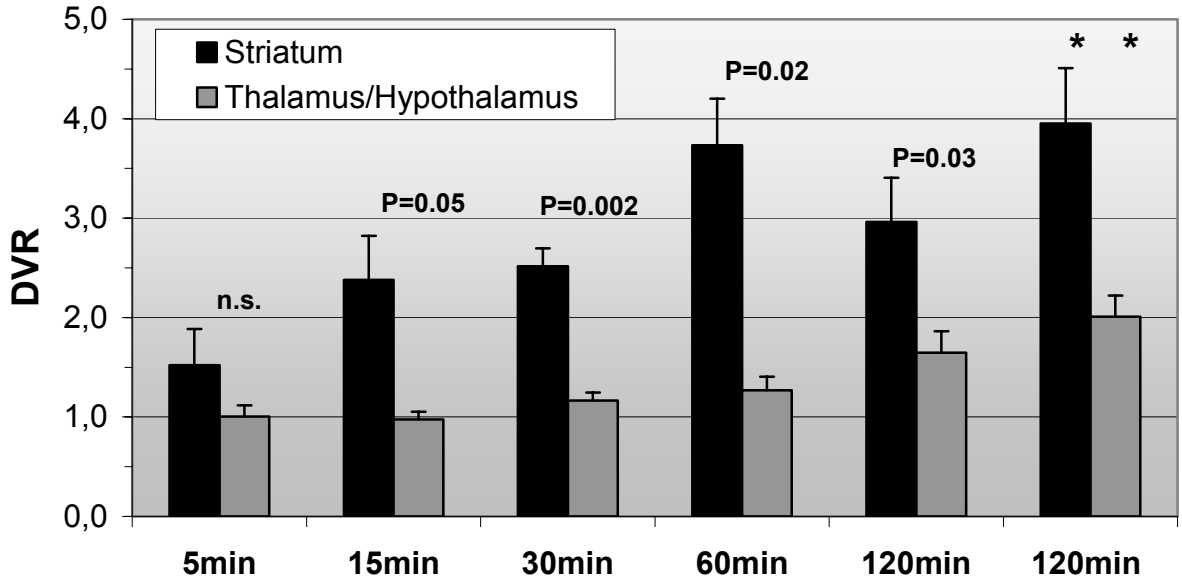

2.2. Paper 2

Preparation and Biodistribution of [^{18}F]FE@CFN (2-[^{18}F]fluoroethyl 4-[N-(1-oxopropyl)-N-phenylamino]-1-(2-phenylethyl)-4-piperidinecarboxylate), a Potential μ-Opioid Receptor Imaging Agent

Radiochim. Acta 95: 33-38 (2007)

AUTHORS: Wolfgang Wadsak[1,2,*]; Leonhard-Key Mien[1,3,4]; Dagmar E. Ettlinger[1]; Sylvia Feitscher[1,4]; Stefan Toegel[1,4]; Rupert Lanzenberger[3]; Janos Marton[5]; Robert Dudczak[1,6]; Kurt Kletter[1] and Markus Mitterhauser[1,4,7].

1 Department of Nuclear Medicine, Medical University of Vienna, Austria

2 Department of Inorganic Chemistry, University of Vienna, Austria

3 Department of Psychiatry, Medical University of Vienna, Austria

4 Department of Pharmaceutical Technology and Biopharmaceutics, University of Vienna, Austria

5 ABX – Advanced Biochemical Compounds, Radeberg, Germany

6 Ludwig-Boltzmann-Institute for Nuclear Medicine, Vienna, Austria

7 Hospital Pharmacy of the General Hospital of Vienna, Austria

Abstract

PET imaging of the μ-opioid receptor (OR) is still restricted to [^{11}C]carfentanil ([^{11}C]CFN) but its use is limited due to its short half-life and high agonistic potency. Recently, the radiosynthesis of [^{18}F]fluoroalkyl esters of CFN was proposed, unfortunately yielding products not suitable for human PET due to their low specific activities. Therefore, our rationale was the reliable radiosynthesis of a [^{18}F]fluoroethylated CFN derivative overcoming these drawbacks and its preliminary bioevaluation in rats.

The [^{18}F]fluoroethyl ester of carfentanil, [^{18}F]FE@CFN (2-[^{18}F]fluoroethyl 4-[N-(1-oxopropyl)-N-phenylamino]-1-(2-phenylethyl)-4-piperidinecarboxylate), and its corresponding inactive standard compound were prepared. Purification of [^{18}F]FE@CFN was achieved via solid phase extraction. Whole body biodistribution was investigated in rats and μ-OR selective binding was measured autoradiographically in rat brain slices.

[^{18}F]FE@CFN was prepared with excellent purity (>98%) and sufficient yields. Specific activity surpassed the level required for safe administration. In rats, considerable uptake was observed in ileum, lung, kidney and heart. Uptake in the rat brain peaked at 5 min (0.21 %ID/g). On autoradiographic slices, highest uptake was seen in the olfactory bulb and cerebral cortex whereas almost no uptake in the cerebellum was observed, matching the known distribution of μ-OR in the rat brain excellently.

Our simplified synthesis of [^{18}F]FE@CFN, for the first time, overcomes the shortcomings of [^{11}C]CFN and the previously suggested alternatives: (1) longer half-life; (2) easy production and (3) adequate specific activity should make a wider application possible. Hence, [^{18}F]FE@CFN may become a valuable PET tracer for the imaging of the μ-OR in human brain and heart.

Summary

PET imaging of the μ-opioid receptor (OR) is still restricted to [^{11}C]carfentanil ([^{11}C]CFN) but its use is limited due to its short half-life and high agonistic potency. Recently, the radiosynthesis of [^{18}F]fluoroalkyl esters of CFN was proposed, unfortunately yielding products not suitable for human PET due to their low specific activities. Therefore, our rationale was the reliable radiosynthesis of a [^{18}F]fluoroethylated CFN derivative overcoming these drawbacks.

The [^{18}F]fluoroethyl ester of carfentanil, [^{18}F]FE@CFN (2-[^{18}F]fluoroethyl 4-[N-(1-oxopropyl)-N-phenylamino]-1-(2-phenylethyl)-4-piperidinecarboxylate), and its corresponding inactive standard compound were prepared. Purification of [^{18}F]FE@CFN was achieved via a simple solid phase extraction method. [^{18}F]FE@CFN was prepared with excellent purity (>98%) and sufficient yields. Specific activity surpassed the level required for safe administration. We therefore conclude that our simplified synthesis of [^{18}F]FE@CFN, for the first time, overcomes the shortcomings of [^{11}C]CFN and the previously suggested alternatives: (1) longer half-life; (2) easy production and (3) adequate specific activity should make a wider application possible. Hence, [^{18}F]FE@CFN may become a valuable PET tracer for the imaging of the μ-OR in human brain and heart.

KEY WORDS: opioid receptor; carfentanil; fluorine-18; fluoroalkylation; PET

Introduction

The existence of a specific opiate receptor (OR) was demonstrated by Candace B. Pert and Sol H. Snyder in 1973 [1]. Since that time, a number of OR subtypes have been revealed [2]. Of the three major classes of opioid receptors (OR) - μ, κ and δ - the μ receptor is by far the one most important. Activation of the μ-OR by an agonist such as morphine causes symptoms such as analgesia, sedation, reduced blood pressure, itching, nausea, euphoria, decreased respiration, miosis and decreased bowel motility. Although tolerance to respiratory depression develops relatively quickly, it is the single most adverse side effect of opioid use. In medicine, opioids are widely used as effective analgesics for severe pain (www.opiods.com).

Fentanyl, an artificial opioid analgesic with a potency of about 80 times that of morphine, was synthesized in the late 1950s. Lateron, several fentanyl analogues were developed. Carfentanil (CFN) is an extremely potent (analgesic potency 10,000 times that of morphine), synthetic opiate binding to the μ-subtype of the OR with very high affinity (Ki = 0.051 nM). In rats, CFN was found to be 90 and 250 times more selective for μ-OR compared to δ- and κ-subtypes, respectively [3].

Today, positron emission tomography (PET) of the μ-OR is still restricted to [^{11}C]CFN although the short half life of carbon-11 (20 min) together with the unavoidably low specific activities limit its application to PET centres with an on-site production facility. Nevertheless, continuous work is done with [^{11}C]CFN concerning various topics such as alcohol abuse and detoxification [4], therapeutic effectiveness in heroin addicts [5], pain activation [6, 7] or temporal lobe epilepsy [8].

Recent findings demonstrated that μ-OR imaging with PET could, beside its application in the human brain, become a very useful tool also in cardiology resulting in a better insight in the cardiovascular pathophysiology, especially in the ischemic heart and in arrhythmias. Furthermore, cardiovascular effects of drug abuse and

chronic μ-OR stimulation could be evaluated and quantified [9-11]. Although the booming interest of the community is demonstrated by the afore mentioned publications, the drawbacks of the short half-life of [^{11}C]CFN and its extremely high potency still have to be overcome to allow a broader application of μ-OR imaging with PET.

Therefore, different strategies to ameliorate the applicability of [^{11}C]CFN have been followed lately, resulting in derivatives labelled with either carbon-11 [12] or fluorine-18 [13-15].

Our group recently presented a feasible method for the synthesis of [^{18}F]fluoroethyl ester ligands based on their methylester relatives proving biologically more stable than methyl or ethyl esters [16-20]. Simultaneously to our investigations regarding the preparation of a [^{18}F]fluoroethylated CFN, the radiosynthesis of [^{18}F]fluoroalkyl esters of CFN was described elsewhere [21]. There, the authors conclude: (1) the fluoroethyl ester is favourable to the fluoropropyl compound; and (2) the specific activity achieved with their radiosynthesis is less than required for the application in human PET imaging.

Thus, our aim was the simplified preparation and improved radiosynthesis of [^{18}F]FE@CFN with high specific activities.

Materials and Methods

General

All reagents and chemicals were purchased from Merck (Darmstadt, Germany), Sigma-Aldrich Chemical (Steinheim, Germany) or Riedel-de Haen (Seelze, Germany) and used without further purification. [^{18}F]Fluoride was produced via the ^{18}O(p,n)^{18}F reaction in a GE PETtrace cyclotron (16.5 MeV protons). $H_2{}^{18}O$ (>97%) was purchased from Rotem (Leipzig, Germany). Solid phase extraction cartridges

(SepPak® C18plus) were purchased from Waters Associates (Milford, MA). Melting points were measured with a Büchi-535 instrument. The ^{1}H-NMR and ^{13}C-NMR spectra were obtained with a Bruker 500 spectrometer at 20°C in DMSO-d_6, $CDCl_3$ and D_2O, respectively.

Precursor and Standard Synthesis

For inactive precursor and standard syntheses, analytical thin-layer chromatography was performed on Macherey-Nagel Alugram® Sil G/UV254 40x80 mm aluminium sheets (Dueringen, Germany) with the following eluent systems (v/v): [A]: chloroform-methanol 9:1; [B]: ethyl acetate-methanol 8:2. The spots were visualized with a 254 nm UV lamp or with 5% phoshomolybdic acid in ethanol. Preparative system: pump: Merck/Knauer K-1800; column: Phenomenex 100A, Nucleosil C18; flow: 5 mL/min; eluent: methanol-water-acetic acid 70:30:0.1 (v/v/v); UV detector: Merck/Knauer K-2501, λ = 254 nm. Column chromatography was performed on silica gel (Kieselgel 60, Merck (0.040-0.063 mm)).

Benzyl 4-[(1-oxopropyl)phenylamino]-1-(2-phenylethyl)-4-Piperidinecarboxylate (**1a,** figure 1) was prepared according to a literature method [22, 23].

Desmethylcarfentanil free acid (**1b**) precursor was synthesized by hydrogenolysis of **1a** (4 bar, 16 h). The fluoroalkylation of **1b** was performed via **1c** [23] with 1-brom-2-fluoroethan in dry N,N-Dimethylformamide. NMR assignments are based on a standard reference [24].

4-[N-(1-oxopropyl)-N-Phenylamino]-1-(2-phenylethyl)-4-piperidinecarboxylic acid (1b)

A solution of Benzyl 4-[N-(1-oxopropyl)-N-Phenylamino]-1-(2-phenylethyl)-4-piperidinecarboxylate (**1a**) (470 mg, 1 mmol) in ethanol (50 mL) was hydrogenolysed in the presence of Pd/C 10 % (100 mg) at room temperature and 4 bar for 16 h. The

catalyst was removed by filtration and the solvent was evaporated in vacuum. The residual white powder was purified by column chromatography on silica gel. Eluent systems: 1. chloroform-methanol 9:1 to 7:3. 2. methanol-acetic acid 9:1. TLC: R_f[A] = 0.13; R_f[B] = 0.1. The crude product was purified by preparative RP-HPLC (t_R = 17.6 min).

2-Fluoroethyl 4-[N-(1-oxopropyl)-N-Phenylamino]-1-(2-phenylethyl)-4-piperidine-carboxylate (1d)

To a stirred suspension of 4-[N-(1-oxopropyl)-N-phenylamino]-1-(2-phenylethyl)-4-piperidine-carboxylic acid sodium salt (**1c**) (100 mg, 0.248 mmol) in dry N,N-Dimethylformamide (6 mL) under argon atmosphere 2-bromo-1-fluoroethane (40 mg, 0.273 mmol) was added. The solution was stirred at room temperature for 24h. The reaction mixture was poured onto water (50 mL) and extracted with chloroform (3x25 mL). The organic phase was dried (Na_2SO_4). The solvent was evaporated in vacuum and the residual oil was purified by column chromatography on silica gel (50 g) with hexane-ethyl acetate 1:1 (v/v). The pure fractions were collected and the eluent was evaporated yielding an oily residue – R_f[A] = 0.76; R_f[B] = 0.78 – The residue was dissolved in dry diethyl ether (5 mL) and a solution of 2 M HCl in diethyl ether was given. The crystalline product was filtered off and dried in vacuum ($3x10^{-1}$ mbar).

Radiosynthesis

Radio-analytical thin-layer chromatography (radio-TLC) was performed using silicagel 60 F254 plates from Merck. Analysis of radio-TLC plates was performed using a digital autoradiograph (Berthold Technologies, Bad Wildbad, Germany). Analytical high-performance liquid chromatography (HPLC) was performed using a LiChrospher 100 RP-18 column (5 µm, 250 x 4 mm) from Merck on a Merck-Hitachi LaChrom L-

7100 system equipped with a Merck-Hitachi LaChrom L-7400 UV detector at 235 nm and a lead-shielded NaI-radiodetector (Berthold Technologies).

2-Bromoethyl triflate

2-Bromoethyl triflate was prepared according to a literature method [25] starting from tri-fluoromethanesulfonic anhydride and 2-bromoethanol.

2-Bromo-1-[^{18}F]fluoroethane ([^{18}F]BFE)

No-carrier-added (n.c.a.) aqueous [^{18}F]fluoride was added to a 2.5 mL v-vial containing kryptofix 2.2.2. (13.3 µmol), potassium carbonate (10.0 µmol) and acetonitrile (1.0 mL, 19.1 mmol) and heated to 100°C. Azeotropic drying was performed by subsequent addition of at least four 250 µL portions of acetonitrile. To the dried complex 2-bromoethyl triflate (20 µL, 77.8 µmol) and acetonitrile (80 µL, 1.5 mmol) were added, the vial was sealed and heated at 100°C (10 min).

Distillation

Volatiles were distilled using a smooth stream of nitrogen (6 mL/min) through a washing flask (containing 195 µL of DMSO and 5 µL of anhydrous DMF at ambient temperature) into the product trap containing 300 µL of anhydrous DMF at 0°C. A total of 200 µL of acetonitrile was added in small portions to the reaction vessel to achieve quantitative distillation of [^{18}F]BFE.

[^{18}F]FE@CFN (2a)

10 mg (26.3 µmol) CFN-acid (1b) were dissolved in 300 µL dichloromethane, 28 µL tetrabutylammonium hydroxide solution (TBAH, 1 M in methanol) was added and dichloromethane was evaporated. The dried complex was reconstituted in 1000 µL anhydrous DMF. A calculated aliquot of this solution was added to the distilled [^{18}F]BFE to achieve the desired molarity. The reaction was carried out for 5–20 min at temperatures from 20–150°C.

Product purification

The product solution was diluted with a total of 35 mL water and loaded onto a preconditioned C18plus SepPak® cartridge. After washing with a further 10 mL of water, the purified [^{18}F]FE@CFN was quantitatively eluted with 1.2 mL of ethanol.

Quality control

Chemical and radiochemical impurities were detected using radio-HPLC (mobile phase: 65% (water/ethanol/acetic acid 87.5/10/2.5 (v/v/v), 2.5 g/L ammonium acetate, pH 3.5)/35% acetonitrile) and radio-TLC (mobile phase: 95% acetonitrile/5% water). Residuals of kryptofix 2.2.2 were analyzed by TLC according to the [^{18}F]FDG monograph in the European Pharmacopoeia (mobile phase: 90% methanol/10% ammonia (v/v); iodine chamber).

Results

Precursor and Standard Synthesis

4-[N-(1-oxopropyl)-N-Phenylamino]-1-(2-phenylethyl)-4-piperidinecarboxylic acid (1b)

Yield: 170 mg (44 %) – melting point: 230.0-233.5°C – 1H-NMR (DMSO-d_6) δ = 12.43 (brs, 1H, COO<u>H</u>); 7.19-7.49 (m, 7H, CH_2CH_2<u>Ph</u>, NPh); 7.14 (m, 3H, N<u>Ph</u>); 2.59-2.64 (m, 2H, <u>CH_2</u>CH_2Ph); 2.52-2.54 (m, 2H, CH_2<u>CH_2</u>Ph); 2.33-2.34-2.43 (m, 4H, 2x<u>CH_2</u>CH_2); 2.04-2.13 (m, 2H, <u>CH_2</u>CH_2); 1.75 (q, J = 7.4 Hz, 2H, CH_3<u>CH_2</u>CO); 1.52 (m, 2H, <u>CH_2</u>CH_2); 0.80 (t, J = 7.4 Hz, 3H, <u>CH_3</u>CH_2CO) – 13C-NMR (DMSO-d_6) δ =174.23 (<u>C</u>OOH); 173.96 (CH_3CH_2<u>C</u>O); 139.05 (NPh-C1); 137.32 (βPh-C1); 130.99 (NPh-C3,5); 130.49 (βPh-C3,5); 129.93 (βPh-C2,6); 129.50 (βPh-C4); 129.46 (NPh-C4); 127.71 (NPh-C2,6); 60.21 (C-4); 57.22 (<u>CH_2</u>CH_2Ph); 49.85 (C-2,6); 30.98 (CH_2<u>CH_2</u>Ph); 30.31 (C3,5); 29.13 (CH_3<u>CH_2</u>CO); 9.77 (<u>CH_3</u>CH_2CO) – $C_{23}H_{28}N_2O_3$ (380,48).

2-Fluoroethyl 4-[N-(1-oxopropyl)-N-Phenylamino]-1-(2-phenylethyl)-4-piperidine-carboxylate (1d)

Yield: 110 mg (48 %) **1d** HCl – melting point: 210.0-211.7°C – 1c base: 1H-NMR ($CDCl_3$) δ = 7.22-7.45 (m, 7H, $CH_2CH_2\underline{Ph}$, NPh); 7.13-7.19 (m, 3H, N$\underline{Ph}$); 4.65 (dm, J = 47.5 Hz, 2H, $CH_2\underline{CH_2}F$); 4.45 (dm, J = 29.1 Hz, 2H, $\underline{CH_2}CH_2F$); 2.69-2.78 (m, 2H, $\underline{CH_2}CH_2Ph$); 2.53-2.59 (m, 2H, $CH_2\underline{CH_2}$); 2.45-2.52 (m, 2H, $\underline{CH_2}CH_2$); 2.30-2.37 (m, 2H, $\underline{CH_2}CH_2$); 1.88 (q, J = 7.4 Hz, 2H, $CH_3\underline{CH_2}CO$); 1.67 (m, 2H, $\underline{CH_2}CH_2$); 0.96 (t, J = 7.4 Hz, 3H, $\underline{CH_3}CH_2CO$) – 1c HCl: 13C-NMR (D_2O+CD_3OD) δ = 177.37 ($\underline{C}OOCH_2CH_2F$); 172.96 ($CH_3CH_2\underline{C}O$); 137.42 (NPh-C1); 136.12 (βPh-C1); 130.05 (NPh-C3,5); 129.99 (βPh-C3,5); 129.85 (βPh-C2,6); 129.07 (βPh-C4); 128.70 (NPh-C4); 127.38 (NPh-C2,6); 81.83 ($CH_2\underline{CH_2}F$, J = 165.4 Hz); 65.09 ($\underline{CH_2}CH_2F$, J = 18.8 Hz); 60.61 ($\underline{CH_2}CH_2Ph$); 57.31 (C-4); 49.36 (C-2,6); 30.05 ($CH_2\underline{CH_2}Ph$); 29.82 (C3,5); 28.57 ($CH_3\underline{CH_2}CO$); 8.53 ($\underline{CH_3}CH_2CO$) – $C_{25}H_{31}FN_2O_3$ (426,52).

Radiosynthesis

A reaction scheme of the synthesis is presented in figure 2, showing the optimized conditions used in the two-step preparation of [^{18}F]FE@CFN.

Yields depending upon varying reaction conditions are presented in figure 3: a reaction temperature of 150°C with a precursor concentration of at least 5 mM should be applied for more than 5 min for satisfactory preparation of [^{18}F]FE@CFN. The product was identified by co-elution of the radioactive solution with the inactive reference standard both on HPLC and radio-TLC (TLC – R_f values: FE@CFN: 0.7-0.8, BFE/fluoride: 0.0; HPLC – retention times: precursor: 3.9 min; FE@CFN: 8.3 min; BFE: 3.4 min). Radiochemical purity in the final solution exceeded 98% (specific radioactivity up to 154 GBq/µmol (4,162 Ci/mmol)). The radiosynthesis evinced radiochemical yields of >75% (based on [^{18}F]BFE). An average 40 µAh cyclotron

irradiation yielded more than 1.5 GBq purified and ready for application formulated [^{18}F]FE@CFN.

Discussion

General

[^{11}C]CFN has played an important role in neuroimaging of the μ-OR for more than a decade. Despite the high agonistic potency of the compound and its limitations in availability due to the short half-life (20 min) prominent research groups have demonstrated their interest in μ-OR imaging for psychiatry and cardiology. Lately, some modified analogues have been synthesized and evaluated for PET, but none of the compounds exhibited satisfactory properties.

Since the potency of the ethyl ester analogue of CFN is 13-times less than that of unmodified CFN [26] the fluoroethylated compound is discussed to exhibit a similarly reduced potency. Therefore, Henriksen et al. [21] proposed that the required specific activity of the final product solution will also be reduced. Furthermore, pharmacological effects of CFN cannot be excluded for administration of more than 2.1 μg/70 kg [27]. Disregarding this (assumedly) reduced potency of [^{18}F]FE@CFN, the specific activity at the time of injection has to be >75.2 GBq/μmol for the safe administration of 370 MBq of [^{18}F]FE@CFN. Our preparation surpassed this value reproducibly, revealing values of up to 154 GBq/μmol in contrast to Henriksen at al. [21] who only found 35 GBq/μmol.

Thus, our method for the preparation of [^{18}F]FE@CFN could overcome the previous shortcomings by (1) displaying satisfactory high specific activities; (2) assuring its wider availability and (3) guaranteeing its safe use also in human PET studies.

Radiosynthesis

The presented method was already applied for a variety of PET- radiotracers and proved reliable and feasible throughout various preclinical [17, 19, 20] and even clinical experiments [16, 18, 28]. During the radiosynthesis, the use of a washing flask in the distillation is indispensable to provide reactive, highly purified [^{18}F]BFE, a prerequisite for successful syntheses [16, 17, 20]. Unfortunately, this purification of the intermediate substrate also accounts for the major loss of activity throughout the preparation. Radiochemical yield for the subsequent conversion reaction depended on reaction temperature and time as well as amount of precursor. The described method uses solid phase extraction (SPE) for product purification and is easy to adapt for a remotely controlled synthesis module. As a further improvement, no semi-preparative HPLC system is needed throughout the preparation. Thus, a significant reduction in the overall synthesis time – 55 min (this work) versus 100 min [21] – was achieved and the instrumental requirements were kept to a minimum. The biodistribution experiments revealed high uptake for ileum, heart, lung, and kidney – all organs known to possess high μ-OR densities – whereas muscle and bone showed little uptake (table 1.). Thus, de-fluorination seems to play a subordinate role in peripheral metabolism whereas ester cleavage seems rather probable due to increased liver uptake. This fact was also discussed in a preliminary abstract [13]. Again, also considerable uptake was observed in the heart supporting previous findings about μ-OR in this organ. [^{18}F]FE@CFN therefore could become an interesting PET tracer for the imaging of the cardiovascular pathophysiology and especially for quantification of cardiovascular effects of drug abuse and chronic μ-OR stimulation.

Autoradiographic rat brain images showed uptake in μ-OR rich regions. Cerebral cortex and olfactory bulb showed high tracer accumulation whereas almost no uptake

of [^{18}F]FE@CFN could be observed in the cerebellum (Fig. 4). This excellent congruence with the known distribution of the μ-OR in the rat brain further substantiates the selectivity of the radiotracer. Further investigations are under way to enlighten the specificity of μ-OR binding and the metabolic stability of [^{18}F]FE@CFN prior to its use in human PET studies.

Conclusion

[^{18}F]FE@CFN was prepared with excellent purity in sufficient radiochemical yields to serve for routine PET imaging. The specific activity was well above the level required for its safe administration. Thus, our method for the preparation of [^{18}F]FE@CFN, for the first time, overcomes the shortcomings of [^{11}C]CFN: due to (1) the longer half-life; (2) its easy production and (3) the adequate specific activity a wider application should become possible.

Acknowledgements

Parts of the presented work were supported by a research grant from the Austrian National Bank (“Jubiläumsfonds der Österreichischen Nationalbank”), project number #8263.

References

[1] Pert CB, Snyder SH.1973 Opiate receptor. Demonstration in nervous tissue. Science **179**:1011-1014.

[2] Fowler CJ, Fraser GL. 1994. Mu-, delta-, kappa-opioid receptors and their subtypes. A critical review with emphasis on radioligand binding experiments. Neurochem Int **24**: 1336-1341.

[3] Frost JJ, Wagner HN Jr, Dannals RF, Ravert HT, Links JM, Wilson AA, Burns HD, Wong DF, McPherson RW, Rosenbaum AE. 1985. Imaging opiate receptors in the human brain by positron tomography. J Comp Ass Tomogr **9**: 231-236.

[4] Heinz A, Reimold M, Wrase J, Hermann D, Croissant B, Mundle G, Dohmen BM, Braus DH, Schumann G, Machulla HJ, Bares R, Mann K. 2005. Correlation of stable elevations in striatal mu-opioid receptor availability in detoxified alcoholic patients with alcohol craving: a positron emission tomography study using carbon 11-labeled carfentanil. Arch Gen Psych **62**: 57-64.

[5] Greenwald MK, Johanson CE, Moody DE, Woods JH, Kilbourn, MR, Koeppe RA, Schuster CR, Zubieta JK. 2003. Effects of buprenorphine maintenance dose on mu-opioid receptor availability, plasma concentrations, and antagonist blockade in heroin-dependent volunteers. Neuropsychopharmacology **28**: 2000-2009.

[6] Sprenger T, Berthele A, Platzer S, Boecker H, Tolle TR. 2005. What to learn from in vivo opioidergic brain imaging? Eur J Pain **9**: 117-121.

[7] Bencherif B, Fuchs PN, Sheth R, Dannals RF, Campbell JN, Frost JJ. 2002. Pain activation of human supraspinal opioid pathways as demonstrated by [11C]-carfentanil and positron emission tomography (PET). Pain **99**: 589-598.

[8] Madar I, Lesser RP, Krauss G, Zubieta JK, Lever JR, Kinter CM, Ravert HT, Musachio JL, Mathews WB, Dannals RF, Frost JJ. 1997. Imaging of delta- and mu-opioid receptors in temporal lobe epilepsy by positron emission tomography. Ann Neur **41**: 358-367.

[9] Villemagne PS, Dannals RF, Ravert HT, Frost JJ. 2002. PET imaging of human cardiac opioid receptors. Eur J Nucl Med Mol Imag **29**: 1385-1388.

[10] Kienbaum P, Heuter T, Michel MC, Scherbaum N, Gastpar M, Peters J. 2001. Chronic mu-opioid receptor stimulation in humans decreases muscle sympathetic nerve activity. Circulation **103**: 850-855.

[11] Kienbaum P, Heuter T, Scherbaum N, Gastpar M, Peters J. 2002. Chronic mu-opioid receptor stimulation alters cardiovascular regulation in humans: differential effects on muscle sympathetic and heart rate responses to arterial hypotension. J Cardiovasc Pharm **40**: 363-369.

[12] Jewett DM, Kilbourn MR. 2004. In vivo evaluation of new carfentanil-based radioligands for the mu opiate receptor. Nucl Med Biol **31**: 321-325.

[13] Henriksen G, Platzer S, Schuetz J, Schmidhammer H, Rafecas ML, Schwaiger M, Wester HJ. 2003. ^{18}F-Fluorinated agonists and antagonists for imaging of μ-opioid receptors: approaches to ^{18}F-Carfentanil, ^{18}F-Sufentanil and ^{18}F-Cyprodime J Lab Compd Radiopharm **46**: 175 (abstract)

[14] Henriksen G, Platzer S, Hauser A, Herz M, Boecker H, Toelle TR, Schwaiger M, Wester HJ. 2004. 18F-labeled 4-anilidopiperidenes: promising alternatives to 11C-carfentanil from mu-opioid receptor imaging with PET. Eur. J. Nucl Med Mol Imag 31: 250 (abstract)

[15] Henriksen G, Platzer S, Hauser A, Willoch F, Berthele A, Schwaiger M, Wester HJ. 2005. 18F-Labeled sufentanil for PET-imaging of μ-opioid receptors. Bioorg. Med Chem Lett 15**:** 1773-1777

[16] Wadsak W, Mitterhauser M. 2003. Synthesis of [^{18}F]FETO, a novel potential 11-beta hydroxylase inhibitor. J Lab Compd Radiopharm 46: 379-388

[17] Wadsak W, Mitterhauser M, Mien LK, Toegel S, Keppler B, Dudczak R, Kletter K. 2003. Radiosynthesis of 3-(2'-[18F]fluoro)-flumazenil ([18F]FFMZ). J Lab Compd Radiopharm 46: 1229-1240

[18] Mitterhauser M, Wadsak W, Wabnegger L, Sieghart W, Viernstein H, Kletter K, Dudczak R. 2003. In vivo and in vitro evaluation of [^{18}F]FETO with respect to the adrenocortical and GABAergic system in rats. Eur J Nucl Med Mol Imag 30: 1398-1401

[19] Mitterhauser M, Wadsak W, Wabnegger L, Mien LK, Toegel S, Langer O, Sieghart W, Viernstein H, Kletter K, Dudczak R. 2004. Biological evaluation of 2'-[^{18}F]fluoroflumazenil ([^{18}F]FFMZ), a potential GABA receptor ligand for PET. Nucl Med Biol 31: 291-295

[20] Mitterhauser M, Wadsak W, Mien LK, Hoepping A, Viernstein H, Dudczak R, Kletter K. 2005. Synthesis and biodistribution of [^{18}F]FE@CIT, a new potential tracer for the dopamine transporter. Synapse 55: 73-79

[21] Henriksen G, Herz M, Schwaiger M, Wester HJ. 2005. Synthesis of [^{18}F]fluoroalkyl esters of carfentanil. J Lab Compd Radiopharm 48: 771-779

[22] Janssen PAJ, Van Daele GHP. 1976. N-(4-piperidinyl)-N-phenylamides and carbamates. US Patent 3,99,834

[23] Van Daele PG, De Bruyn MF, Boey JM, Sanczuk S, Agten JT, Janssen PA. 1976. Synthetic Analgesics: N-(1-[2-Arylethyl]-4-substituted 4-Piperidinyl) N-Arylalkanamides. Arzneimittel-Forschung (Drug Research) 26: 1521-1531

[24] Casy AF, Iorio MA, Podo F. 1981. ^{13}C NMR studies of isomeric piperidine derivatives with opiate properties and related compounds. Org Magn Res 15: 275 (abstract)

[25] Chi D, Kilbourn M, Katzenellenbogen J, Welsh M. 1987. A rapid and efficient method for the fluoroalkylation of amines and amides. Development of a method suitable for incorporation of the shortlived positron emitting radionuclide fluorine-18. J Org Chem 52**:** 658-664

[26] Janssen PAJ, Van Daele GHP. 1979. N-(4-piperidinyl)-N-phenylamides. US Patent 4,179,569

[27] Zubieta JK, Smith YR, Bueller JA, Xu Y, Kilbourn MR, Jewett DM, Meyer CR, Koeppe RA, Stohler CS. 2001. Regional mu opioid receptor regulation of sensory and affective dimensions of pain. Science 293: 311-315

[28] Wadsak W, Mitterhauser M, Rendl G, Schuetz M, Mien LK, Dudczak R, Kletter K, Karanikas G. 2006. [^{18}F]FETO for adrenocortical PET imaging: a pilot study in healthy volunteers. Eur J Nucl Med Mol Imaging 33: 669-672

Captions

FIGURE 1 Derivatives of Carfentanil; *Abbreviations*: Bn: benzyl group; CFN: Carfentanil

FIGURE 2 Reaction Scheme for the Preparation of [^{18}F]FE@CFN.

FIGURE 3 The dependence of the radiochemical yield of [^{18}F]FE@CFN on (a) reaction temperature (prec. conc. 5 mM, 20 min); (b) precursor concentration (150°C, 20 min); and (c) reaction time (prec. conc. 5 mM, 150°C). All given values represent arithmetic means ± SD for n≥3.

FIGURE 4 Autoradiography of an ex-vivo mid-brain slice from a single rat, 5 min. after i.v. administration of [^{18}F]FE@CFN (Not published data).

TABLE 1 Values counted in various organs at different time points after administration of 0.5–1.5 MBq [^{18}F]FE@CFN as percent injected dose per gram organ (% ID/g; mean values ± SD; n=5) (Not published data).

Figures and Tables

FIGURE 1

	R	**Name**
	CH_3	CFN
1a	Bn	
1b	H	CFN-acid
1c	Na	CFN-acid sodium salt
1d	CH_2CH_2F	FE@CFN
2a	$CH_2CH_2{}^{18}F$	[^{18}F]FE@CFN

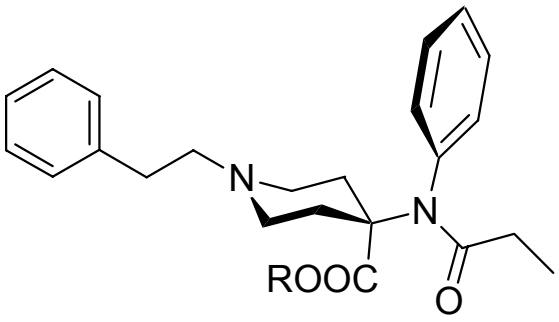

FIGURE 2

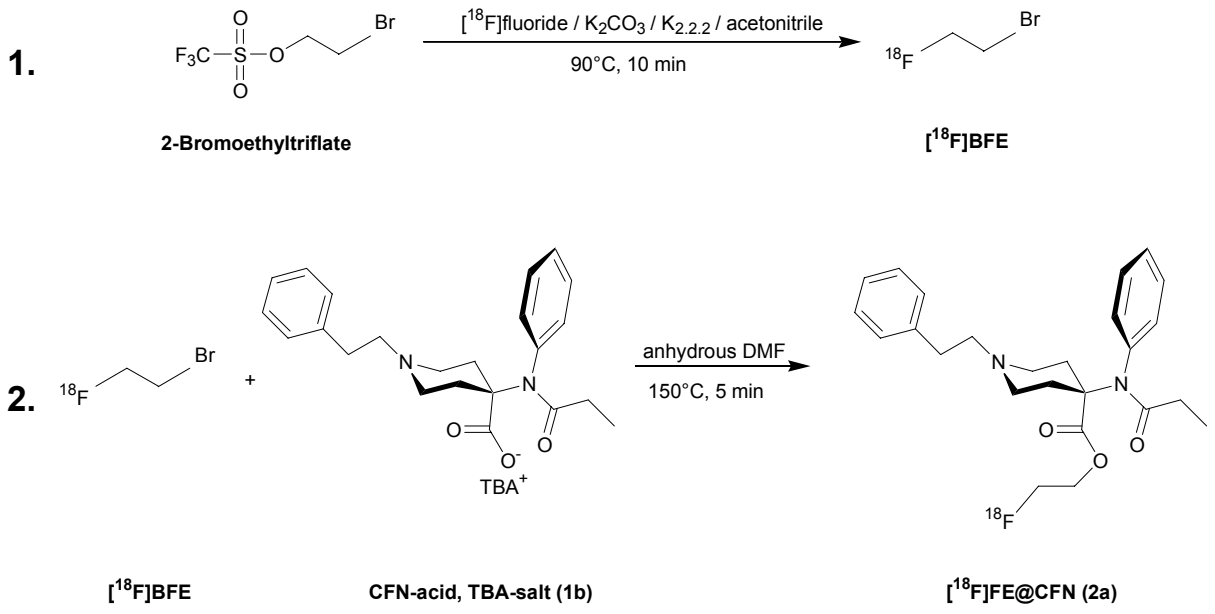
1.
F3C
S
O
Br
[18F]fluoride / K2CO3 / K2.2.2 / acetonitrile
90°C, 10 min
18F
2-Bromoethyltriflate
[18F]BFE
2.
anhydrous DMF
150°C, 5 min
TBA+
[18F]BFE
CFN-acid, TBA-salt (1b)
[18F]FE@CFN (2a)

FIGURE 3

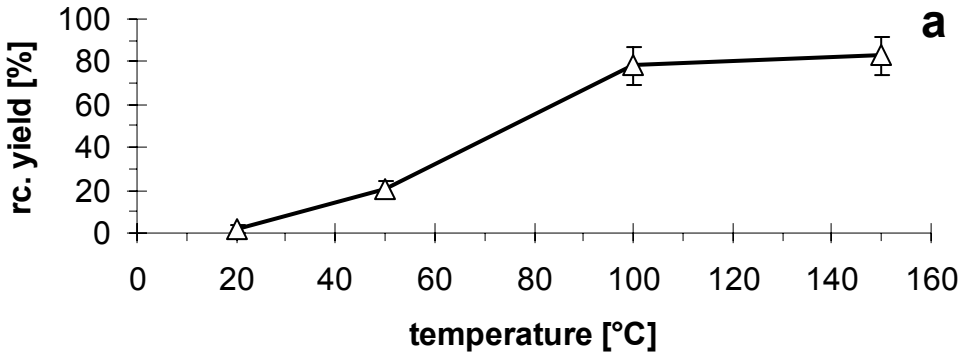
a
rc. yield [%]
100
80
60
40
20
0
0
20
40
60
80
100
120
140
160
temperature [°C]

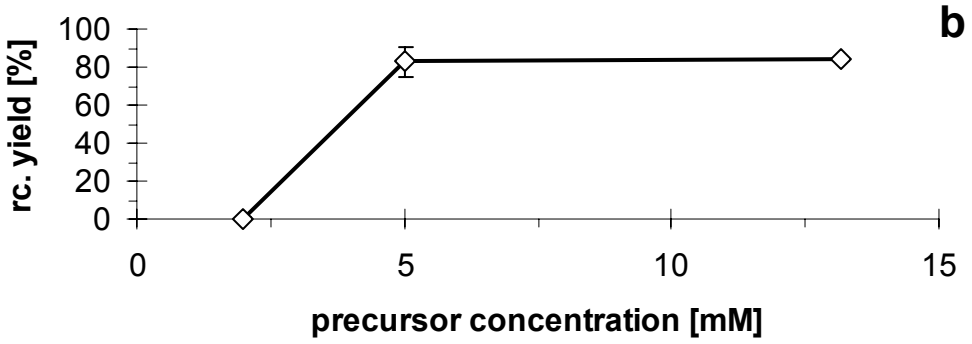
b
rc. yield [%]
100
80
60
40
20
0
0
5
10
15
precursor concentration [mM]

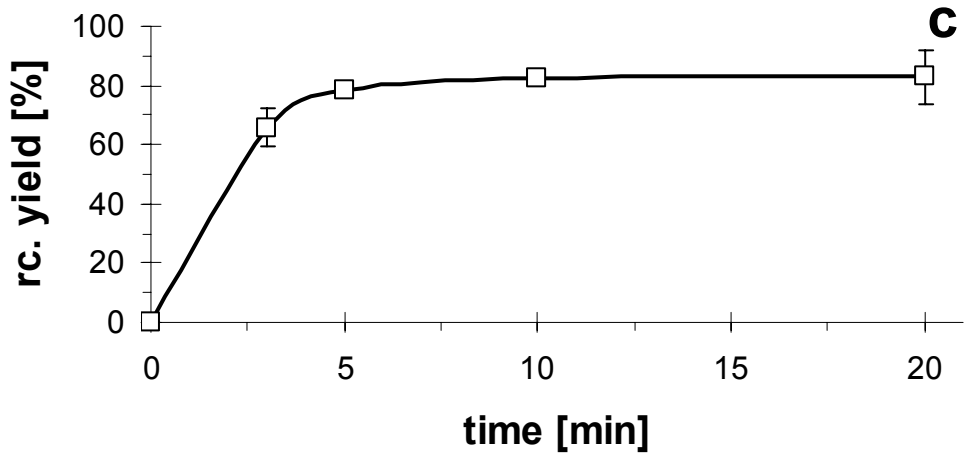
c
rc. yield [%]
100
80
60
40
20
0
0
5
10
15
20
time [min]

Figure 4.

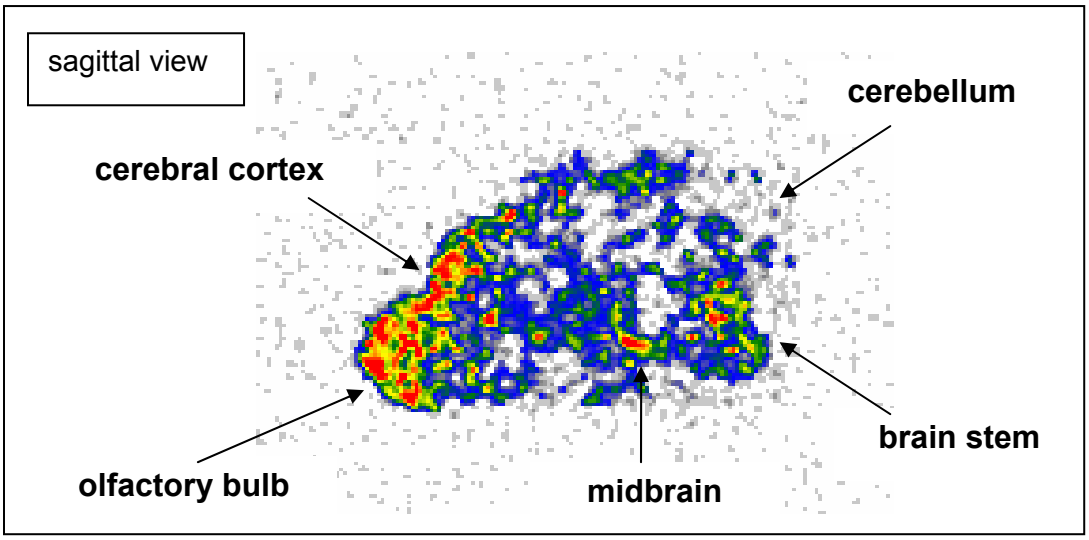
sagittal view
cerebellum
cerebral cortex
brain stem
olfactory bulb
midbrain

Table 1.

Tissue	**5 min**	**15 min**	**30 min**	**60 min**
blood	0.30 ± 0.05	0.18 ± 0.03	0.17 ± 0.02	0.14 ± 0.02
brain	0.21 ± 0.03	0.17 ± 0.06	0.11 ± 0.04	0.14 ± 0.10
carcass	0.18 ± 0.05	0.21 ± 0.04	0.25 ± 0.03	0.25 ± 0.02
colon	0.33 ± 0.10	0.26 ± 0.07	0.43 ± 0.12	0.37 ± 0.05
fat	0.07 ± 0.04	0.28 ± 0.12	0.62 ± 0.19	0.60 ± 0.11
femur	0.31 ± 0.03	0.28 ± 0.05	0.26 ± 0.02	0.26 ± 0.04
heart	0.66 ± 0.06	0.37 ± 0.08	0.29 ± 0.04	0.19 ± 0.01
ileum	0.95 ± 0.29	3.43 ± 0.50	3.16 ± 0.50	1.14 ± 0.20
kidney	2.22 ± 0.51	1.10 ± 0.20	1.04 ± 0.07	0.61 ± 0.04
liver	0.98 ± 0.34	1.71 ± 0.47	1.85 ± 0.18	1.72 ± 0.38
lung	2.34 ± 0.43	0.96 ± 0.23	0.67 ± 0.07	0.39 ± 0.03
muscle	0.27 ± 0.04	0.23 ± 0.04	0.16 ± 0.02	0.13 ± 0.01
pituitary gland	2.40 ± 0.39	3.16 ± 0.70	3.15 ± 0.60	2.66 ± 1.10
tail	0.46 ± 0.20	0.65 ± 0.15	0.44 ± 0.12	0.40 ± 0.13

2.2. Paper 3 submitted

Title: Preparation and first Preclinical Evaluation of [^{18}F]FE@SUPPY as a new PET-Tracer for the Adenosine A_3 Receptor.

Running Title: [^{18}F]FE@SUPPY–Preparation and Evaluation

Authors: Wolfgang Wadsak[1], Leonhard-Key Mien[1,2,3], Karem Shanab[4], Dagmar Ettlinger[1], Daniela Haeusler[1,2], Karoline Sindelar[1], Helmut Spreitzer[4], Helmut Viernstein[2], Robert Dudczak[1], Kurt Kletter[1], Markus Mitterhauser[1,2,5,*]

[1] Dept of Nuclear Medicine, Medical University of Vienna, Austria

[2] Dept of Pharmaceutical Technology and Biopharmaceutics, University of Vienna, Austria

[3] Dept of Psychiatry and Psychotherapy, Medical University of Vienna, Austria

[4] Dept of Drug and Natural Product Synthesis, Faculty of Life Sciences, University of Vienna, Austria

[5] Hospital Pharmacy of the General Hospital of Vienna, Austria

Abstract

Changes of the adenosine A3 receptor subtype (A3AR) expression have been shown in a variety of pathologies, especially (1) neurological and affective disorders, (2) cardiac diseases, (3) oncological diseases and (4) inflammation processes. Recently, (5-(2-fluoroethyl) 2,4-diethyl-3-(ethylsulfanylcarbonyl)-6-phenylpyridine-5-carboxylate, FE@SUPPY) was presented as a high affinity ligand for the A3AR with good selectivity. Hence, our aims were (1) the development of a suitable labeling precursor; (2) the establishment of a reliable radiosynthesis for the fluorine-18 labeled analogue, [^{18}F]FE@SUPPY; and (3) a first biodistribution study of [^{18}F]FE@SUPPY in rats.

Methods: A suitable labeling precursor, 5-(2-tosyloxyethyl) 2,4-diethyl-3-(ethylsulfanylcarbonyl)-6-phenylpyridine-5-carboxylate (Tos@SUPPY), was developed and the reference standard compound, FE@SUPPY, was synthesized according to a previously published method. The radiosynthesis of [^{18}F]FE@SUPPY was conducted in a one-pot reaction starting from cyclotron produced [^{18}F]fluoride. To the dried [^{18}F]fluoride-aminopolyether complex, Tos@SUPPY in acetonitrile was added, the vial was sealed and heated. Purification was achieved using semi-preparative HPLC and solid phase extraction. Biodistribution studies followed an established protocol: male Sprague-Dawley rats were injected with [^{18}F]FE@SUPPY and were subsequently sacrificed by exsanguination in ether anesthesia at different points of time. Organs were removed, weighed and counted.

Results: 1.7g recrystallized Tos@SUPPY was obtained (52%) as white crystalline powder. 136.8mg FE@SUPPY was obtained after purification (67%) as yellowish oil. Starting from an average of 49.2±13.9GBq [^{18}F]fluoride, 8.9±4.0GBq of formulated [^{18}F]FE@SUPPY (34.9±14.8%, based on [^{18}F]fluoride, corrected for decay) were prepared. Specific radioactivity was 60.8±18.0GBq/µmol. The organ with the highest uptake was the liver (1.87±0.16% I.D./g, 15min; 1.41±0.57% I.D./g, 30min). Organs with pronounced uptake were kidney, lung and heart. Tissues with lowest uptake were colon and testes. Intermediate brain uptake was observed throughout the examined time span.

Conclusion: [^{18}F]FE@SUPPY was prepared in a feasible and reliable manner. Overall yields and radiochemical purity were sufficient for further preclinical and clinical applications. Uptake pattern of [^{18}F]FE@SUPPY congruently follows the

described distribution pattern of the A3AR. The fact that organs reliably displaying high densities of the other adenosine receptor subtypes beside low densities of A3AR, show only low uptake, is encouraging for further studies with [^{18}F]FE@SUPPY for quantitative PET imaging of the A3AR.

Key words: Adenosine, PET, Receptor, Fluorine-18, Radioligand

Introduction

Adenosine is a ubiquitous nucleoside, released from metabolically active or stressed cells. It is known to act as an important regulatory molecule through its activation of cell surface receptors named A_1, A_{2A}, A_{2B}, and A_3 (A1AR, A2AR, A3AR), which all belong to the G-protein–coupled superfamily of receptors. There exists much information on the distribution of the A_1 and A_{2A} receptors because good pharmacological tools including radioligands are available. There are also several studies that have used antibodies to localize adenosine A_1 receptors in brain and A_{2A} receptors in striatum [1,2]. In the case of the A_{2B} and A_3 receptors, there are many open questions regarding the distribution and involvement in pathophysiological processes.

Collectively, adenosine receptors are widespread on virtually every organ and tissue. So, they represent promising drug targets for pharmacological intervention in many pathophysiological conditions that are believed to be associated with changes of adenosine levels such as asthma, neurodegenerative disorders, chronic inflammatory diseases, and cancer [3]. The A3AR is the latest identified adenosine receptor and its involvement in tumors has recently been shown: A3ARs are highly expressed on the cell surface of tumor cells and in human enteric neurons but not in the majority of normal tissues [4-10]. In a very comprehensive study A3AR mRNA expression in various tumor tissues was tested in paraffin-embedded slices using reverse transcription-PCR analysis [11]. A comparison with the A3AR expression in the relevant adjacent normal tissue or regional lymph node metastasis was performed. In addition, A3AR protein expression was studied in fresh tumors and was correlated with that of the adjacent normal tissue. The authors conclude that primary and metastatic tumor tissues highly express A3AR, which indicates that high receptor expression is a characteristic of solid tumors. These findings suggest the A3AR as a potential target for tumor growth inhibition and imaging. The A3ARs are also known to be involved in many other diseases, such as cardiac [12] and cerebral ischemia [13], glaucoma [14], stroke [15] and epilepsy [16]. Western blot analysis showed that A3 receptors are present in rat hippocampal nerve terminal membranes [17] and functionally it has been shown that the A3AR plays a role in the brain neurotransmitter system by directly influencing for instance serotonin [18-20] or glutamate [21]. Unfortunately, although the A3AR is discussed as a good target for

drug development, there is little information on the distribution and the absolute amounts of receptor protein in various body regions in the literature so far: Fredholm et al found high expression of A_3 mRNA in rat testes, intermediate levels in human cerebellum and hippocampus, sheep lung and spleen and low levels in human liver, kidney, heart, intestine, testis and rest of the brain [22]. In a second publication, the authors quantified the mRNA responsible for the expression of the A3AR in hearts of immature, young, and mature rats. They found values comparable (immature) or even higher (1.4 times higher in young and 1.6 times higher in mature rats) [23] compared to other adenosine receptors. The same group investigated the distribution of the mRNA of various adenosine receptors in the rat brain and found low but significant amounts of A_3 mRNA (about a fifth of the A_{2A} mRNA), which were further down-regulated after ovariectomy (2-fold) [24]. Dixon et al found expression of the gene encoding the adenosine A3AR to be widespread in the rat - throughout the CNS and in many peripheral tissues. The authors also concluded that this found pattern of expression is similar to the one observed in man and sheep, which had previously been perceived to possess distinct patterns of A3AR for gene expression in comparison to the rat [25]. However, in these few cases the given values represent the mRNA responsible for the expression rate for the receptors but do not represent absolute receptor densities.

For direct quantification of these receptor densities, autoradiography or positron emission tomography (PET) can be used. Both methods demand selective radiotracers. Recently, Li et al [26] evaluated a series of pyridine derivatives regarding affinity and selectivity on the A3AR. Amongst these compounds, a fluoroethyl ester (5-(2-fluoroethyl) 2,4-diethyl-3-(ethylsulfanylcarbonyl)-6-phenylpyridine-5-carboxylate, FE@SUPPY) was presented with promising properties. An affinity in the nanomolar range (K_i 4.22 nM) as well as excellent selectivity for the A3AR (ratio A_1/A_3 = 2700) was demonstrated. [26] Hence, our aims were (1) the development of a suitable labeling precursor; (2) the establishment of a reliable radiosynthesis for the fluorine-18 labeled analogue, [^{18}F]FE@SUPPY; and (3) a first biodistribution study of [^{18}F]FE@SUPPY in rats.

Materials and Methods

General

Melting points were determined on a Reichert-Kofler hot-stage microscope. Mass spectra were obtained on a Shimadzu QP 1000 instrument (EI, 70 eV). IR spectra were recorded on a Perkin-Elmer FTIR spectrum 1000 spectrometer. Elemental analyses were performed at the Microanalytical Laboratory, University of Vienna (Austria). ^{1}H- and ^{13}C-NMR spectra were recorded on a Bruker Avance DPX-200 spectrometer at 27 °C (200.13 MHz for ^{1}H, 50.32 MHz for ^{13}C). Radio-analytical thin-layer chromatography (radio-TLC) was performed using silicagel 60 F254 plates from Merck. Analysis of radio-TLC plates was performed using a digital autoradiograph (Instant Imager, Canberra-Packard, Rüsselsheim, Germany). Analytical high-performance liquid chromatography (HPLC) was performed using a Merck-Hitachi LaChrom system equipped with an L-7100 pump, an L-7400 UV detector and a lead-shielded NaI-radiodetector (Berthold Technologies, Bad Wildbach, Germany). The semi-preparative HPLC system consisted of a Sykam S1021 pump and an UV detector and a radioactivity detector in series.

Solid phase extraction (SPE) cartridges (SepPak® C18plus) were purchased from Waters Associates (Milford, MA). All starting materials for precursor and reference standard syntheses, were commercially available and used without further purification. (Ethyl benzoylacetate, Fluka 12990; Ethylene glycol, Riedel-de Haën 24204; Ammonium acetate, Sigma-Aldrich A7330; Propionaldehyde, Fluka 81870; Ethanethiol, Fluka 04290; 2,2-Dimethyl-1,3-dioxane-4,6-dione, Fluka 63395; Propionyl chloride, Fluka 81970) 5-(2-hydroxyethyl) 2,4-diethyl-3-(ethylsulfanylcarbonyl)-6-phenylpyridine-5-carboxylate (OH@SUPPY; **1**) was prepared according to a literature method [26]. [^{18}F]Fluoride was produced via the ^{18}O(p,n)^{18}F reaction in a GE PETtrace cyclotron (16.5 MeV protons; GE medical systems, Uppsala, Sweden). $H_2{}^{18}O$ (>97%) was purchased from Rotem Europe (Leipzig, Germany). Anion exchange cartridges (PS-HCO3) for [^{18}F]fluoride fixation were obtained from Macherey-Nagel (Dueringen, Germany).

Precursor chemistry – 5-(2-tosyloxy*ethyl) 2,4-diethyl-3-(ethylsulfanylcarbonyl)-6-phenylpyridine-5-carboxylate (Tos@SUPPY*; **2***)*

To a stirred mixture of OH@SUPPY (**1;** 2.40 g, 6.2 mmol) and triethylamine (1.68 g, 2.3 mL, 16.6 mmol) in THF (30 mL) at 0°C, a solution of toluene-4-sulfonyl chloride (2.36 g, 12.3 mmol) in THF (10 mL) was added dropwise. After the reaction mixture was refluxed for 62 h, the solvent was evaporated *in vacuo* and the residue was recrystallized from diethyl ether. A reaction scheme is presented in Figure 1.

Reference standard – 5-(2-fluoroethyl) 2,4-diethyl-3-(ethylsulfanylcarbonyl)-6-phenyl-pyridine-5-carboxylate (FE@SUPPY; **3***)*

The reference compound was obtained according to [26]. Briefly, OH@SUPPY (**1**) was treated with diethylaminosulfur trifluoride (DAST) at -78°C. Purification was performed using column chromatography.

Radiosynthesis – 5-(2-[^{18}F]fluoroethyl) 2,4-diethyl-3-(ethylsulfanylcarbonyl)-6-phenyl-pyridine-5-carboxylate ([^{18}F]FE@SUPPY; **3a***)*

No-carrier-added (n.c.a.) aqueous [^{18}F]fluoride was fixed on an anion exchange cartridge (carbonate form) on-line and separated from excess water. Subsequently, [^{18}F]fluoride was eluted with a solution containing the aminopolyether Kryptofix 2.2.2. (4,7,13,16,21,24-hexaoxo-1,10-diaza-bicyclo[8.8.8]hexacosane; 20 mg, 53.2 µmol) and potassium carbonate (4.5 mg, 32.6 µmol) in acetonitrile/water (70/30 vol/vol; V=1.0 mL). This solution was heated to 100°C and azeotropic drying was performed by subsequent addition of at least four 250 µL portions of acetonitrile.

To the dried [^{18}F]fluoride-aminopolyether complex, 8-10 mg of Tos@SUPPY (14.7-18.5 µmol) in acetonitrile was added, the vial was sealed and heated to 75°C for 20 min (*see* Figure 1). After cooling to room temperature, the crude reaction mixture was subjected to semi-preparative reversed-phase HPLC (HPLC: column: Chromolith® SemiPrep RP-18e, 100x10 mm (Merck 1.52016.0001), mobile phase: acetonitrile/ water/acetic acid (60/38.8/1.2 v/v/v; 2.5 g/L ammonium acetate; pH 3.2); flow: 10 mL/min). The [^{18}F]FE@SUPPY fraction was diluted with 80 mL water and fixed on a C18plus SepPak®. After washing with 10 mL water the pure product was eluted with 1.5 mL ethanol, sterile filtered (0.22 µm Millipore GS®) and formulated with 0.9% sodium chloride solution (10 mL).

Biodistribution experiments

All biodistribution studies followed a protocol of the NIH Animal Care and Use Committee also approved by the Austrian law on animal experiments. The procedure followed the protocol established in previous studies [27-29]. Briefly, male Sprague-Dawley rats/Him:OFA (n=20, 263-318 g) were injected with 0.37-1.41 MBq [^{18}F]FE@SUPPY (180-225 µL) through the tail vein. Subsequently the rats were sacrificed by exsanguination from the abdominal aorta in ether anesthesia after 5, 15, 30, 60 and 120 minutes (n=4, respectively). The organs were removed, dry weighed and counted (Cobra II auto-gamma counter, Canberra Packard, Canada). Radioactivity is expressed as percentage injected dose per gram tissue (% I.D./g).

Results

Precursor chemistry

1.7 g recrystallized Tos@SUPPY was obtained (52%) as white crystalline powder (Mp 107°C). For NMR-analysis, the solvent signal was used as an internal standard which was related to TMS with δ = 7.26 ppm (^{1}H in $CDCl_3$), δ = 77.0 ppm (^{13}C in $CDCl_3$).

^{1}H-NMR (200 MHz, $CDCl_3$): δ (ppm) 7.61 (d, 2H, *J* = 8.2 Hz, OTs H-2, H-6), 7.42 (m, 2H, Ph H-2, H-6), 7.28 (m, 3H, Ph H-3, H-4, H-5), 7.19 (d, 2H, *J* = 7.94, OTs H-3, H-5), 4.09 (t, 2H, *J* = 4.61, $OC\underline{H}_2CH_2$), 3.84 (t, 2H, *J* = 4.67, $C\underline{H}_2OSO_2$), 3.06 (q, 2H, *J* = 7.32, $SC\underline{H}_2CH_3$), 2.80 (q, 2H, *J* = 7.44, $NCC\underline{H}_2CH_3$), 2.59 (q, 2H, *J* = 7.56, $CC(C\underline{H}_2CH_3)C$), 2.34 (s, 3H, OTs CH_3), 1.30 (m, 6H, $CC(CH_2C\underline{H}_3)C$, $NCCH_2C\underline{H}_3$), 1,09 (t, 3H, *J* = 7,57, $SCH_2C\underline{H}_3$). ^{13}C-NMR (50 MHz, $CDCl_3$): δ (ppm) 195.2 ($\underline{C}OS$), 167.9 ($\underline{C}OO$), 159.6 (C-6), 157.1 (C-2), 148.1 (C-4), 145.0 (OTs C-1), 139.6 (OTs C-4), 133.1 (Ph C-1), 132.5 (C-3), 129.7 (OTs C-3, C-5), 128.9 (Ph C-4), 128.3 (Ph C-3, C-5), 128.1 (OTs C-2, C-6) 127.8(Ph C-2, C-6), 125.6 (C-5), 66.6 ($\underline{C}H_2OSO_2$), 62.5 ($O\underline{C}H_2CH_2$), 29.1 ($NC\underline{C}H_2CH_3$), 24.5 ($CC(\underline{C}H_2CH_3)C$), 24.0 ($S\underline{C}H_2CH_3$), 21.5 (OTs CH_3), 15.7 ($CC(CH_2\underline{C}H_3)C$), 14.5 ($NCCH_2\underline{C}H_3$), 14.0 ($SCH_2\underline{C}H_3$).

IR cm^{-1} (KBr): 3454, 2978, 2931, 2880, 1738, 1657 MS: m/z (%) 540 (M^+ - 1, 0.21), 481 (31), 480 (98), 436 (27), 264 (14), 199 (36), 154 (42), 91 (100), 65 (20).

Elemental analysis: Calculated molecular weight for $C_{28}H_{31}NO_6S_2$ was C, 62.08; H, 5.77; N, 2.59 and the analysis found a good agreement C, 61.96; H, 5.73; N, 2.53.

Reference standard

136.8 mg FE@SUPPY was obtained after purification (67%) as yellowish oil. NMR-analysis (^{1}H and ^{13}C) was performed and results were in full accordance with the literature. [26]

Radiosynthesis

Until now, 10 high scale radiosyntheses were performed. Starting from an average of 49.2 ± 13.9 GBq (average ± SD; range: 29.9 – 67.0 GBq) [^{18}F]fluoride, 8.9 ± 4.0 GBq of formulated [^{18}F]FE@SUPPY (34.9 ± 14.8 %, based on [^{18}F]fluoride, corrected for decay) were prepared within 97.8 ± 10.0 minutes. Radiochemical purity determined via radio-TLC and radio-HPLC always exceeded 98%. Specific radioactivity was determined via HPLC and found to be 60.8 ± 18.0 GBq/µmol (1640 ± 490 Ci/mmol) at the end of synthesis (EOS). [^{18}F]FE@SUPPY was found to be stable for at least 10 hours (checked by chromatography).

Biodistribution experiments

All values are shown in Table 1. The organ with the highest uptake was the liver showing 1.87±0.16% I.D./g at 15 min and 1.41±0.57% I.D./g at 30 min. Other organs with pronounced uptake were kidney, lung and heart. The tissues with the lowest uptake were colon and testes. Blood activity was 0.04-0.09% I.D./g throughout the whole experiment. Intermediate brain uptake was observed throughout the examined time span (0.20-0.33% I.D./g). Remaining activity in the carcass accounted for 0.10-0.23% I.D./g.

Discussion

General

According to the distribution pattern of the A3AR described in literature [22-24], the only limitation for the successful PET quantification could lie in too low receptor densities. But since many PET studies have already been successfully performed on the A1AR and A2AR systems, and Jenner et al and Rose'Meyer et al [23,24] found densities of the A3AR comparable (in the heart even higher) to those of A1AR and A2AR, it was consecutively one would expect sufficient target receptors for quantitative PET imaging of the A3AR. Li et al [26] published a series of chemical

structures, with most of them displaying reasonable affinities for the A3AR. Amongst all those investigated structures containing a fluorine atom, FE@SUPPY was the most affine compound for the A3AR. Furthermore, FE@SUPPY contains its fluorine label at its fluoroethyl ester function, a moiety known to serve as a good radiolabeling target.

It can be expected, that [^{18}F]FE@SUPPY, after passing the blood brain barrier or other tissue membranes, is cleaved by esterase by forming 2-[^{18}F]fluoroethanol and the acid of SUPPY (2,4-diethyl-3-(ethylsulfanylcarbonyl)-6-phenylpyridine-5-carboxylic acid). 2-[^{18}F]Fluoroethanol would easily re-diffuse from tissue and would not contribute to the receptor signal leading to lower non-specific accumulation compared to tracers primarily forming hydrophilic radioactive metabolites.

Precursor and reference standard

The preparation and purification of the precursor molecule as well as the reference compound were accomplished straight forward without any significant problems. Surprisingly, the tosylation reaction was unexpectedly sluggish (62 hours under refluxing in THF).

Radiosynthesis

For the preparation of [^{18}F]fluoroethyl esters, there are two major ways: (1) fluoroethylation of the free acid compound and (2) direct radiofluorination of a precursor molecule containing a preformed ethyl ester function with a good leaving group (such as tosylate, triflate or mesylate). Fluoroethylations are useful for molecules originally designed as [^{11}C]methyl esters since they share the very same precursor (i.e. the free acid). These precursors are easily translated into the corresponding [^{18}F]fluoroethyl esters. [27-30] In contrast, direct radiofluorination demands rather sophisticated precursor chemistry but can be performed in a one-pot reaction which is easier to automate. Hence, the latter way is usually preferred and was chosen for the preparation of [^{18}F]FE@SUPPY. The described radiosynthesis was straight forward with a negligible failure rate (2 out of 54).

Biodistribution experiments

As presented in Table 1, the organ displaying the highest uptake was the liver followed by the kidney. Since our group has demonstrated recently that

[^{18}F]fluoroethyl esters are primarily metabolized by carboxylic esterases, high kidney uptake could be explained by the renal excretion route of the major expected metabolite, [^{18}F]fluoroethanol [27, 31-34]. High liver uptake could be explained by metabolism taking place in the CYP-rich hepatosomes.

Fredholm et al. [22] summarized the distribution of adenosine receptor subtypes and stated high expression of adenosine A_1 and A_{2A} receptors in various brain regions. Since we found only moderate uptake in brain, high binding to those receptor subtypes appears improbable. Additionally, high expression of adenosine A_1 receptors is found in heart, and high expression of adenosine A_{2A} receptors is found in thymus and spleen. Again, the uptake of [^{18}F]FE@SUPPY in these organs is moderate to low, indicating a high selectivity of this novel PET-ligand to the A_3 subtype as stated by Li et al [26], earlier. Organs reliably expressing A_3 mRNA are lung (intermediate levels), liver, kidney, heart and intestines (low levels) [22]. Calculating tissue-to-blood ratios as a more accurate indicator for accumulation over time we found uptake of [^{18}F]FE@SUPPY in all of these regions (*see* Figure 2). Highest values are displayed for liver, kidney and lung tissue. All of these three organs and spleen reach their peak activity already after 5 minutes.

It is noteworthy that the tissue-to-blood ratio of the brain – although only at an intermediate level – is the only one increasing over the whole time course of the experiment (up to 5.4 ± 0.6 after 120 minutes). This fact is encouraging for further applications of [^{18}F]FE@SUPPY in the central nervous system besides its high potential for oncological and cardiological PET imaging.

Conclusion

[^{18}F]FE@SUPPY, the first PET-ligand for the adenosine A_3 receptor, was prepared in a feasible and reliable manner, starting from a suitable labeling precursor (Tos@SUPPY). Overall yields and radiochemical purity were sufficient for further preclinical and clinical applications. The uptake pattern of [^{18}F]FE@SUPPY congruently follows the described distribution pattern of the A3AR (as far as assessable). The fact that organs known to reliably display high densities of the other adenosine receptor subtypes beside low densities of A3AR, show only low uptake is encouraging for further studies with [^{18}F]FE@SUPPY for the quantitative imaging of the A3AR.

Acknowledgements

The authors thank Karola Weber and Birgit Schmidt for their help in setting up the synthesis. Especially, Dr Herbert Kvaternik and Drs Bornatowicz and Hruby at the ARC are acknowledged for providing their expertise and facilities. Sylvia Hiessberger at BSM Diagnostica is acknowledged for organizing talents. This research was funded by the Austrian Science Fund (FWF P19383-B09) awarded to M. Mitterhauser.

References

[1] Hettinger BD, Leid M and Murray TF. Cyclopentyladenosine-induced homologous down-regulation of A1 adenosine receptors (A1AR) in intact neurons is accompanied by receptor sequestration but not a reduction in A1AR mRNA expression or G protein alpha-subunit content. *J Neurochem* 1998;71:221-230.

[2] Rosin DL, Robeva A, Woodard RL, Guyenet PG and Linden J. Immunohistochemical localization of adenosine A2A receptors in the rat central nervous system. *J Comp Neurol*. 1998;401:163-186.

[3] Gessi S, Cattabriga E, Avitabile A, et al. Elevated expression of A3 adenosine receptors in human colorectal cancer is reflected in peripheral blood cells. *Clinical Cancer Research.* 2004;10:5895-5901.

[4] Gessi S, Varani K, Merighi S, et al. Pharmacological and biochemical characterization of A3 adenosine receptors in Jurkat T cells. *Br J Pharmacol.* 2001;134:116-26.

[5] Merighi S, Varani K, Gessi S, et al. Pharmacological and biochemical characterization of adenosine receptors in the human malignant melanoma A375. *Br J Pharmacol.* 2001;134:1215-26.

[6] Suh BC, Kim TD, Lee JU, Seong JK, Kim KT. Pharmacological characterization of adenosine receptors in PGT-beta mouse pineal gland tumour cells. *Br J Pharmacol.* 2001;134:132-42.

[7] Gessi S, Varani K, Merighi S, et al. A3 adenosine receptors in human neutrophils and promyelocytic HL60 cells: a pharmacological and biochemical study. *Mol Pharmacol*. 2002;61:415-24.

[8] Fishman P, Bar-Yehuda S, Madi L, Cohn I. A3 adenosine receptor as a target for cancer therapy. *Anticancer Drugs.* 2002;13:1-8.

[9] Fishman P, Bar-Yehuda S, Ardon E, et al. Targeting the A3 adenosine receptor for cancer therapy: inhibition of prostate carcinoma cell growth by A3AR agonist. *Anticancer Res*. 2003;23:2077-83.

[10] Christofi FL, Zhang H, Yu JG, et al. Differential gene expression of adenosine A1, A2a, A2b, and A3 receptors in the human enteric nervous system. *J Comp Neurol.* 2001;439:46-64.

[11] Madi L, Ochaion A, Rath-Wolfson L, et al. The A3 adenosine receptor is highly expressed in tumor versus normal cells: potential target for tumor growth inhibition. *Clin Cancer Res.* 2004;10:4472-9.

[12] Liang BT, Jacobson K. A. A Physiological role of the adenosine A3 receptor: Sustained cardioprotection. *Proc. Natl. Acad. Sci. U.S.A.* 1998;95:6995-9.

[13] von Lubitz, DKJE, Ye W, McClellan J, Lin RCS. Stimulation of adenosine A3 receptors in cerebral ischemia. Neuronal death, recovery, or both? *Ann. N.Y. Acad Sci.* 1999;890:93-106.

[14] Avila MY, Stone RA, Civan MM. Knockout of A3 adenosine receptors reduces mouse intraocular pressure. *Invest Opthalmol Visual Sci.* 2002;43:3021-6.

[15] von Lubitz DK, Simpson KL, Lin RC. Right thing at a wrong time? Adenosine A3 receptors and cerebroprotection in stroke. *Ann N Y Acad Sci.* 2001;939:85-96.

[16] Laudadio MA, Psarrapoulou. The A3 receptor agonist 2-Cl-IB-MECA facilitates epileptiform discharges in the CA3 area of immature rat hippocampal slices. *Epilepsy Res.* 2004;59:83-94.

[17] Lopes LV, Rebola N, Pinheiro PC, Richardson PJ, Oliveira CR, Cunha RA. Adenosine A3 receptors are located in neurons of the rat hippocampus. *Neuroreport.* 2003;26:1645-8.

[18] Okada M, Kawata Y, Kiryu K, et al. Effects of adenosine receptor subtypes on hippocampal extracellular serotonin level and serotonin reuptake activity. *J Neurochem.* 1997;69:2581-8.

[19] Sawynok J. Adenosine receptor activation and nociception. *Eur J Pharmacol.* 1998;347:1-11.

[20] Zhu CB, Hewlett WA, Feoktistov I, Biaggioni I, Blakely RD. Adenosine receptor, protein kinase G, and p38 mitogen-activated protein kinase-dependent up-regulation of serotonin transporters involves both transporter trafficking and activation. *Mol Pharmacol.* 2004;65:1462-74.

[21] Macek TA, Schaffhauser H, Conn PJ. Protein kinase C and A3 adenosine receptor activation inhibit presynaptic metabotropic glutamate receptor (mGluR) function and uncouple mGluRs from GTP-binding proteins. *J Neurosci*. 1998;18:6138-46.

[22] Fredholm BB, Arslan G, Halldner L, Kull B, Schulte G, Wasserman W. Structure and function of adenosine receptors and their genes. *Naunyn-Schmiedeberg's Arch Pharmacology.* 2000;362:364–374.

[23] Jenner TL, Mellick AS, Harrison GJ, Griffiths LR, Rose'Meyer RB. Age-related changes in cardiac adenosine receptor expression. *Mech Ageing Dev*. 2004;125:211-7.

[24] Rose'Meyer RB, Mellick AS, Garnham BG, Harrison GJ, Massa HM, Griffiths LR. The measurement of adenosine and estrogen receptor expression in rat brains following ovariectomy using quantitative PCR analysis. *Brain Res Brain Res Protoc.* 2003;11:9-18.

[25] Dixon AK, Gubitz AK, Sirinathsinghji DJ, Richardson PJ, Freeman TC. Tissue distribution of adenosine receptor mRNAs in the rat. *Br J Pharmacol.* 1996;118:1461-8.

[26] Li AH, Moro S, Forsyth N, Melman N, Ji XD, Jacobson KA. Synthesis, CoMFA analysis, and receptor docking of 3,5-diacyl-2, 4-dialkylpyridine derivatives as selective A3 adenosine receptor antagonists. *J Med Chem.* 1999;42:706-21.

[27] Mitterhauser M, Wadsak W, Mien LK, et al. Synthesis and Biodistribution of [^{18}F]FE@CIT, a new potential tracer for the Dopamine Transporter. *Synapse* 2005;55:73-79.

[28] Wadsak W and Mitterhauser M. Synthesis of [^{18}F]FETO, a novel potential 11-β hydroxylase inhibitor. *J Label Compd Radpharm.* 2003;46:379-88.

[29] Wadsak W, Mien L-K, Ettlinger D, et al. Preparation and Biodistribution [^{18}F]FE@CFN (2-[^{18}F]fluoroethyl-4-[N-(1-oxopropyl)-N-phenylamino]-1-(2-phenylethyl)-4-piperidine-carboxylate) a Potential μ-Opioid Receptor Imaging Agent. *Radiochim Acta* 2007;95:33-8.

[30] Wadsak W, Mitterhauser M, Mien L-K, et al. Radiosynthesis of 3-(2´-[^{18}F]fluoro)-flumazenil ([^{18}F]FFMZ). *J Label Compd Radpharm.* 2003; 46:1229-40.

[31] Mitterhauser M, Wadsak W, Wabnegger L, et al. In vivo and in vitro evaluation of [^{18}F]FETO with respect to the adrenocortical and GABAergic system in rats. *Eur J Nucl Med Mol Imaging*. 2003;30:1398-1401.

[32] Mitterhauser M, Wadsak W, Wabnegger L, et al. Biological evaluation of 2´-[^{18}F]fluoroflumazenil ([^{18}F]FFMZ), a potential GABA receptor ligand for PET. *Nucl Med Biol.* 2004;31:291-295.

[33] DE Ettlinger, W Wadsak, LK Mien, et al. [^{18}F]FE@CIT: Metabolische Überlegungen/ Metabolic considerations [abstract]. *Nuklearmedizin – Nuclear Medicine* 2006; 45:A155.

[34] Ettlinger DE, Wadsak W, Mien L-K, et al. The metabolic profile of [^{18}F]FETO. *Eur J Nucl Med Mol Imaging*. 2006;33:928-31.

Figure 1 – Reaction scheme for the preparation of Tos@SUPPY, FE@SUPPY and [^{18}F]FE@SUPPY starting from OH@SUPPY.

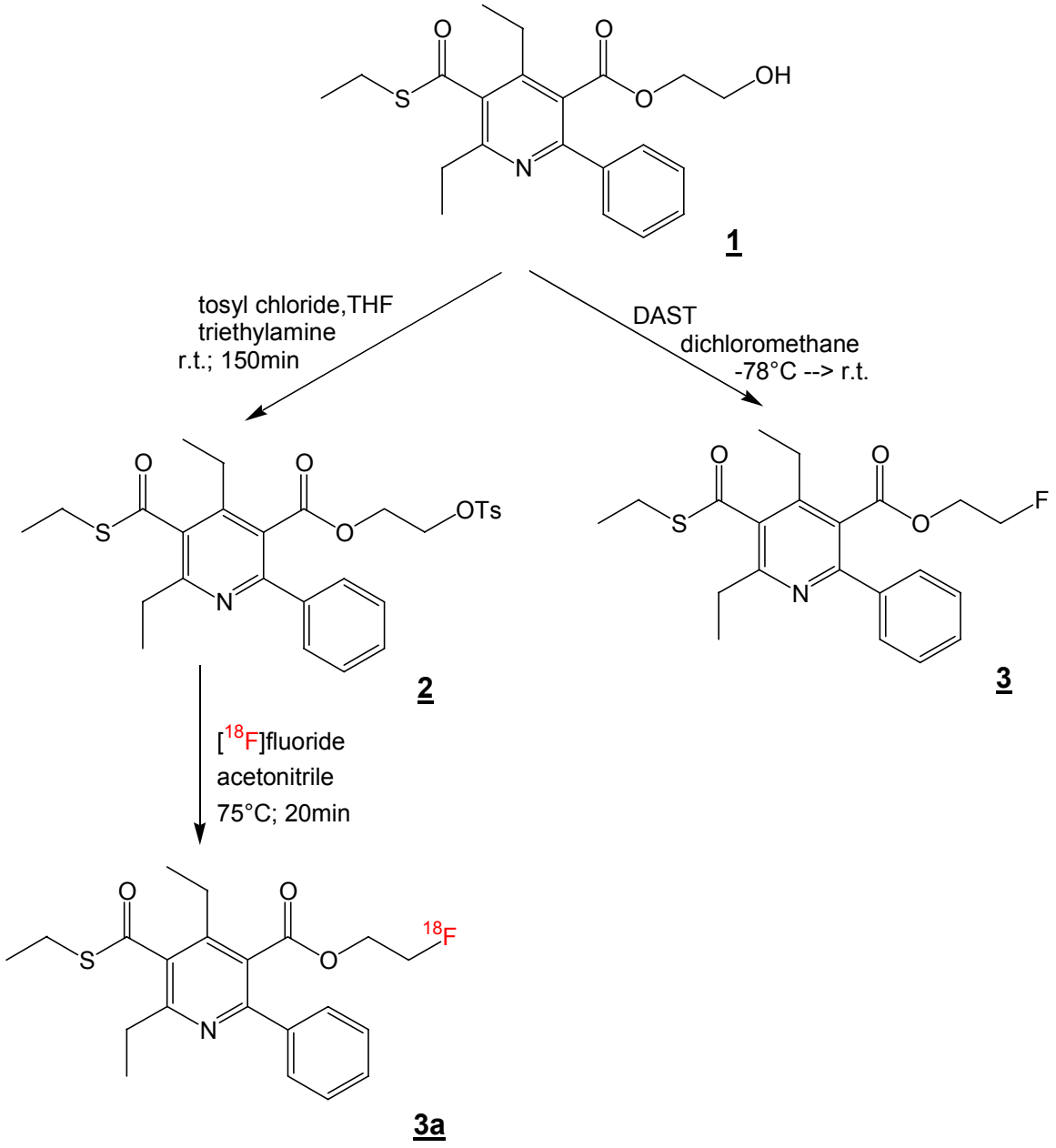

Figure 2 – Tissue-to-blood uptake ratios of [^{18}F]FE@SUPPY in organs of assumed moderate-to-high A3AR densities [22-24] at different time points. Values were calculated by division of tissue (% I.D./g) by blood (% I.D./g) for each individual subject (e.g. brain (rat1) / blood (rat1); brain (rat2) / blood (rat2); etc.). Given bars represent arithmetic means ± standard deviation of these values grouped for each time point (n = 4).

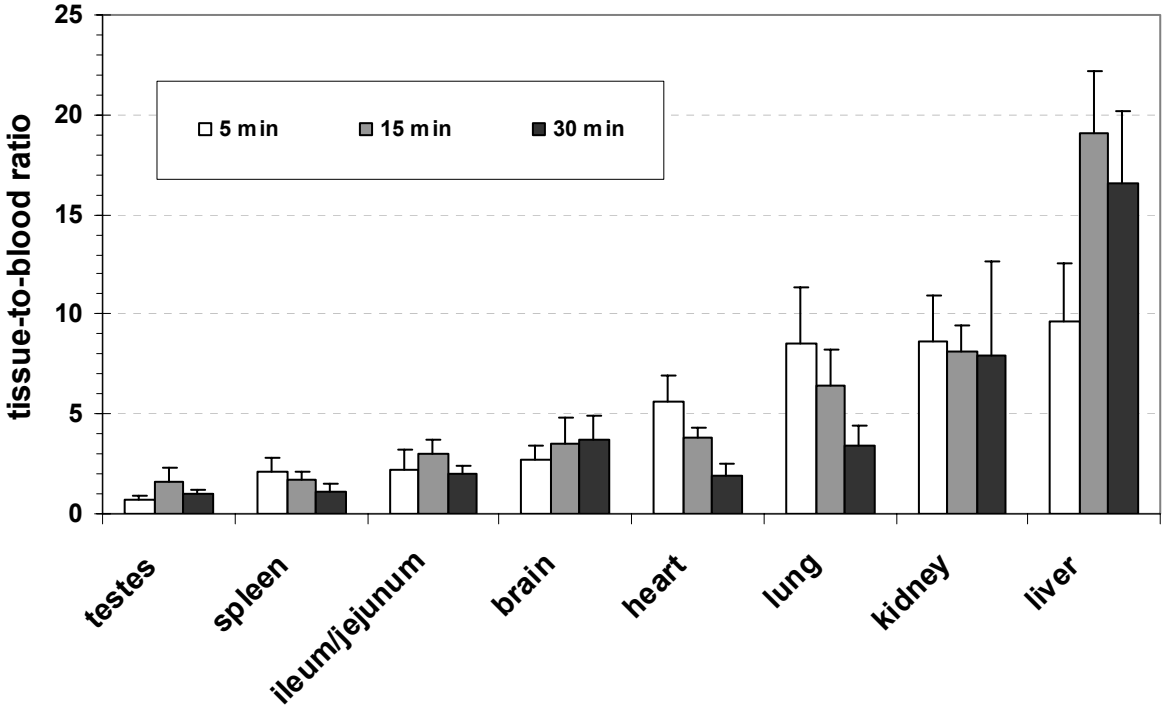

Table 1 – Biodistribution of [^{18}F]FE@SUPPY in rats at different time points. Values represent % injected dose per gram (% I.D./g; arithmetic means ± standard deviation; n ≥ 3)

Tissue	**5min**	**15min**	**30min**	**60min**	**120min**
blood	0,090 ± 0,027	0,076 ± 0,033	0,081 ± 0,019	0,038 ± 0,012	0,038 ± 0,013
testes	0,063 ± 0,025	0,160 ± 0,067	0,084 ± 0,030	0,019 ± 0,005	0,039 ± 0,011
liver	0,880 ± 0,333	1,871 ± 0,161	1,415 ± 0,567	0,326 ± 0,169	0,072 ± 0,015
spleen	0,200 ± 0,089	0,180 ± 0,086	0,098 ± 0,042	0,007 ± 0,007	0,020 ± 0,001
fat	0,155 ± 0,095	0,417 ± 0,105	0,435 ± 0,167	0,114 ± 0,056	0,112 ± 0,012
colon	0,066 ± 0,025	0,160 ± 0,103	0,041 ± 0,010	0,003 ± 0,003	0,005 ± 0,005
ileum/jejunum	0,192 ± 0,080	0,299 ± 0,052	0,168 ± 0,065	0,583 ± 0,083	0,231 ± 0,031
kidney	0,800 ± 0,318	0,806 ± 0,121	0,571 ± 0,180	0,070 ± 0,045	0,011 ± 0,001
muscle	0,152 ± 0,096	0,244 ± 0,091	0,123 ± 0,045	0,024 ± 0,001	0,004 ± 0,003
femur	0,217 ± 0,080	0,245 ± 0,061	0,133 ± 0,049	0,021 ± 0,019	0,025 ± 0,002
thymus	0,244 ± 0,142	0,299 ± 0,090	0,111 ± 0,062	0,008 ± 0,005	0,001 ± 0,000
heart	0,528 ± 0,211	0,380 ± 0,075	0,165 ± 0,072	0,059 ± 0,041	0,033 ± 0,004
lung	0,695 ± 0,157	0,634 ± 0,171	0,290 ± 0,135	0,079 ± 0,041	0,035 ± 0,015
brain	0,257 ± 0,106	0,332 ± 0,080	0,297 ± 0,123	0,200 ± 0,050	0,210 ± 0,090
carcass	0,234 ± 0,162	0,208 ± 0,064	0,168 ± 0,052	0,098 ± 0,046	0,154 ± 0,048

2.2. Paper 4

Title: Simple and fully automated preparation of [*carbonyl*-^{11}C]WAY-100635

Running Title: “Simple preparation of WAY”

Authors: Wolfgang Wadsak[1,*], Leonhard-Key Mien[1,2,3], Dagmar E Ettlinger[1], Rupert R Lanzenberger[2], Daniela Haeusler[1,3], Robert Dudczak[1], Kurt Kletter[1] and Markus Mitterhauser[1,3,4]

1 Department of Nuclear Medicine, Medical University of Vienna, A-1090 Vienna, Austria

2 Department of Psychiatry, Medical University of Vienna, A-1090 Vienna, Austria

3 Department of Pharmaceutical Technology and Biopharmaceutics, University of Vienna, A-1090 Vienna, Austria

4 Hospital Pharmacy of the General Hospital of Vienna, A-1090 Vienna, Austria

Summary

So far, [*carbonyl*-^{11}C]WAY-100635 is the PET-tracer of choice for $5HT_{1A}$-receptor-imaging. Since the preparation is still a challenge, we aimed at (1) the evaluation of various essential parameters for the successful preparation, (2) the simplification of the radiosynthesis and (3) the establishment of a safe and fully automated system. The preparation is based on a commercial synthesizer and all chemicals are used without further processing. We found a low failure rate (7.7%), high average yield (4.0±1.0 GBq) and a specific radioactivity of 292±168 GBq/µmol (both at the end of synthesis, EOS).

Key words

WAY-100635 / Serotonin / 5-HT / Radiosynthesis / Carbon-11

Introduction

Carbon-11 labelled WAY-100635 (*N*-(2-(1-(4-(2-methoxyphenyl)-1-piperazinyl)ethyl))-*N*-(2-pyridyl)-cyclohexane-carboxamide; WAY) was introduced into positron emission tomography (PET) as a highly potent and selective antagonist at the $5HT_{1A}$ receptors more than a decade ago. Since $5HT_{1A}$ receptors are implicated in the pathogenesis of anxiety, depression, eating disorders and motion sickness, they are an important target for drug therapy [1,2]. The visualisation and quantification of this receptor is a basis for further exploration of molecular pathologies causing psychiatric conspicuousness. The most extensively studied tracers are two carbon-11 labelled WAY-100635 derivatives, [*O-methyl*-^{11}C]- and [*carbonyl*-^{11}C]WAY-100635 [3-8]. [*O-methyl*-^{11}C]WAY-100635 is rapidly metabolized to [*O-methyl*-^{11}C]WAY-100634, both passing the blood-brain barrier and other polar radioactive metabolites [1, 9-12]. Since [*carbonyl*-^{11}C]WAY-100635 is solely metabolized to radioactive polar metabolites that do not cross the blood–brain barrier [10], it became the PET-tracer of choice.

Since the radiosynthesis is especially technically demanding we aimed at developing a simple and automated preparation method using a commercially available synthesizing module. Automated methods for radiosyntheses are favourable, because

- carbon-11 preparations demand heavy lead shielding and do not allow manual operation,
- the short half-life of carbon-11 makes a short total synthesis time a prerequisite for routine preparation,
- it is easier to comply with “good manufacturing practise” (GMP) with automated methods, and
- it is easier to perform repeated preparations for routine demands.

There are very few publications dealing with the automated or semi-automated preparation of [^{11}C]labelled WAY-100635 [7,8], and [*carbonyl*-^{11}C]WAY-100635 is still considered as one if not the most challenging PET-tracer. Hence, we aimed at (1) the evaluation of various previously not investigated parameters essential for the successful preparation and purification, (2) consecutively the simplification of this challenging PET-radiosynthesis and (3) the establishment of a safe and fully automated system for routine applications. This investigation should help others to avoid unnecessary, expensive and time consuming troubles during the

implementation of this important $5HT_{1A}$ radioligand and to simplify its preparation drastically.

Materials and Methods

General

Cyclohexylmagnesium chloride (2.0 M in diethylether, No. 256692 200 mL; “Grignard’s reagent”), tetrahydrofurane (THF without stabilizing agent; No. 40,175-7 100 mL), thionyl chloride (99%, No. 23,046-4 5 mL) and triethylamine (TEA, 99.5%, No. 47,128-3 100 mL) were obtained from Sigma Aldrich (St. Louis, MO, USA). WAY-100634 (“precursor”) was obtained from ABX (No. 320, ABX-Advanced Biochemical Compounds Dresden, Germany), C18plus SepPak® cartridges were obtained from Waters (Waters® Associates Milford, MA, USA). Millex GS® 0.22 µm sterile filters were purchased from Millipore® (Bedford, MA, USA).

Testing of loop material

PE (polyethylene): $[^{11}C]CO_2$ (85.5 ± 10 GBq, n=40, flow 3 mL/min) was passed through a 80 cm long polyethylene tube (PE, Portex fine bore polythene tubing REF 800/100/280; 0.86 mm x 1.52 mm; FC 334104; Portex Ltd, UK), impregnated with 0.5 mL cyclohexylmagnesium chloride, diluted with 1.0 mL THF. After trapping was complete, the reaction mixture was eluted with a thionyl chloride solution (5 µL in 400 µL THF) and transferred to a solution containing 3.5 mg WAY-100634 in 20 µL TEA and 40 µL THF, previously prepared in the reactor. The reaction was allowed to proceed for 4 min at 70°C. After cooling to room temperature, the activity was counted and the crude reaction mixture was subjected to analytical HPLC. The corresponding product peak (retention time: 6-8 min) was corrected for decay compared to the by-product eluting with the front. This corrected value was then related to the measured activity at the end of bombardment (EOB).

FEP (Fluoroethylene-propylene): $[^{11}C]CO_2$ (33 ± 4.5 GBq, n=14, flow 3 mL/min) was passed through a 80 cm long FEP tube (Cat. 1520 0.03 inch x 1/16 inch; Upchurch Scientific, Oak Harbor, WA, USA), impregnated with 0.5 mL cyclohexylmagnesium chloride, diluted with 1.0 mL THF. The consecutive processing was conducted analogous to the steps described in the section above (PE).

ETFE (Ethylen-Tetrafluoroethylene): [^{11}C]CO_2 (30 ± 23 GBq, n=12, flow 3 mL/min) was passed through a 80 cm long TEFZEL® tube (ETFE; Cat. 1528 0.03 inch x 1/16 inch, Upchurch Scientific), impregnated with 0.5 mL cyclohexylmagnesium chloride, diluted with 1.0 mL THF. The consecutive processing was conducted analogous to the steps described in the section above (PE).

Determination of the effect of amount of precursor

After trapping was complete, the reaction mixture was eluted from the PE loop with a thionyl chloride solution (5 µL in 400 µLTHF) and transferred to a solution containing variable amounts of WAY-100634 in 20 µL TEA and 40 µL THF (1.5 – 5.0 mg), previously prepared in the reactor. The reaction was allowed to proceed for 4 min at 70°C. After cooling to room temperature, the activity was counted and the crude reaction mixture was subjected to analytical HPLC. The corresponding product peak (retention time: 6-8 min) was corrected for decay compared to the by-product eluting with the front.

Testing of preparative HPLC-columns

XTerra: The crude aqueous solution was purified by preparative HPLC (column: Waters® XTerra, 10 µm, 300 x 7.8 mm, No.188001166; mobile phase: methanol/0.1M ammonium formate/TEA 65/35/0.3 (v/v/v); flow 6 mL/min). The desired product peak eluted after approximately 7 minutes and peak cutting time was 40-50 seconds.

µ-Bondapak: The crude aqueous solution was purified by preparative HPLC (column: Waters® µ-Bondapak, 10 µm, 300 x 7.8 mm, No. N3078B0110S18; mobile phase: methanol/0.1M ammonium formate/TEA 65/35/0.3 (v/v/v); flow 6 mL/min). The desired product peak eluted after approx. 5 minutes and peak cutting time was 40 seconds.

Gemini: The crude aqueous solution was purified by preparative HPLC (column: Phenomenex® Gemini, 10 µm, 110 Å, 250 x 10 mm, No. 00G-4436-NO; mobile phase: methanol/0.1M ammonium formate/TEA 70/30/0.3 (v/v/v); flow 10 mL/min). The desired product peak eluted after approx. 7 minutes and peak cutting time was only 25 seconds.

Influence of the inert gas

The composition of the inert working gas, a previously addressed parameter [8], was investigated using the following set-up: PE loop, 3.5 mg precursor, µ-Bondapak column for HPLC purification. Pure helium (6.0) and nitrogen (6.0) were compared regarding overall yield and product quality.

Automated set-up

A scheme of the synthesis apparatus is presented in Figure 3. All details given in the following section refer to this figure.

Prior to synthesis, 80 cm of the PE tubing were tightly wound around a chopstick (diameter approx. 6 mm) and fixed with scotch tape to fit inside the reaction vial pin hole (AD2). Care should be taken to avoid squeezing. Luer fittings were connected on both ends, and immediately prior to start of synthesis the loop was impregnated with cyclohexylmagnesium chloride (0.5 mL) in THF (1 mL) with a flow of 3 mL/min.

Cyclotron produced [^{11}C]CO_2 (43.5 – 90 GBq, mean 73 ± 13) was trapped at -150°C (liquid nitrogen; cool trap, AD1). Then, it was passed through the specially prepared synthesis loop (AD2) under heating of the cool trap to 0°C using 3 mL/min nitrogen-flow. After the activity reached its maximum, the reaction mixture was manually eluted with a thionyl chloride solution (3 µL in 400 µLTHF) and transferred on-line into the reaction vial (AD3) containing a solution of 3.5 mg WAY-100634 in 20 µL TEA and 40 µL THF (exhaust through V19). After 4 minutes at 70°C, the reaction was quenched by addition of 1000 µL distilled water (V2) and the crude mixture was subjected to the HPLC injector (V11) passing the fluid detector. The product peak – as obtained by preparative HPLC – was cut from the chromatogram via V7, diluted with 80 mL water and captured on the pre-conditioned C18plus SepPak (V14a, V12a). After washing with a further 10 mL of water (V6b, V14b, V12a), the purified product was eluted from the SepPak with 1.5 mL ethanol (V5b, V6a, V14b, V12b). After formulation with 10 mL physiological saline solution (AD4) and on-line sterile filtration under aseptic conditions (V13 → laminar air flow hot cell), the product was subjected to quality control.

Statistical analysis was performed using the Microsoft Excel® integrated analysis tool. Unpaired independent two-tailed t-tests were made between two data sets and a

significance level of $p < 0.001$ was considered highly significant. Descriptive statistical analysis was performed using mean values and the standard deviation.

Quality control

HPLC analysis was performed with a Merck-Hitachi LaChrom L-7100 pump with a Merck-Hitachi LaChrom L-7400 UV detector at 254 nm and a NaI-radiodetector (Berthold technologies, Bad Wildbach, Germany) using a µ-Bondapak C-18 column (5 µm, 300 x 3.9 mm, WAT027324, Waters®). Mobile phase: 0.1M ammonium formate/acetonitrile 55/45 (v/v) at a flow rate of 2 mL/min. Residual solvents were analysed by gas chromatography (HP 6890 series system with a flame ionisation detector (FID)): carrier gas: He; flow 2.7 mL/min; 45°C (2.5min); 20°C/min to 110°C; 30°C/min to 200; 200°C (10min); FID: 270°C. pH and osmolality were determined for safe administration. Radionuclidic purity was assessed by recording of the corresponding gamma spectrum (annihilation radiation at 511 keV and sum peak at 1022 keV) and additional measurement of the physical half-life.

Results

Effect of loop material

Comparative results are presented in Figure 1. The yields range from 0.8 ± 0.7% (FEP) over 2.5 ± 2% (ETFE) up to 27 ± 10% (PE).

Influence of amount of precursor

Results are presented in Figure 2. It is evident, that there is insignificant conversion below 2 mg of the precursor. For reliable conversion a minimum amount of 3.5 mg of the precursor appears to be reasonable. Higher amounts result in an insignificant increase.

Effect of preparative HPLC-columns

Results are presented in Table 1. Statistical evaluations showed, that the method using the Gemini column is superior with regard to preparation efficiency and quality of the purified product (overall product yield, specific activity, precursor contamination).

Influence of the inert gas

A comparison of N_2 (n=34) and He (n=20) as module working gases showed no significant impact on radiochemical yields (2.42 vs. 2.98 GBq; p=0.10), synthesis time (28 vs. 29 min; p=0.72) and radiochemical purity (98.1 vs. 98.3%; p=0.67) of the readily prepared tracer.

Automated apparatus

A scheme is presented in Figure 3. The presented set-up proved to be reliable and feasible. From a total of 92 routine patient syntheses we observed only 7 failures (7.6%, every 13th). Out of the 6 failures, 3 were due to operator mistakes (assembling mistake, pinched off trapping loop, missing preparative peak), 2 due to chemical problems (no conversion) and 1 because of a technical problem (valve fault).

Using the optimum reaction parameters in the automated module, average yields of 4 ± 1GBq (12.0 ± 3.6%) with a specific radioactivity of 292 ± 168GBq/µmol were obtained within 29 ± 3 minutes overall. The radiochemical purity averaged > 98%, and the contamination of the final product solution with WAY-100634 was below 0.2 µg/mL.

Discussion

Due to its difficult preparation, [*carbonyl*-^{11}C]WAY-100635 still has to be considered as one of the, if not the most, demanding PET-tracers. Two different methods have been introduced, the “wet” method [3-5] and the “dry” method [6-8]. In the “wet” method the three main reaction steps are performed in a traditional one-pot wet-chemical way, whereas the “dry” method uses a loop impregnated with the immobilized reaction partners for steps one and two (see Figure 4). The obtained adduct is then flushed into the precursor solution for the reaction step 3. Only the “dry” method could be performed automatically in a commercially available module at our department and therefore was our method of choice.

General

So far, it was understood that the synthesis of [*carbonyl*-^{11}C]WAY-100635 is especially sensitive to traces of moisture and therefore demands freshly distilled

solvents and vigorously dried reaction partners. In this study, we present for the first time, that there is no need to distil THF or thionyl chloride and there is no demand to especially process WAY-100634, TEA and the Grignard reagent. All chemicals were used as commercially available, without further purification. One essential finding concerns the influence of stabilizer (2,6-di-tert-butyl-p-cresol) in THF: no conversion can be achieved if stabilized THF is used! The given THF product is – to the best of our knowledge – the only available directly usable solvent for this purpose.

Loop material

McCarron et al. [7] reported that polypropylene (PP) guarantees successful trapping efficiency. Since PP is not easily available from a commercial source, Matarrese et al. [8] compared PP with FEP, and found no significant difference in the preparation yields. However, during our set up procedure, we found very low trapping and subsequent conversion using FEP and therefore alternatively evaluated ETFE and PE. As evident from Figure 1, only PE permits a reproducible preparation of [*carbonyl*-^{11}C]WAY-100635. These findings could be explained by the known differences in mixing in flow-through reactions using tightly coiled polymers due to the differences in wall friction. Although PE is not recommended as a material for thionyl chloride storage, we did not observe any secondary reactions. Furthermore, PE is very cheap and easily available from commercial suppliers.

Amount of precursor

Initially, it was reported, that the successful use of the wet method required 13-60 mg of precursor to achieve yields of 0.78 GBq (0.7% radiochemical yield at EOB) [4,7]. Hwang et al. [5] reported a one-pot synthesis demanding 2-3 mg of precursor for average yields of 30 mCi (1.11 GBq; 2.5% EOS) of [*carbonyl*-^{11}C]WAY-100635. In case of the dry method, McCarron et al. [7] suggested the use of 3.5 mg of precursor. Since there was no evaluation published regarding the influence of amount of precursor upon conversion yield, we conducted these experiments using 1.5-5.0 mg of the precursor. Our data show a distinct dependency (Figure 2), suggesting that 3.5 mg of the precursor is very suitable for safe routine application.

Preparative HPLC-columns

Due to the amount of precursor demanded for the radiosynthesis of [*carbonyl*-^{11}C]WAY-100635, the purification is a challenging step: WAY-100634 exhibits affinity for the $5HT_{1A}$ receptor and has to be limited to a maximum of 0.2 µg/kg body weight [13]. McCarron et al. [7] even suggested a sample enrichment device to obtain higher resolution of the preparative HPLC. To keep technical requirements to a minimum, we decided to omit sample enrichment and directly inject the quenched aqueous solution on an adequate HPLC column. From the three evaluated columns, µBondapak and XTerra showed poor pH stability leading to decreased resolution and short lifetime. High back-pressure allowed for a maximum flow of 6 mL/min. In contrast, Gemini showed a back pressure of 145 bar at a flow of 10 mL/min. Exceptional pH stability resulted in extended product life at comparable costs. Additionally, resolution between WAY-100634 and [*carbonyl*-^{11}C]WAY-100635 was increased, diminishing precursor contamination in the final product solution to a tenth. This result reflects the higher efficiency (more theoretical plates) of the Gemini column. Interestingly, the specific radioactivity was increased significantly.

Influence of the inert gas

Matarrese et al. [8] discussed the importance of the use of argon as carrier gas: due to its higher molecular weight, argon should diminish the contact with disturbing moisture in the vessel. In contrast, helium has the tendency to leak and is lighter than air. Nevertheless, we observed satisfactory yields both with helium and nitrogen, and therefore attach little value to that parameter.

Automated apparatus

The presented method is very simple, allowing the routine preparation of [*carbonyl*-^{11}C]WAY-100635 with a commercially available synthesizer module. With this set-up a 20-minutes reduction of the overall synthesis time as compared to [8] was achieved. As compared to the published failure rate of 14.9% [5], the presented method can be conducted very reproducibly with a failure rate of only 7.6%. Yields are constantly high, in average 4.0 GBq (2.4-6.3 GBq).

Although it is commonly known that the set-up of a reliable synthesis of [*carbonyl*-^{11}C]WAY-100635 is a challenge, it took us less than 6 months from point zero to the first patient synthesis. Until now, 92 routine investigations have been performed. For

illustrative purposes two examples are presented in Figure 5 showing the undisputed quality of [*carbonyl*-^{11}C]WAY-100635 as the tracer of choice for $5HT_{1A}$ receptor imaging [14].

Conclusion

A simple and feasible method for the routine preparation of [*carbonyl*-^{11}C]WAY-100635 is presented here. Detailed experimental evaluations of the essential parameters were conducted, and on their basis an automatic set-up was generated. The preparation is based on a commercially available synthesizer module and all chosen chemicals can be used without further processing. The presented set-up allows the reproducible preparation of [*carbonyl*-^{11}C]WAY-100635 with high specific radioactivities and yields up to 6.3 GBq.

Acknowledgements

The authors thank Thomas Zenz for reliable technical support and Dr. Oliver Langer for his initial interest in the project. Parts of the project were supported by a grant from the Austrian Science Fund (FWF P16549).

References

1. Houle, S., DaSilva, J. N., Wilson, A. A.: Imaging the 5-HT_{1A} receptors with PET: WAY-100635 and analogues. Nucl. Med. Biol. **27**, 463 (2000).
2. Passchier, J., van Waarde, A.: Visualisation of serotonin-1A (5-HT1A) receptors in the central nervous system. Eur. J. Nucl. Med. **28**, 113 (2001).
3. Mathis, C. A., Simpson, N.R., Mahmood, K., Kinahan, P. E., Mintun, M. A.: [^{11}C]WAY-100635: a radioligand for imaging 5-HTIA receptors with positron emission tomography. Life Sci. **55**, 403 (1994).
4. Pike, V. W., McCarron, J. A., Lammertsma, A. A., Hume, S. P., Poole, K. G., Grasby , P. M., Malizia, A., Cliffe, I. A., Fletcher, A., Bench, C.: First delineation of 5-HT1A receptor in human brain with PET and [C-11]WAY-100635. Eur. J. Pharmacol. **283**, R1 (1995).
5. Hwang, D. R., Simpson, N. R., Montoya, J., Mann, J. J., Laruelle, M.: An improved one-pot procedure for the preparation of [^{11}C-carbonyl]-WAY100635. Nucl. Med. Biol. **26**, 815 (1999).
6. Wilson, A. A., DaSilva, J. N., Houle, S.: Solid-phase radiosynthesis of [^{11}C]WAY100635. J. Label. Compd. Radiopharm. **38**,149 (1996).
7. McCarron, J. A., Turton, D. R., Pike, V. W., Poole, K. G.: Remotely-controlled production of the 5-HT_{1A} receptor radioligand, [*carbonyl*-^{11}C]WAY-100635, via ^{11}C-carboxylation of an immobilized Grignard reagent. J. Label. Compd. Radiopharm. **38**, 941 (1996).
8. Matarrese, M., Sudati, F., Soloviev, D., Todde, S., Turolla, E. A., Kienle, M. G., Fazio, F.: Automation of [^{11}C]acyl chloride syntheses using commercially available ^{11}C-modules. Appl. Radiat. Isot. **57**, 675 (2002).
9. Osman, S., Lundkvist, C., Pike, V. W., Halldin, C., McCarron, J. A., Hume, S. P., Luthra, S. K., Bench, C. J., Grasby, P. M., Swahn, C.-G., Wikström, H., Barf, T., Ginovart, N., Farde, L., Cliffe, I. A., Fletcher, A.: Radioactive metabolites of the 5HT1A receptor radioligand, [*O*-methyl-^{11}C]WAY100635, in rat, monkey and humans plus evaluation of the brain uptake of the metabolite [*O*-methyl-^{11}C]WAY100634 in monkeys. J. Label. Compd. Radiopharm. **37**, 283 (1995).

10. Pike, V. W., McCarron, J. A., Lammertsma, A. A., Osman, S., Hume, S. P., Sargent, P. A., Bench, C. J., Cliffe, I. A., Fletcher, A., Grasby, P. M.: Exquisite delineation of 5-HT1A receptors in human brain with PET and [carbonyl-^{11}C]WAY-100635. Eur. J. Pharmacol. **301**, R5 (1996).

11. Cliffe, I. A.: A retrospect on the discovery of way-100635 and the prospect for improved 5-HT_{1A} receptor PET radioligands. Nucl. Med. Biol. **27**, 441 (2000).

12. Osman, S., Lundkvist, C., Pike, V. W., Halldin, C., McCarron, J. A., Swahn, C.-G., Farde, L., Ginovart, N., Saijnder, K., Luthra, S. K., Gunn, R. N., Bench, C. J., Sargent, P. A., Grasby, P. M.: Characterisation of the appearance of radioactive metabolites in monkey and human plasma from the 5-HT1A receptor radioligand, [carbonyl-^{11}C]WAY-100635—Explanation of high signal contrast in PET and an aid to biomathematical modelling. Nucl. Med. Biol. **25**, 215 (1998).

13. Hume, S. P., Ashworth, S., Opacka-Juffry, J., Ahier, R. G., Lammertsma, A. A., Pike, V. W., Cliffe, I. A., Fletcher, A., White, A. C.: Evaluation of [O-methyl-^{3}H]WAY-100635 as an in vivo radioligand for 5-HT1A receptors in rat brain. Eur. J. Pharmacol. **271**, 515 (1994).

14. Lanzenberger, R., Mitterhauser, M., Spindelegger, C., Wadsak, W., Klein, N., Mien, L. K., Holik, A., Attarbaschi, T., Mossaheb, N., Sacher, J., Geiss-Granadia, T., Kletter, K., Kasper, S., Tauscher, J.: Reduced serotonin-1A receptor binding in social anxiety disorder. Biol. Psych., in press (2006). DOI:10.1016/j.biopsych.2006.05.022

Captions

Table 1: Comparison of three different HPLC columns and their influence on selected radiochemical parameters. Each given value represents arithmetic mean ± standard deviations.

Figure 1: Influence of the loop material on the combined trapping and conversion yield. Each given value represents arithmetic mean ± standard deviation ($n \geq 7$). (★) Values differ significantly ($p<0.05$; unpaired two-tailed t-test) (★★) Values differ highly significantly ($p<0.001$; unpaired two-tailed t-test)

Figure 2: Influence of the amount of precursor upon the conversion yield. Values represent arithmetic means ± standard deviation ($n \geq 7$).

Figure 3: Graphical illustration of the set-up of the commercially available Nuclear Interface module. AD … activity detector; V … valve; LAF … laminar air flow.

Figure 4: Schematic illustration of the three major steps in the radiosynthesis of [*carbonyl*-^{11}C]WAY-100635. Steps 1 and 2 are performed inside the coated PE loop (with immobilized Grignard's reagent; AD2); step 3 is conducted in the reaction vial (AD3) at 70°C for 4 minutes.

Figure 5: Parametric $5HT_{1A}$ receptor distribution superimposed on high-resolution single-subject structural MR images (matrix 256*256*128, resolution 0.78*0.86*1.56mm, MPRAGE sequence). The white crosses show the commissura anterior in the coronal, sagittal and axial view of a healthy male subject (A) and a male patient suffering from social anxiety disorder (B). The colour table indicates values of regional $5HT_{1A}$ receptor binding potential (Bmax/KD) for each voxel. The $5HT_{1A}$ receptor binding potential is significantly reduced across all brain regions in the patient compared to the healthy control subject, although radiochemical variables are comparable. Areas with low $5HT_{1A}$ receptor densities as the reference region, cerebellum, show no specific binding calculated by the simplified reference tissue model using PMOD. The PET data were acquired on a GE Advance PET camera measuring a series of 30 successive time frames (15*1min, 15*5min) in 3D mode within a total acquisition time of 90 minutes. [*carbonyl*-^{11}C]WAY-100635 was injected as bolus. Emission

data were scatter corrected, 35 contiguous slices (matrix 128*128*35) with a slice thickness of 4.25 mm were reconstructed by using an iterative filtered back-projection algorithm. Spatial resolution of the final reconstructed volume was 4.36 mm full-width-half-maximum at the centre of the field of view. Radiochemical parameters represent values at time of injection. Further details are found in (Lanzenberger et al., 2006).

column	**Yield (EOS) [GBq]**	**Yield (EOS) [%]#**	**Preparation time [min]**	**Spec. radioactivity [GBq/µmol]**	**Conc. of WAY-100634 [µg/mL]**	**Radiochem. purity [%]§**
X-Terra	1.55 ± 1.09 (★)	5.6 ± 3.41 (n.s.)	30 ± 7	37.4 ± 35.0 (n.s.)	1.21 ± 0.58 (n.s.)	96.8 ± 1.2
µ-Bondapak	2.26 ± 0.94 (★)	7.2 ± 3.43 (n.s.)	28 ± 5	45.6 ± 30.2 (n.s.)	1.54 ± 1.38 (n.s.)	98.1 ± 1.5
Gemini	4.00 ± 0.96 (★★)	12.03 ± 3.65 (★★)	29 ± 3	292.4 ± 168.2 (★★)	0.16 ± 0.35 (★★)	98.3 ± 0.8

#) at the end of synthesis (EOS), corrected for decay, based on [^{11}C]CO_2 (EOB, end of bombardment)

§) determined by analytical radio-HPLC (conditions see methods section – quality control)

(★) values differ significantly ($p<0.05$; n = 16-54; unpaired two-tailed t-test)

(★★) values differ highly significantly ($p<0.001$; n = 16-54; unpaired two-tailed t-test)

(n.s.) values differ not significantly ($p>0.05$; n = 16-54; unpaired two-tailed t-test)

Table 1: Comparison of three different HPLC columns and their influence on selected radiochemical parameters. Each given value represents arithmetic mean ± standard deviations.

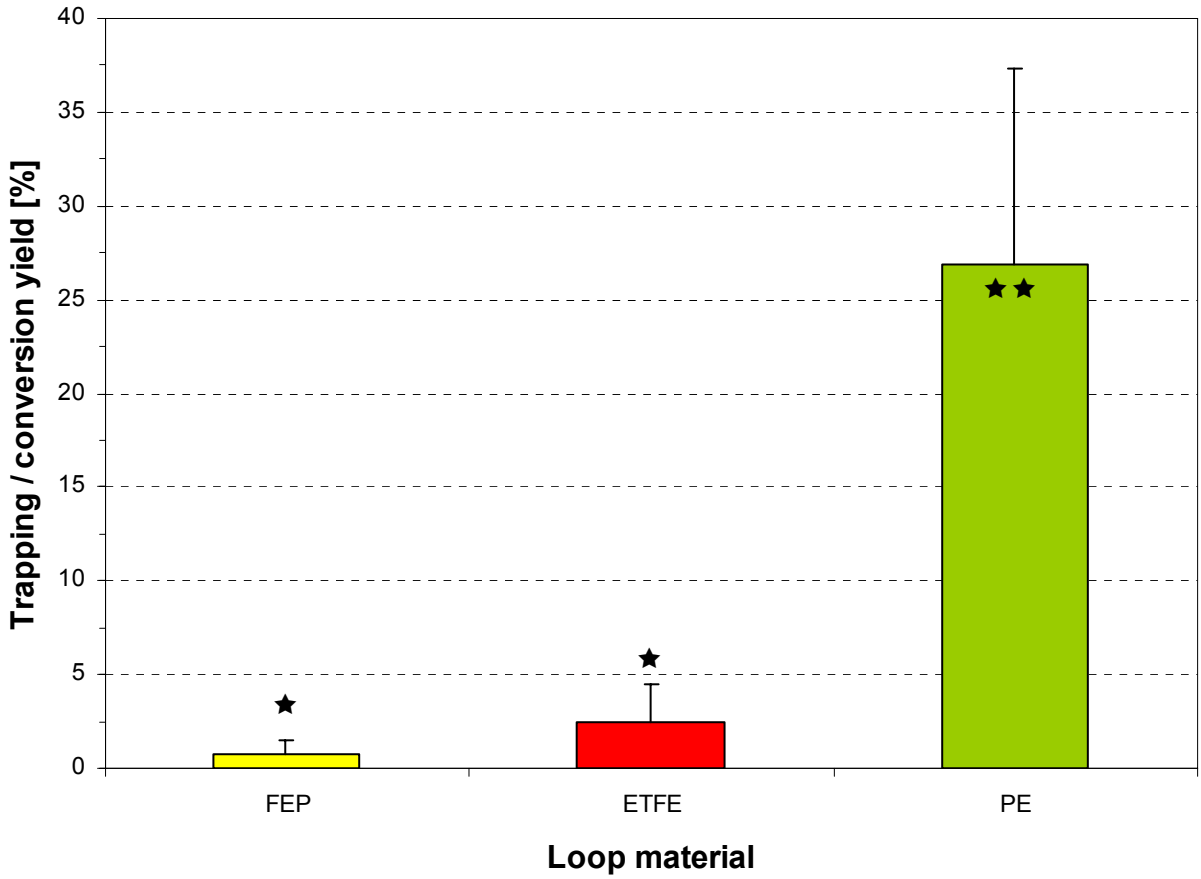

Figure 1: Influence of the loop material on the combined trapping and conversion yield. Each given value represents arithmetic mean ± standard deviation (n ≥ 7). (★) Values differ significantly ($p<0.05$; unpaired two-tailed t-test) (★★) Values differ highly significantly ($p<0.001$; unpaired two-tailed t-test)

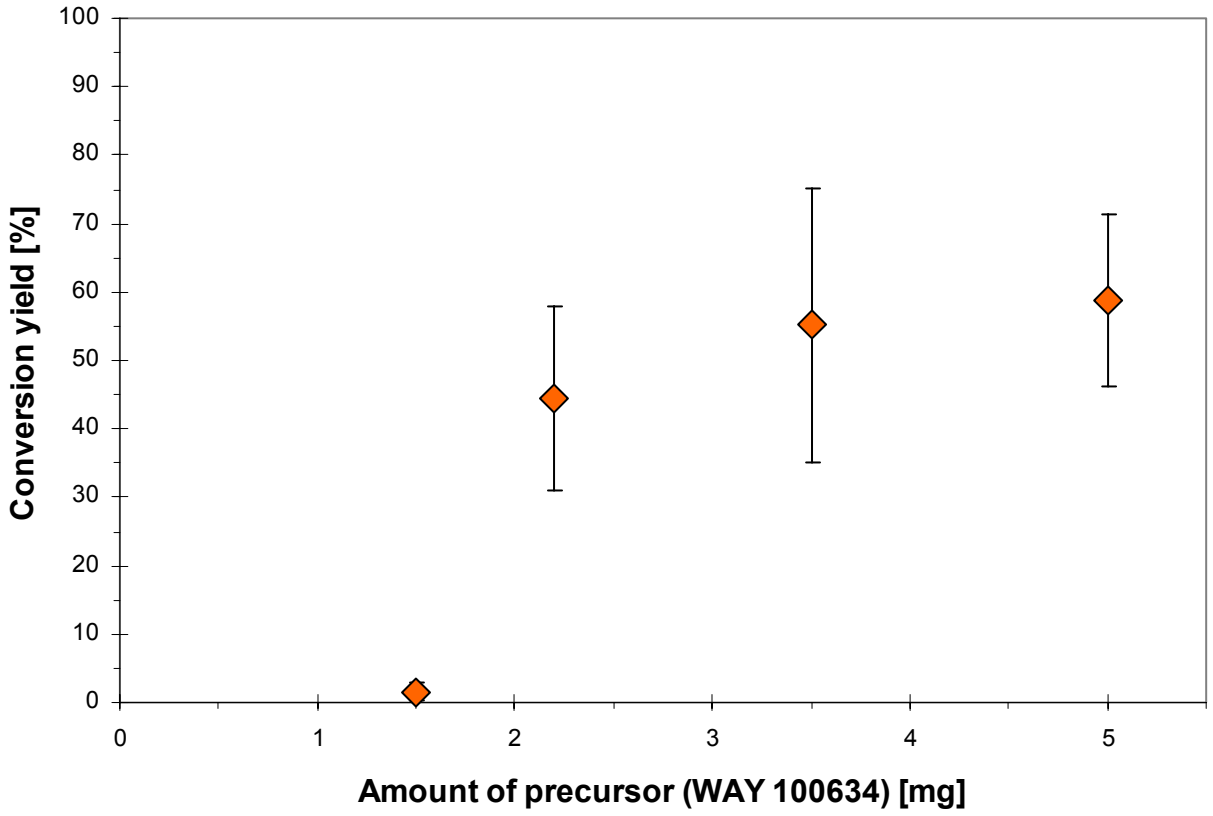

Figure 2: Influence of the amount of precursor upon the conversion yield. Values represent arithmetic means ± standard deviation (n ≥ 7).

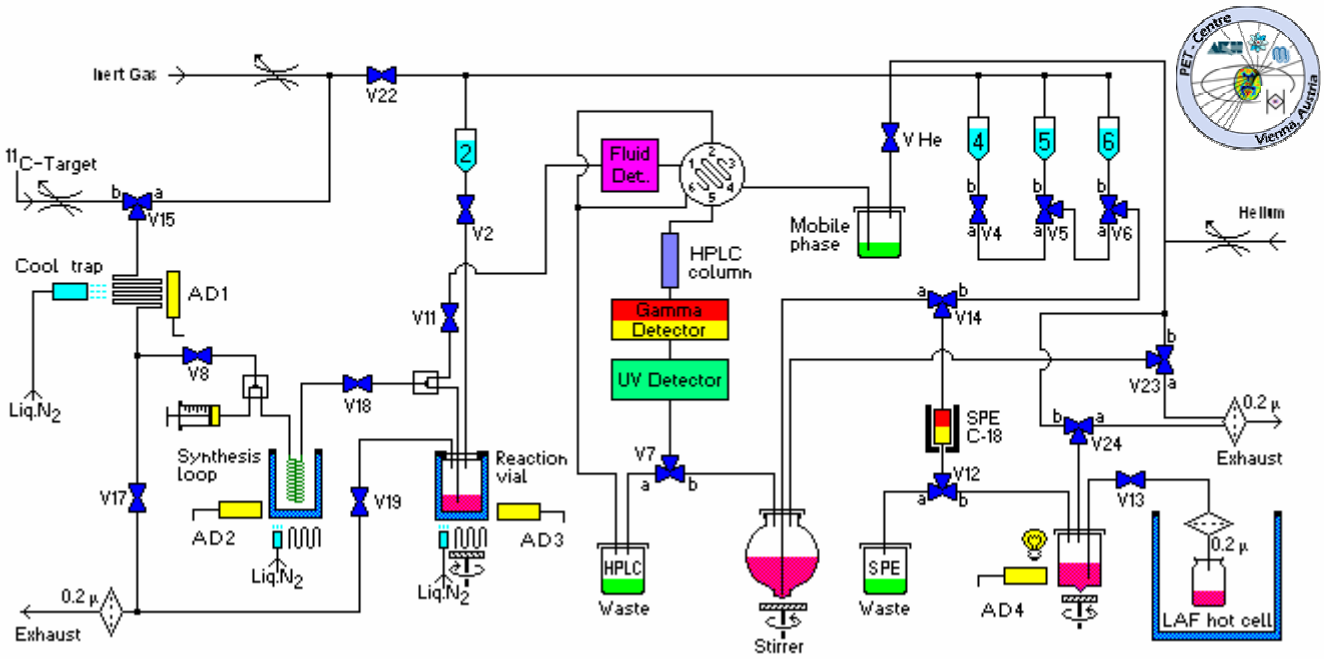

Figure 3: Graphical illustration of the set-up of the Nuclear Interface module. AD … activity detector; V … valve; LAF … laminar air flow.

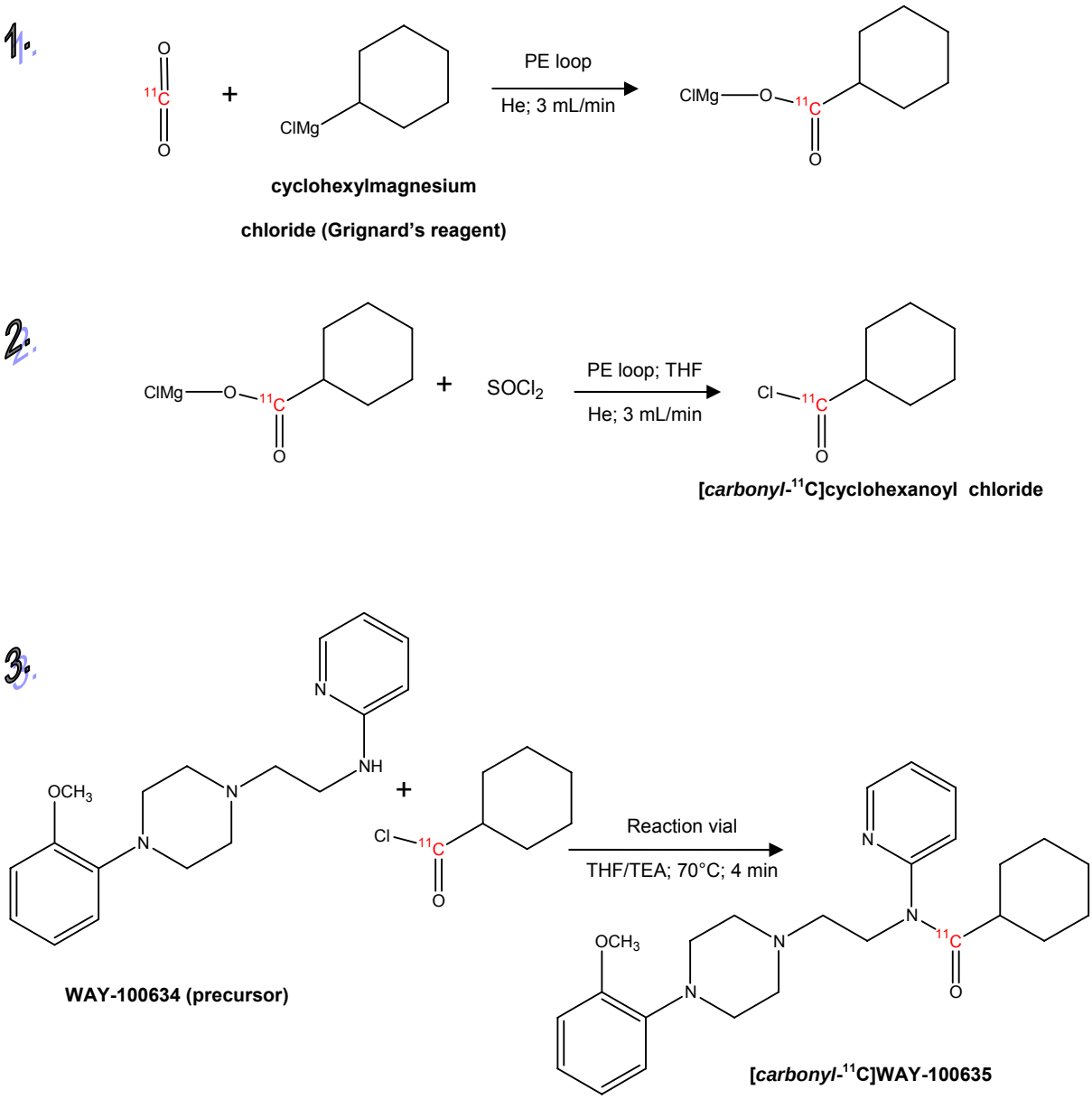

Figure 4: Schematic illustration of the three major steps in the radiosynthesis of [*carbonyl*-^{11}C]WAY-100635. Steps 1 and 2 are performed inside the coated PE loop (with immobilized Grignard's reagent; AD2); step 3 is conducted in the reaction vial (AD3) at 70°C for 4 minutes.

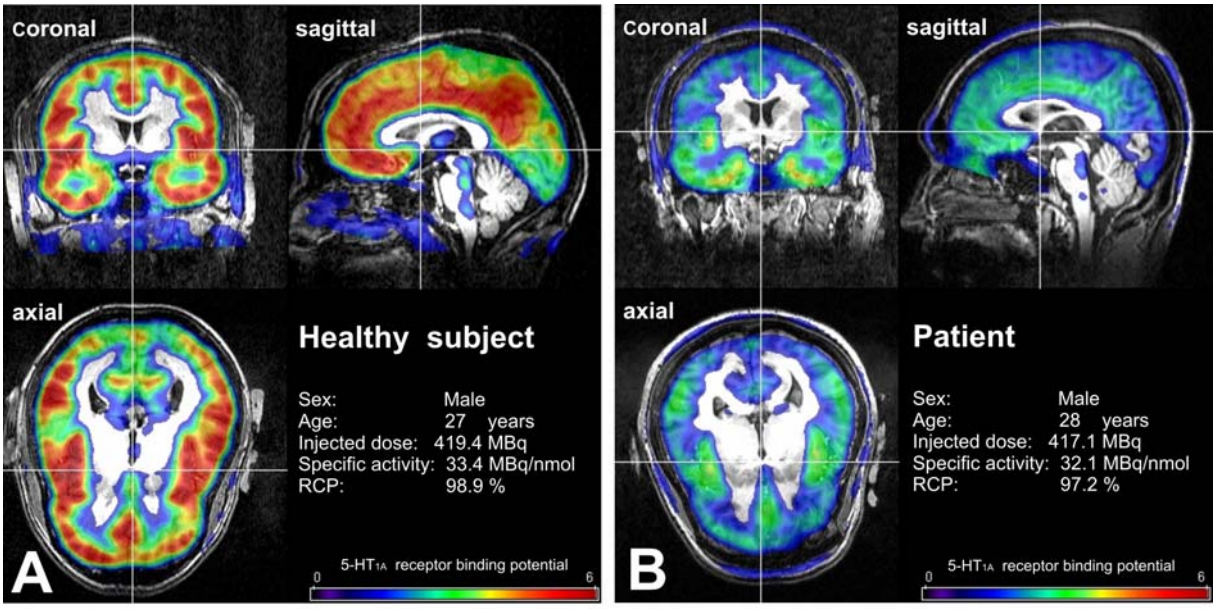

Figure 5: Parametric $5HT_{1A}$ receptor distribution superimposed on high-resolution single-subject structural MR images (matrix 256*256*128, resolution 0.78*0.86*1.56mm, MPRAGE sequence). The white crosses show the commissura anterior in the coronal, sagittal and axial view of a healthy male subject (A) and a male patient suffering from social anxiety disorder (B). The colour table indicates values of regional $5HT_{1A}$ receptor binding potential (Bmax/KD) for each voxel. The $5HT_{1A}$ receptor binding potential is significantly reduced across all brain regions in the patient compared to the healthy control subject, although radiochemical variables are comparable. Areas with low $5HT_{1A}$ receptor densities as the reference region, cerebellum, show no specific binding calculated by the simplified reference tissue model using PMOD. The PET data were acquired on a GE Advance PET camera measuring a series of 30 successive time frames (15*1min, 15*5min) in 3D mode within a total acquisition time of 90 minutes. [*carbonyl*-^{11}C]WAY-100635 was injected as bolus. Emission data were scatter corrected, 35 contiguous slices (matrix 128*128*35) with a slice thickness of 4.25 mm were reconstructed by using an iterative filtered back-projection algorithm. Spatial resolution of the final reconstructed volume was 4.36 mm full-width-half-maximum at the centre of the field of view. Radiochemical parameters represent values at time of injection. Further details are found in (Lanzenberger et al., 2006).

3. Conclusions

The presented thesis aimed at the establishment and the development of four innovative PET-tracers for neuroimaging. The targets of the presented compounds work are the dopamin transporter (= DAT) imaged with [^{18}F]FE@CIT, the mu opioid subtype receptor (= μOR) imaged with [^{18}F]FE@CFN, the adenosine 3 subtype receptor (= A3AR) imaged with [^{18}F]FE@SUPPY and the serotonin 1A subtype receptor (= 5-HT1A) imaged with [carbonyl-^{11}C]WAY 100635

In the establishment of [carbonyl-^{11}C]WAY 100635 at the PET centre of the Vienna General Hospital, we gained new insights on the radiosynthesis of this high demanding four step radiosynthesis resulting in the implementation of an automated radiosynthesis for the daily routine production.

The considerations for the development of new fluorine-18 fluoroethylated neuroimaging tracers are based on the long radiochemical expertise of the local working group. The choice for the selected targets was inspired by the “fruitful” cooperation with the department of psychiatry of the Vienna General Hospital, especially with Dr R. Lanzenberger, head of the local neuroimaging group.

The new developed PET-tracers of this PhD thesis will broaden the PET in vivo neuroimaging spectrum and, furthermore, enable new insights in the neurotransmitter systems of the human brain. Especially with the focus on clinical psychiatry questions such as pathophysiological meachanisms of the serotonergic system and their related diseases, e.g. social anxiety disorders, these PET-tracers will provide additional information.

Moreover, the introduced tracers can also be strongly employed for drug developement research by answering questions of pharmacokinetics and drug dose

regimen *(microdosing concept)* and there enable the evaluation of the biological selectivity of newly developed drugs for the pharmaceutical industry.

Outlook and future perspectives

For the tracers [^{18}F]FE@CIT ,[^{18}F]FE@CFN and [^{18}F]FE@SUPPY the required preclinical evaluations were accomplished and a the clinical application will be the next step Especially, [^{18}F]FE@CIT has the potential to be implemented for the daily routine DAT-neuroimaging at the PET centre of the Vienna General Hospital due to its fast, convenient radiosynthesis, feasibility and high product yields Moreover, optimizations of this radiosynthesis are schedulded with a newly designed precursor compound, which contains a tosylate leaving group, thus enabling the direct fluorination via one-pot one-step reaction. This will result in overall time reduction and allowing will an easier approach for the automatization. For [^{18}F]FE@SUPPY, first micro-PET studies are in process.

To conclude, the newly gained aspects for fluorine-18 fluoroethylations and for carbon-11 radiochemistry (with the focus on the primary precursor [^{11}C]CO_2 are enlightning the demanding and complex synthesis mechanisms.

The special emphasis on preparative aspects of radiochemical parameters specific (radioactivity, yield and radiochemical purity) were fully fulfilled for all presented PET-tracers.

4. Appendix

Automatization approach of radiosyntheses

Due to radiation safe guarding guidelines for the operating personnel and operational safety requirements for the production of PET radiopharmaceuticals the implementation of automated and remotely controlled radioyntheses of PET radiotracers performed by synthesizer module is always the desired main aim. The radiosyntheses production in a hospital PET centre have special requirements:

1) Due to short physical half life of positron emitters the starting production activity ranges in [GBq] levels to yield sufficent amount of the desired PET tracer at the end of radiosyntheses. Thus the radiation burden for the operating personnel have to be minimized.

2) The need of hospital daily routine production of PET radiopharmaceuticals requires rapid, reproducible, safe and reliable radiosyntheses.

3) Each produced radiopharmaceutical batch has to fulfill pharmaceutical quality assurance standards, respectively given Good Manufacturing Practice guidelines (GMP).

With these three prerequistes in mind the employment of synthesizer modules for the automatization of radiosyntheses is the *"logical"* approach for appropriating these three demands.

1) The automated set-up for the radiosynthesis of [^{18}F]FE@SUPPY

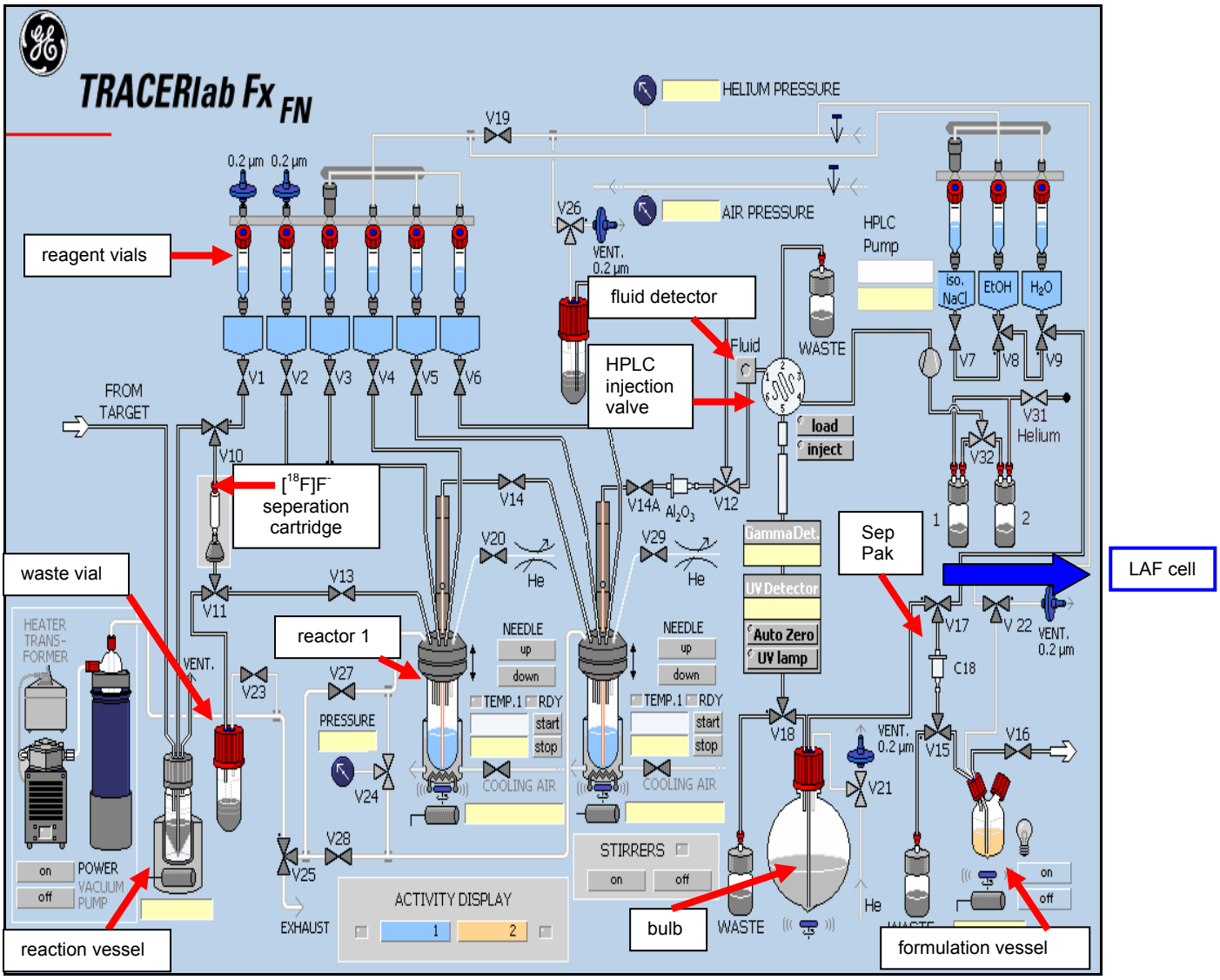

This Figure shows the scheme of the employed synthesizer module Tracer lab FX $_{FN}$ for the automated [^{18}F]FE@SUPPY radiosynthesis. All following given operation steps are related to this scheme. Cyclotron produced n.c.a [^{18}F]F$^-$ was inserted by the operator manually in reaction vessel due to reason that there is no direct connection line to the target. Then for the azeotropic drying process the reaction vessel content was transferred via V10 (= Valve) through a [^{18}F]F$^-$ cartidge for seperation of unreacted oxygen-18 enriched H_2O^{16}. This undesired oxygen-18 enriched H_2O^{16} is transferred via V11 into the waste vial. The desired [^{18}F]F$^-$ is eluated from the catridge with a 16.0mg- 20.0mg K $_{2.2.2.}$/ 3.5-4.5mg K_2CO_3 dissolved in a solution of [70-80]ACN/ [30-20] water (v/v) , which is stored in reagent vial V1, this eluated mixture is transferred via V13 into the reactor 1. In this reactor 1 the azeotropic dryness operation of [^{18}F]F$^-$ is performed by first addition of two x 500.0µl ACN portions and then followed by a second addition of four x 250.0µl ACN from reagent vial V2. The heating temperature is 100°C for 10.0 minutes. After this activiation the obtained K $_{2.2.2.}$ / [^{18}F]F$^-$ complex in reactor 1 is reacting with a precusor amount of 1.5mg- 10.0mg Tos@SUPPY, which is stored in reagent vial V3. After the reaction temperature of 75.0°C for 20.0 minutes is fulfilled , this crude mixture is then subjected to the radio HPLC injector V12 passing the fluid detector for purification process. The product peak [^{18}F]FE@SUPPY- as obtained by semi-preparative HPLC- was cut automatically from the chromatogram via V18, diluted

with 80.0ml water stored in a reagent vial (so called “bulb”) and captured on pre-conditioned C18 SepPak® plus or C18 SepPak® light V17. After washing with a further 10.0ml of water stored in V9 via V17 and V15 into the waste vial. The purified product was eluted from the SepPak with different ethanol volumina in a range of 0.6- 2.5ml stored in V8 via V17 and V15 into the formulation vial (= formul. vial). After formulation with 10.0ml physiological saline solution stored in V7 via V17 and V15 and on-line sterile filtration with different tested sterile filter types under aseptic conditions via V22→ laminar air flow hot cell (blue arrow LAF cell), the product [^{18}F]FE@SUPPY was subjected to quality control.

2) Original Standard Operation Procedures protocol (= SOP) for [carbonyl-^{11}C]WAY 100635 of the PET centre of Vienna General Hospital (added on the next pages)

6. Acknowledgements (Danksagungen)

“ *…und sie bewegt sich doch…*”, um mit dem Ausspruch Galileis einen Vergleich mit diesem Dissertationsprojekt aufzustellen und gleichzeitig einen Versuch für eine „treffende und aufrichtige„ Einleitung für meine Danksagungen zu bemühen, möchte ich auf diesem Wege meinen tiefsten Dank folgenden Personen übermitteln:

Meiner einzigartigen, geliebten und fantastischen Frau Mutter, die mich immer, ohne Unterlaß und bedingunglos unterstützt hat und mir dieses wunderschöne Leben ermöglicht hat. Ihr ganz speziell widme ich diese Dissertation, die sie hoffentlich auch ein wenig „stolz“ macht. ***(Oka-san, arigatou !!!)***

Diese Dissertation ist auch nur realisierbar gewesen durch die hervorragenden Arbeitsbedingungen, die mir das Department für pharmazeutische Technologie und Biopharmazie und die Universitätsklinik für Nuklearmedizin der Medizinischen Universität Wien, ermöglicht, respektive geschaffen haben. Ich möchte hier an dieser Stelle meinen besonderen Dank, den „Professores“ Viernstein H (Danke für Ihre Unterstützung und Hilfe), Dudczak R, und Kletter K. (Danke, für Ihr stetes Lob und unerschütterlichen Glauben an mich) aussprechen.

Für das immer angenehme Arbeitsklima im „Schreibraum“ bedanke ich mich sehr bei Harald und Fritz (auf viele heitere Arbeitsstunden im fensterlosen Raum !).

Für die immer sehr angeregten und konstruktiven Vorschläge für verbesserte Radiosynthesen möchte ich mich bei Oliver und Aiman recht herzlichst bedanken.

Weiters meiner hervorragenden und einmaligen „ neuroimaging“ Arbeitsgruppe:

Für die spannenden und „fruchtbaren“ Diskussionen und interessanten Projekte ein „*dickes*“ Dankeschön an Euch, Dagmar, Dani, Rupert, Christoph, Karem und Evi (mögen wir noch viele bahnbrechende Entdeckungen erforschen!).

Insbesonders, möchte ich meine Gruppenarbeitskollegin, *Karo* ♦ ☺, in diesem Kontext nennen. Es ist mir wirklich eine echte Freude, jemanden gefunden zu haben, der sich für C-11; F-18 Module, azeotrope Trockung und Konsorten so begeistern kann wie ich ! Es ist auch sehr sehr fein, daß wir immer stets so angeregte Fachdiskussionen führen und einfach über alles reden können. (*„Zauberlehrling“*, Du bist mein allerbester und talentierster Azubi ! Auf viele weitere *„fliegende Precursors“*, *„les products“* und ganz viele Witze und noch mehr coole Radiosynthesen !)

Für meine unglaublichen, stets tiefst beeindruckenden und wirklich humorvollen *„Mentores“* *Markus* und *Wolfi*- meinen innigsten und aufrichtigsten Dank. Es ist wirklich schwer für mich in Worte zu fassen, was Ihr mir bedeutet, aber soviel ohne Euch beide wäre ich nicht da, wo ich jetzt bin, an der „*Olympspitze*“ meiner Träume ! Ich hätte das nie ohne Eure ungebrochene Hilfe, Förderung und Euer Verständnis geschafft ! Ihr seid mir stets Vorbilder gewesen und werdet es immer sein ! Dankeschön für einfach alles ! Und auf weitere viele viele viele und tolle Arbeitsstunden mit Euch beiden !

Meinem lieben ehemaligen Kommilitonen Stefan, der mir immer mit Rat und Tat zur Seite stand, und den ich einfach für sein Wesen so schätze! (Stefan, mein lieber *„Zwillingsbruder“* ! Auf viele weitere Kebap's vom Mustafa mit echt scharfer roter Sauce !)

Meinen *„zivilen“* Freundinnen, Steffi und Eva, die immer mitgefiebert haben während meiner ganzen Dissertationszeit und mich stets wieder aufs Neue motiviert haben ! (Ihr seid einfach unvergleichliche Damen !)

Curriculum vitae of MPharmS Mien Leonhard-Key

Personal data:

Date of birth: November the 6th. 1974

Place of birth: Vienna, Austria

Citizenship: Austrian

Marital status: Unmarried

Education:

1980-1984: Elementary school am Judenplatz 1010 Vienna

1984-1993: High school BRG 1 Stubenbastei 1010 Vienna

1993-1995: Fulfilling military service at LWSR 22 Karlskaserne 1220 Vienna

1994-xxxx : Study of nutrition science at university of Vienna

1995-2003: Study of pharmacy at the university of Vienna

Practical experiences:

June – July 2002 practical training in the pharmacy of the General Hospital of Vienna (AKH Wien)

August - October 2002 study project "radiolabelling of Nanocoll® with In-111" at the department of nuclear medicine of the Vienna general hospital under supervision of Doz Mitterhauser M and Dr Wadsak W (see publication list reference number [13])

January 2003 Poster presentation of "radiolabelling of Nanocoll® with In-111" at the ÖGN congress (Linz)

April - October 2003 Diploma thesis "Radiosynthesis of [^{18}F]FFMZ, a new ligand for the GABA A subtype receptor PET imaging" under supervision of Dr Wadsak and Doz Mitterhauser (see references [12] and [14])

January 2004 Poster presentation of "Purification and Quality control of 3- (2' [^{18}F]fluoro)-flumazenil" at the ÖGN congress (Bad Gastein)

March 2004 - August (planned) 2007 PhD thesis: "New innovative fluorine-18 labelled radiotracers developed for the PET neuroimaging and new insights of the [carbonyl-^{11}C]WAY 100635 radiosynthesis for the 5-HT1A subreceptor PET imaging" under supervision of Doz Mitterhauser M, Dr Wadsak W and Dr Lanzenberger R.

December 2003- March 2007 co-worker in the FWF – project (FWF P16549) "

Implementation of the automated radiosynthesis of [carbonyl -^{11}C] WAY 100635 for the 5-HT_{1A} subtype receptor PET imaging" under supervision of Doz Mitterhauser and Dr Wadsak in cooperation with Dr Lanzenberger (references [1] and [3])

January 2005 study project "Radiosynthesis and biological evaluation of [^{18}F]FE@CIT, a new ligand for the dopamine transporter PET imaging" under supervision of Doz Mitterhauser and Dr Wadsak (see reference [10])

April 2005 study project "Radiosynthesis and biological evaluation of [^{18}F]FE@CFN, a new ligand for the mu subtype opioid rececptor" under supervision of Dr Wadsak and Doz Mitterhauser (see reference [2])

April 2006 study project " Radiosynthesis and biological evaluation of [^{18}F]FE@SUPPY, a new ligand for the Adenosine 3 subtype receptor PET imaging" under supervision of Dr Wadsak and Doz Mitterhauser

January 2006 oral presentation "Improvements and optimization of the automated radiosynthesis of [Carbonyl-^{11}C]WAY100635" at the ÖGN (Bad Gastein)

January 2007 oral presentation "Die optimierte Radiosynthese von [Carbonyl-^{11}C] WAY 100635" at the ÖGN (Linz)

March 2007 invited lecture "There was a WAY, Erfahrungen eines Radiopharmazeuten bei der [carbonyl-^{11}C]WAY Implementierung" for the "VO+ SE Positronen Emissions Tomographie/Molekulares Imaging"

Practical supervision of diploma theses :

Practical supervision of the diploma thesis of Ms. Feitscher S for the study project [^{18}F]FE@CFN and of the diploma theses of Ms Schmidt B and of Ms Weber K for the study project of [^{18}F]FE@SUPPY and [^{18}F]FE@SUPPY 2.

Laboratory teaching experiences:

Since March 2005 laboratory assistant for the "Praktikum für magistrale und industrielle Arzneimittelherstellung" and for the "Grundpraktikum aus pharmazeutischer Technologie" at the department of Pharmaceutical Technology and Biopharmaceutics, University of Vienna

Post graduation courses:

August 2005-September 2006 Attending the postgraduate Diploma Course Radiopharmaceutical Chemistry/Radiopharmacy at the ETH ZURICH with final graduation in October 2006

Publication list:

[1] Wadsak W, Mien LK, Ettlinger DE, Lanzenberger R , Dudczak R , Haeusler D, Kletter K, Mitterhauser M 2007. The simple and fully automated preparation of [carbonyl-^{11}C]WAY-100635. Radchim Acta **95**: 417-22

[2] Wadsak W, Mien LK, Ettlinger DE, Feitscher S, Toegel S, Lanzenberger R, Marton J, Dudczak R, Kletter K, Mitterhauser M 2006. Preparation and Radiosynthesis of [^{18}F]FE@CFN (2-[18F]fluoroethyl 4-[N-(1-oxopropyl)-N-phenylamino]-1-(2-phenylethyl)-4-piperidinecarboxylate), a Potential μ-Opioid Receptor Imaging Agent. Radchim Acta **95**:33-8.

[3] Lanzenberger RR, Mitterhauser M, Spindelegger C, Wadsak W, Klein N, Mien LK, Holik A, Attarbaschi T, Mossaheb N, Sacher J, Geiss-Granadia T, Kletter K, Kasper S, Tauscher J 2007. Reduced Serotonin-1A Receptor Binding in Social Anxiety Disorder. Biol Psychiatry **61**:1081-9.

[4] Ettlinger DE, Wadsak W, Mien LK, Machek M, Wabnegger L, Rendl G, Karanikas G, Viernstein H, Kletter K, Dudczak R, Mitterhauser M 2006. [^{18}F]FETO: metabolic considerations. Eur J Nucl Med Mol Imaging **33:** 928-31.

[5] Wadsak W, Mitterhauser M, Rendl G, Schuetz M, Mien LK, Ettlinger DE, Dudczak R, Kletter K, Karanikas G 2006. [^{18}F]FETO for adrenocortical PET imaging: a pilot study in healthy volunteers. Eur J Nucl Med Mol Imaging **33:** 669-72.

[6] Toegel S, Mien LK, Wadsak W, Eidherr H, Viernstein H, Kluger R, Ettlinger D, Kletter K, Dudczak R, Mitterhauser M 2006. In vitro evaluation of no carrier added, carrier added and cross-complexed [^{90}Y]-EDTMP provides evidence for a novel "foreign carrier theory". Nucl Med Biol **33:** 95-9.

[7] Toegel S, Hoffmann O, Wadsak W, Ettlinger D, Mien LK, Wiesner K, Nguemo J, Viernstein H, Kletter K, Dudczak R, Mitterhauser M 2006. Uptake of bone-seekers is solely associated with mineralisation! A study with ^{99m}Tc-MDP, ^{153}Sm-EDTMP and ^{18}F-fluoride on osteoblasts. Eur J Nucl Med Mol Imaging **33:** 491-4.

[8] Wadsak W, Wirl-Sagadin B, Mitterhauser M, Mien LK, Ettlinger DE, Keppler BK, Dudczak R, Kletter K 2006. NCA nucleophilic radiofluorination on substituted benzaldehydes for the preparation of [^{18}F]fluorinated aromatic amino acids. Appl Radiat Isot **64:** 355-9.

[9] Mitterhauser M, Toegel S, Wadsak W, Mien LK, Eidherr H, Kletter K, Viernstein H, Kluger R, Engel A, Dudczak R 2005. Binding studies of [^{18}F]-fluoride and polyphosphonates

radiolabelled with [^{99m}Tc], [^{111}In], [^{153}Sm] and [^{188}Re] on bone compartments: verification of the pre vivo model? Bone **37:** 404-12.

[10] Mitterhauser M, Wadsak W, Mien LK, Hoepping A, Viernstein H, Dudczak R, Kletter K 2005. Synthesis and biodistribution of [^{18}F]FE@CIT, a new potential tracer for the dopamine transporter. Synapse **5:** 573-9.

[11] Mitterhauser M, Togel S, Wadsak W, Mien LK, Eidherr H, Wiesner K, Viernstein H, Kletter K, Dudczak R 2004. Binding studies of [^{18}F]-fluoride and polyphosphonates radiolabelled with [^{111}In], [^{99m}Tc], [^{153}Sm], and [^{188}Re] on bone compartments: a new model for the pre vivo evaluation of bone seekers? Bone **34:** 835-44.

[12] Mitterhauser M, Wadsak W, Wabnegger L, Mien LK, Togel S, Langer O, Sieghart W, Viernstein H, Kletter K, Dudczak R 2004. Biological evaluation of 2'-[^{18}F]fluoroflumazenil ([18F]FFMZ), a potential GABA receptor ligand for PET. Nucl Med Biol **31:** 291-5.

[13] Mitterhauser M, Wadsak W, Mien LK, Eidherr H, Roka S, Zettinig G, Angelberger P, Viernstein H, Kletter K, Dudczak R. 2003. The labelling of Nanocoll with [^{111}In] for dual-isotope scanning. Appl Radiat Isot **59:** 337-42.

[14] Wadsak W, Mitterhauser M, Mien LK, Toegel S, Keppler B, Dudczak R, Kletter K 2003. Radiosynthesis of 3-(2'- [18F]-fluoro-flumazenil ([18F]FFMZ) via distillation of 2-bromo-[^{18}F]-fluoroethane. J Label Compd Radiopharm **46:** 1229-40.